



febrero, 2015

tesis doctoral realizada por **Ahmed Elyamani Ali Mohamed**

Integrated monitoring and structural analysis strategies for the study of large historical construction. Application to Mallorca cathedral

Universitat Politècnica de Catalunya
Departament d'Enginyeria de la Construcció

Barcelona, febrero de 2015

dirigida por:
Pere Roca i Fabregat

tesis doctoral realizada por:
Ahmed Elyamani Ali Mohamed

Integrated monitoring and
structural analysis
strategies for the study of
large historical
construction. Application
to Mallorca cathedral

TESIS DOCTORAL

This page is intentionally left blank.

Integrated monitoring
and structural analysis
strategies for the study
of large historical
construction. Application
to Mallorca cathedral

tesis doctoral realizada por:

Ahmed Elyamani Ali Mohamed

dirigida por:

Pere Roca i Fabregat

Barcelona, febrero de 2015

Universitat Politècnica de Catalunya
Departament d'Enginyeria de la Construcció

TESIS DOCTORAL

This page is intentionally left blank.



CURSO ACADÉMICO:2014-2015

ACTA DE CALIFICACIÓN DE TESIS DOCTORAL

Nombre y apellidos

Ahmed Elyamani Ali Mohamed

Programa de doctorado

Ingeniería de la Construcción

Unidad estructural responsable del programa

Departamento de Ingeniería de la construcción

RESOLUCIÓN DEL TRIBUNAL

Reunido el Tribunal designado a tal efecto, el doctorando / la doctoranda expone el tema de la su tesis doctoral titulada “*Integrated monitoring and structural analysis strategies for the study of large historical construction. Application to Mallorca cathedral*”

Acabada la lectura y después de dar respuesta a las cuestiones formuladas por los miembros titulares del tribunal, éste otorga la calificación:

- NO APTO APROBADO NOTABLE SOBRESALIENTE

(Nombre, apellidos y firma)		(Nombre, apellidos y firma)	
Presidente/a		Secretario/a	
(Nombre, apellidos y firma)	(Nombre, apellidos y firma)	(Nombre, apellidos y firma)	(Nombre, apellidos y firma)
Vocal	Vocal	Vocal	Vocal

_____, _____ de _____ de _____

El resultado del escrutinio de los votos emitidos por los miembros titulares del tribunal, efectuado por la Escuela de Doctorado, a instancia de la Comisión de Doctorado de la UPC, otorga la MENCIÓN CUM LAUDE:

- SÍ NO

(Nombre, apellidos y firma)	(Nombre, apellidos y firma)
Presidente de la Comisión Permanente de la Escuela de Doctorado	Secretaria de la Comisión Permanente de la Escuela de Doctorado

Barcelona a _____ de _____ de _____

This page is intentionally left blank.

*"I constantly sought knowledge and truth,
and it became my belief that
for gaining access to the effulgence and closeness to God,
there is no better way than that of searching for truth and knowledge".*

Al-Hasan Ibn Al-Haytham
(c. 965 in Basra – c. 1040 in Cairo)

This page is intentionally left blank.

Acknowledgments

First of all, I would like to thank Allah for everything he has given me. Without His help in every single moment of my life I wouldn't be able to achieve anything, *Alhamdulillah*.

I would like to express my sincere grateful to my tutor Prof. Pere Roca for trusting and offering me this PhD scholarship after finishing my MSc thesis under his supervision. I would like to thank him for his guidance, valuable suggestions and careful review of my work. Our fruitful discussions during several meetings motivated me to think deeply and to find logical answers for the problems I faced. I've learned a lot from you Prof. Pere, heartfelt thanks.

Special thanks are to Oriol Caselles for his help in the experimental investigations and for his always availability to answer my questions. Thanks are also to Jaime Clapés for taking care of the technical issues of the dynamic and thermography monitoring systems.

I would like to thank Murat Alaboz, Edwin Reynders, and Filippo Lorenzoni who answered my inquiries. I would like to express my gratitude to Prof. Luis Ramos for our two meetings in Wroclaw and Barcelona. I wish to acknowledge many advices provided by Katrien van Nimmen in using MACEC program.

Thanks are to the SAHC MSc students Matteo Bettoni and Chavon Grande whose works were of a good help to me. Many thanks also go to Yohei Endo and Nuno Mendes for their help in the nonlinear dynamic analysis. I would like to extend my thanks to Anass Attaya and Abdullah Galaa for replying my questions about the soil-structure interaction.

Many individuals from many departments of the Technical University of Catalonia have provided me with important help. Truly grateful to Anna Fabregas from the International Relations Office for her help in obtaining my visa to Spain and the regular renewing of my permit of stay. Thanks are also extended to the secretary of the Department of Construction Engineering. The lectures offered about using the University information resources are deeply acknowledged, special thanks to Marta Garcia-Sanchez. Thanks are to all my colleagues in the Department of Construction Engineering. Thanks to Alexis, André, Augusto, Carles, Cristian, Daniel, Francisco, Isaac, Juliana, Luca, Martha, Oriol, Pablo, Pau, Rubén, Savvas and Tasos. I must also thank a lot Jaume Nos my dear flatmate for all these years and also for his kind parents.

In the Faculty of Archeology of Cairo University, I would like to express my very great appreciation to Professors Azza Farouk, Salwa Gad, Soad Abdelal, Mohamed Hamza

and Moustafa Attia who made my PhD study in Spain possible. My special thanks are extended to the staff of Conservation Department. I would like to express my special thanks to my colleague Dr. Mahmoud Abdelhafez for his help in taking care of all my administrative papers in the University and his sincere moral support.

Due thanks are to all the staff members of the Egyptian Cultural Office in Madrid. In specific, I would like to thank Professors Sayed Soheim, Basem Daoud and Abeer Abdelsalam and Mr. Baher Ahmed and Mr. Hany Elmaadawi.

I would like to thank all my family. Mentioning only acknowledgment words cannot express enough my feelings to my beloved deceased father and mother. Only Allah is able to reward you for all you've done for me from the first moment of my life until the last days of your lives. I would like to express my special thanks to my brother Hany and my sisters Safaa, Basma and Amira. To my beloved wife Rasha, all the acknowledgment words would not be enough to thank you for your encouragement and accepting my travelling alone for all these years. My beloved daughter Rokaya, I hope to compensate you for this long absence and to be the father that you love so much.

The financial support to do this PhD within the framework of the FP7 European funded research project "*New Integrated Knowledge-based approaches to the protection of Cultural Heritage from Earthquake-induced Risk*" is fully acknowledged. Also, the financial support from Bauhaus University to attend the summer school course on "Model Validation and Simulation" is acknowledged.

Abstract

Historical structures are vital to the realization of how the technical, artistic, and scientific skills of the human kind have developed over time. These structures are one of the motors of the tourism industry, and therefore, the studies related to their conservation do not only have social benefits but as well economical ones. It is unfortunately that many countries rich with valuable architectural heritage are characterized by high seismic activity, Italy and Turkey are obvious examples. Due to earthquakes, many invaluable historical structures have been lost forever. Consequently, there is an increasing need for more research on the topic of seismic assessment and protection of this class of buildings.

This work contributes to the methodological approaches adopted for the seismic assessment of historical structures. In many cases, due to the lack of knowledge about the assessed historical structure, it is essential to combine many investigation activities in such approaches. The aim is to minimize any possibly required seismic strengthening interventions (minimum intervention concept) by increasing the level of knowledge about the structure.

In the current research, the employed experimental investigation activities are the dynamic identification tests and the dynamic monitoring. Most approaches for dynamic monitoring are based on the use of a threshold limit which is used to trigger the system when the parameters measured surpass the limit. Here, an alternative is considered that consists of a continuous monitoring system based on the permanent measurement of the ambient vibration. A thermography monitoring is used as a complementary system for the measurement of temperature. The integration between the dynamic investigation and the numerical modeling is essential and it includes two main features. On one hand, tentative structural analyses are carried out to identify important aspects of the dynamic tests and monitoring strategies such as critical points of the structure where to place the sensors. On the other hand, the results of the dynamic investigation are used to perform model updating until obtaining a satisfactory structural model adequately matching the measured dynamic properties of the structure.

Once the structural model is validated, it is used to carry out the seismic assessment of the structure. This assessment is performed using different methods, to cross check the results, including the pushover analysis, the kinematic limit analysis and the nonlinear dynamic analysis. It is then possible with these assessments to identify the seismic behavior of the structure. Using the N2 method, the evaluation of the structural

performance and its safety are carried out. Hence, the needs for any possible seismic strengthening are revealed, keeping in mind, the respect to the “minimum intervention” concept.

As an application, the cathedral of Mallorca (Spain) is taken as a case study. This structure is one of the largest cathedrals built during the Middle Age.

For each of the previously mentioned research steps, the followed criteria and the experience gained are transferred into recommended methodological approaches to be applied to other historical structures. Finally, the integration of these partial steps into one integrated methodology is discussed.

Resumen

Las estructuras históricas son de vital importancia para la comprensión del desarrollo de las habilidades técnicas, artísticas y científicas de la especie humana en el tiempo. Actualmente, estas estructuras son uno de los motores de la industria del turismo, y por ello, los estudios relacionados con su conservación no sólo tienen beneficios sociales, sino también económicos. Por desgracia, muchos países con abundante y en valioso patrimonio arquitectónico se caracterizan por una alta actividad sísmica. Entre ellos, Italia y Turquía son ejemplos obvios. Debido a los terremotos, muchas estructuras históricas de valor incalculable se han perdido para siempre. En consecuencia, existe una creciente necesidad de investigación sobre el tema de la evaluación sísmica y protección de esta clase de edificios.

Este trabajo desea contribuir a la metodología adoptada para la evaluación sísmica de estructuras históricas. En muchos casos, y debido a las limitaciones en la comprensión de una estructura histórica en estudio, es esencial combinar distintas actividades de investigación con la finalidad de aumentar el conocimiento sobre la estructura. El objetivo es reducir al mínimo las intervenciones de refuerzo sísmico que pueden resultar necesarias (aplicando el concepto de intervención mínima) a través del aumentar el nivel de conocimiento acerca de la estructura.

En esta investigación, las actividades experimentales empleadas son las pruebas de identificación dinámicas y la instrumentación dinámica. La mayoría de los enfoques para la instrumentación dinámica se basan en el uso de un umbral que se utiliza para activar el sistema cuando los parámetros medidos superan un límite. En el presente trabajo se considera una alternativa que consta de un sistema de instrumentación continua basado en la medición permanente de la vibración ambiente. Se utiliza un monitoreo termográfico como un sistema complementario para la medición de la temperatura. La integración entre la investigación dinámica y el modelado numérico es esencial. Esta integración incluye dos características principales. Por un lado, los análisis estructurales provisionales se llevan a cabo para identificar aspectos importantes de las pruebas dinámicas y de las estrategias de monitoreo, tales como los puntos críticos de la estructura donde colocar los sensores. Por otra parte, los resultados de la investigación dinámica se utilizan para realizar una actualización del modelo numérico estructural hasta la obtención de un modelo satisfactorio cuyos parámetros dinámicos coincidan satisfactoriamente con los medidos experimentalmente.

Una vez que el modelo estructural se valida, se utiliza para llevar a cabo la evaluación sísmica de la estructura. Esta evaluación se lleva a cabo usando diferentes métodos incluyendo el análisis estático no lineal, el análisis límite cinemático y el análisis dinámico no lineal. Con estas evaluaciones es posible identificar el comportamiento sísmico de la estructura. Utilizando el método de N2, es posible llevar a cabo una evaluación del comportamiento estructural y de la seguridad ante el sismo. Ello permite determinar las necesidades refuerzo sísmico. El refuerzo propuesto debe tener en cuenta el concepto de "intervención mínima".

La catedral de Mallorca (España) se toma como caso de estudio para la aplicación de la metodología propuesta. Esta estructura es una de las mayores catedrales construidas en Europa durante la Edad Media.

Para cada uno de los pasos de la investigación mencionados anteriormente, los criterios seguidos y la experiencia adquirida han sido transferidos a los enfoques metodológicos recomendados para su posible aplicación a otras estructuras históricas. Se presenta una discusión sobre la integración de estos pasos parciales en una metodología global.

Resum

Les estructures històriques són de vital importància per a la comprensió del desenvolupament de les habilitats tècniques, artístiques i científiques de l'espècie humana en el temps. Actualment, aquestes estructures són un dels motors de la indústria del turisme, i per això, els estudis relacionats amb la seva conservació no només tenen beneficis socials, sinó també econòmics. Per desgràcia, molts països amb abundós i valuós patrimoni arquitectònic es caracteritzen per una alta activitat sísmica. Itàlia i Turquia en són exemples obvis. A causa dels terratrèmols, moltes estructures històriques de valor incalculable s'han perdut per sempre. En conseqüència, hi ha una creixent necessitat d'investigació sobre el tema de l'avaluació i protecció sísmica d'aqueste tipus d'edificis.

Aquest treball desitja contribuir a la metodologia adoptada per a l'avaluació sísmica d'estructures històriques. En molts casos, i a causa de les limitacions en la comprensió d'una estructura històrica en estudi, és essencial combinar diferents activitats de recerca amb la finalitat d'augmentar el coneixement sobre l'estructura. L'objectiu és reduir al mínim les intervencions de reforç sísmic que poden resultar necessàries (tot aplicant el concepte d'intervenció mínima) a través d'augmentar el nivell de coneixement sobre l'estructura.

En la present investigació, les activitats de recerca experimentals emprades són les proves d'identificació dinàmiques i la monitorització dinàmica. La majoria dels enfocaments per la monitorització dinàmica es basen en l'ús d'un llindar que s'utilitza per activar el sistema quan els paràmetres mesurats superen un límit. En el present treball es considera una alternativa que consta d'un sistema de monitoratge continu basat en el mesurament permanent de la vibració ambient. Alhora, s'utilitza un monitoratge termogràfic com a sistema complementari per al mesurament de la temperatura. La integració entre la recerca dinàmica i el modelatge numèric és essencial. Aquesta integració inclou dues característiques principals. D'una banda, les anàlisis estructurals provisionals es duen a terme per a identificar aspectes importants de les proves dinàmiques i de les estratègies de monitorització, com ara punts crítics de l'estructura on col·locar els sensors. D'altra banda, els resultats de la recerca dinàmica s'utilitzen per realitzar una actualització d'un model estructural fins a la obtenció d'un model satisfactori del qual els paràmetres dinàmics coincideixin satisfactòriament amb les propietats dinàmiques mesurades experimentalment.

Una vegada validat el model estructural, s'utilitza per dur a terme l'avaluació sísmica de l'estructura. Aquesta avaluació es porta a terme utilitzant diferents mètodes incloent l'anàlisi estàtica no lineal, l'anàlisi límit cinemàtica i l'anàlisi dinàmica no lineal. És llavors possible, amb aquestes avaluacions, caracteritzar el comportament sísmic de l'estructura. Utilitzant el mètode de N2 és possible dur a terme una avaluació del comportament estructural i de la seguretat davant de sísmes. Aquesta avaluació permet determinar les necessitats de reforç sísmic. El reforç finalment proposat ha de tenir en compte el concepte d'intervenció mínima.

La catedral de Mallorca (Espanya) es pren com a cas d'estudi per a l'aplicació de la metodologia proposada. Aquesta estructura és una de les catedrals més grans construïdes a Europa durant l'Edat Mitja.

Per a cada un dels passos de la investigació esmentats anteriorment, els criteris utilitzats i l'experiència adquirida es transfereixen han estat transferits als enfocaments metodològics recomanats l'aplicació a altres estructures històriques. Finalment, es presenta una discussió sobre la integració d'aquests passos parcials en una metodologia global.

TABLE OF CONTENTS

AKNOWLEDGMENTS	i
ABSTRACT	iii
RESUMEN	v
RESUM	vii
CHAPTER 1 INTRODUCTION	
1.1 Introduction	2
1.2 Motivations	2
1.3 Objectives	4
1.3.1 General objectives	4
1.3.2 Specific objectives	4
1.4 Outline of the thesis	5
CHAPTER 2 STATE-OF-THE-ART	
2.1 Introduction	8
2.2 Dynamic identification of historical construction	8
2.2.1 Motivations	8
2.2.2 Testing methods	9
2.2.3 Equipments	13
2.2.4 Applications: from modern to historical structures	21
2.3 Dynamic monitoring of historical construction	29
2.3.1 Motivations	29
2.3.2 Types of dynamic monitoring systems	30
2.3.3 Applications of dynamic monitoring to cultural heritage buildings	32
2.4 Modal parameters identification	36
2.4.1 Introduction	36
2.4.2 Concepts in signal processing	36
2.4.3 Modal parameters identification methods	41
2.5 Infrared thermography	46
2.5.1 Theoretical background	46
2.5.2 Practical considerations	47
2.5.3 Infrared thermography in historical construction: case studies	48
2.6 Updating of finite element models of historical construction	50
2.6.1 Introduction	50
2.6.2 Philosophy of FE model updating	51
2.6.3 Methods of FE model updating	52
2.6.4 Experimental and numerical data correlation techniques	55
2.6.5 Case studies using different updating approaches	56
2.7 Historical masonry properties: literature review	60
2.7.1 Introduction	60
2.7.2 Tensile strength	61
2.7.3 Modulus of elasticity	62
2.7.4 Fracture energy	64
2.8 Seismic assessment of historical construction	66
2.8.1 Introduction	66
2.8.2 Nonlinear static (pushover) analysis	68
2.8.3 Nonlinear time-history (dynamic) analysis	71
2.8.4 Limit analysis	75
2.8.5 N2 method	77
2.8.6 Case studies	79
2.9 Conclusions	82
CHAPTER 3 MALLORCA CATHEDRAL: ONE CENTURY OF STUDIES	

3.1	Introduction	88
3.2	History of construction	88
3.2.1	Introduction	88
3.2.2	Construction, failures and reconstruction	89
3.3	Description of Mallorca cathedral	94
3.4	Previous Inspection	100
3.4.1	Cracking survey	100
3.4.2	Deformations survey	102
3.4.3	Geophysical surveys of columns, buttresses and walls	106
3.4.4	Chemical analysis	108
3.4.5	Dynamic identification	109
3.4.6	Soil investigation	110
3.5	Previous structural assessments	113
3.5.1	Pioneering studies	113
3.5.2	Recent studies	116
3.6	Previous monitoring	126
3.6.1	Static monitoring (González and Roca, 2003-2008; Godde, 2009)	126
3.6.2	Dynamic monitoring (Martínez, 2007; Boromeo, 2010)	127
3.7	Conclusions	129
CHAPTER 4 DYNAMIC IDENTIFICATION OF MALLORCA CATHEDRAL		
4.1	Introduction	132
4.2	Design of tests. Initial modal analysis	132
4.2.1	Considerations	132
4.2.2	Equipment	134
4.2.3	Configuration of setups	135
4.3	Execution of tests and preliminary post processing	136
4.4	Dynamic identification using different methods	140
4.4.1	Frequency domain decomposition (FDD)	141
4.4.2	Reference-based covariance-driven stochastic subspace identification (SSI-cov/ref)	142
4.4.3	Reference-based data-driven stochastic subspace identification (SSI-data/ref)	146
4.4.4	Poly-reference least squares complex frequency domain identification (pLSCF).	148
4.5	Comparison among all methods	150
4.5.1	Natural frequencies	150
4.5.2	Damping ratios	152
4.5.3	Mode shapes	153
4.6	Conclusions	168
CHAPTER 5 DYNAMIC AND THERMOGRAPHY MONITORING OF MALLORCA CATHEDRAL		
5.1	Introduction	173
5.2	Dynamic monitoring of Mallorca cathedral	173
5.2.1	Description of the dynamic monitoring system	173
5.2.2	Data processing methodology	175
5.2.3	Evolution of natural frequencies over time	177
5.2.4	Effects of environmental actions on the dynamic response	181
5.2.5	Response during recorded earthquakes	197
5.3	Thermography monitoring of Mallorca cathedral	201
5.3.1	Description of the thermography monitoring	201
5.3.2	Comparisons between different temperatures	203
5.3.3	Correlation between natural frequencies and different temperatures	206

5.4	Conclusions	209
CHAPTER 6 UPDATING OF MALLORCA CATHEDRAL NUMERICAL MODEL		
6.1	Introduction	212
6.2	Description of the initial FE model	212
6.3	Initial correlation of experimental and numerical modal parameters	214
6.4	Model updating procedure	217
6.4.1	Adjusting in the longitudinal direction	220
6.4.2	Adjusting in the transversal direction	223
6.4.3	Using elastic foundations	224
6.4.4	Damage simulation	226
6.4.5	Final FE model after updating	228
6.5	Conclusions	232
CHAPTER 7 SEISMIC ASSESSMENT OF MALLORCA CATHEDRAL		
7.1	Introduction	236
7.2	Constitutive model and properties of materials	236
7.3	Characterization of the seismic demand	237
7.3.1	Characterization of the seismic demand according to NCSE-02	237
7.3.2	Characterization of the seismic demand according to EC-08	238
7.4	Nonlinear static analysis	240
7.4.1	Introduction	240
7.4.2	The seismic response in the longitudinal ($\pm X$) direction	240
7.4.3	The seismic response in the transversal ($\pm Y$) direction	249
7.4.4	Sensitivity analysis	259
7.5	Kinematic Limit analysis	263
7.6	Nonlinear dynamic analysis	266
7.6.1	Dynamic seismic loading	266
7.6.2	Time step and damping model	274
7.6.3	Results	275
7.7	Evaluation of the seismic performance	280
7.8	Conclusions	283
CHAPTER 8 METHODOLOGICAL CONSIDERATIONS ON SEISMIC ASSESSMENT OF LARGE HISTORICAL STRUCTURES		
8.1	Introduction	286
8.2	Meaning of knowledge-based assessment	286
8.3	Global approach for seismic assessment	287
8.4	Considerations on the dynamic identification	289
8.5	Considerations on the dynamic monitoring	292
8.6	Considerations on numerical model updating	297
8.7	Considerations on seismic assessment	300
CHAPTER 9 CONCLUSIONS AND FUTURE WORK		
9.1	Introduction	304
9.2	Conclusions	304
9.2.1	On the state-of-the-art	304
9.2.2	On the previous studies carried out on Mallorca cathedral	306
9.2.3	On the new studies carried out on Mallorca cathedral	307
9.2.4	On the applied general methodology	311
9.3	Future work	311
9.3.1	On Mallorca cathedral	311
9.3.2	On the studies of historical structures	312
REFERENCES		315

LIST OF FIGURES

Figure 2.1. Basics of FVT: (a) testing scheme; and (b) calculation of the Frequency Response Matrix H (Cantieni, 2005).	10
Figure 2.2. Basics of AVT: (a) testing scheme (R is a reference point and k is a roving point); and (b) calculation of the cross relationship between R and k signals (Cantieni, 2005).	12
Figure 2.3. Excitation mechanisms: (a) Impulse hammer; (b) impulse excitation device for bridges (K.U. Leuven); (c) electrodynamic shaker over three load cells; and (d) eccentric mass vibrator (adapted from Cunha and Caetano, 2006).	14
Figure 2.4. Servo-hydraulic shakers to excite: (a) bridges (vertically); and (b) dams (laterally) (EMPA) (adapted from Cunha and Caetano, 2006).	14
Figure 2.5. A typical deflection-type seismic accelerometer (adapted from Eren, 1999).	16
Figure 2.6. Left: schematic of the force-balance accelerometer (Wilson, 1999a). Right: Titan force-balance accelerometer (www.nanometrics.ca).	17
Figure 2.7. Left: the general force feedback control system (Stuart-Watson, 2006). Right: CMG-5T feedback accelerometer (www.guralp.com).	17
Figure 2.8. Left: A compression-type piezoelectric accelerometer (Eren, 1999). Right: 393B12 piezoelectric accelerometer (www.pcb.com).	18
Figure 2.9. Data acquisition system (Sydenham, 1983).	21
Figure 2.10. Setups of AVT of Fossanova church. Solid arrows show measurement points (De Matteis et al., 2007a).	24
Figure 2.11. FVT of Gothic vaults: (a) preliminary FE mode shapes; (b) measurement and excitation points (1,3,12,18); (c) vertical positioning of accelerometers by adjustable screws of mounting cases; and (d) applying the hammer at excitation points (Atamturktur et al., 2009).	25
Figure 2.12. Choosing optimum sensor locations in Gothic cathedrals: (a) candidate locations are shaded; and (b) optimum locations as dots (Prabhu and Atamturktur, 2013).	27
Figure 2.13. Different monitoring phases across the study of a cultural heritage building, intervention and maintenance (D9.4-NIKER, 2012).	30
Figure 2.14. Types of dynamic monitoring systems: (a) conventional wired based systems; and (b) wireless based systems (Aguilar, 2010).	31
Figure 2.15. Recorded dynamic behavior of Mexico City cathedral during a seismic event: (a) variation of the period; and (b) variation of the damping ratio (Rivera et al., 2008).	34
Figure 2.16. Aliasing: (a) inadequate Nyquist sampling rate; and (b) acceptable Nyquist sampling rate (MC, 2005).	40
Figure 2.17. (a) Minimizing the leakage effect using the exponentially decaying window (Avitabile, 2001); and (b) Hamming, Hanning, and Blackman window functions (adapted from MC, 2005).	40
Figure 2.18. Filters types: (a) low-pass; (b) high-pass; (c) band-pass; and (d) stop-band. Note that the magnitude function of an ideal filter is 1 in the pass-band and 0 in the stop-band (adapted from Jamal and Steer, 1999).	40
Figure 2.19. Example of a stabilization diagram showing the difference between physical and numerical modes. Source: the dynamic identification tests of the current research.	45
Figure 2.20. Examples of IR thermography applied to two walls of the Spanish Fortress in L'Aquila: top: first wall, bottom: second wall (Binda et al., 2011).	49
Figure 2.21. Using IEM in model updating of a masonry arch bridge: (a) 1 st FE model; (b) 2 nd FE model; (c) Stiffness correction coefficients obtained from model	57

updating of the 1 st FE model; and (d) iterative updating of the 1 st FE model (Aoki et al., 2007).	
Figure 2.22. Typical behavior of quasi-brittle materials under uniaxial loading and definition of fracture energy: (a) tensile loading; and (b) compressive loading (Lourenço, 1996).	65
Figure 2.23. Some examples of damage to historical structures: (a) and (b) Lorca earthquake (Spain); (c) and (d) L'Aquila earthquake (Italy); and (e) Van earthquakes (Turkey).	67
Figure 2.24. N2 method procedure: (a) elastic response spectrum; (b) elastic response spectrum in AD format; (c) the capacity curve (in grey) and the equivalent bi-linear curve (in black); (d) inelastic response spectrum; and (e) performance point.	79
Figure 2.25. Nonlinear dynamic analysis of (a) minaret: deformed shape (left) and collapsed part in blue (right) (Peña et al., 2010); and (b) chimney: deformed shape (left) and collapsed part in dark gray (right) (Minghini et al., 2014).	81
Figure 3.1. Mallorca Cathedral: aerial view (left); and external view showing the apse area and the south façade (right).	89
Figure 3.2. Plan showing the progress of Mallorca cathedral construction from 1306 to 1601. The indicated years are for the approximate end of the construction of each part.	90
Figure 3.3. Historical intervention in 1739 on the flying arches at: (a) the 4th northern bay; and (b) the 7th northern bay. The counting is from the east façade.	93
Figure 3.4. The west façade: (a) comparison between the original façade (left) and the new façade of Baptist (right); and (b) the dismantling in 1855.	93
Figure 3.5. Gaudí reforms in Mallorca cathedral: the choir in the central nave (left); and the choir moved to the presbytery (right) (from Gibert, 2010).	94
Figure 3.6. Mallorca cathedral: plan (top); longitudinal section (center); and transversal section (bottom) (from Director Plan of Mallorca Cathedral).	95
Figure 3.7. Comparing the cross section of Mallorca cathedral (always to the left) with the cross section of the cathedrals of: (a) Girona; (b) Milan; (c) Beauvais; (d) Reims; (e) Amiens; and (f) Paris (Salas, 2001).	97
Figure 3.8. Internal views of Mallorca cathedral: looking at apse and south nave, note the large rose window (top left); looking at west façade and north nave, note the slenderness of columns and the upper and lower clerestories (top right); looking from apse at central nave (bottom left); and main nave vaults (bottom right).	98
Figure 3.9. Additional weights: (a) over the transversal arches keys; and (b) over the vaults keys.	99
Figure 3.10. Cracking in columns: a cracked wedge near to the column corner (left); and documentation of the cracked faces (right).	101
Figure 3.11. Separation between a vault and supporting arch (left); developed crack in a vault (right).	101
Figure 3.12. Developed crack across mortar joints in a clerestory wall.	101
Figure 3.13. Deformed columns: internal column (left); and column at triumphal arch (right).	102
Figure 3.14. Deformation survey: (a) bays' deformed shapes (numbering from east to west); and (b) values of deformations (cm) at each of the seven bays in the same order of (a) (from Clemente, 2006).	103
Figure 3.15. Fourth bay construction: (a) lateral chapel (1391-1406) then columns (1406-1426); (b) lateral vault (1453-1454); (c) lateral vault (1458); and (d) central vault (1459-1460) (Domenge, 1997).	104
Figure 3.16. Evidences of using of ties in Mallorca cathedral construction: northern	104

nave of 7th bay (left); northern nave of 6th bay (center); and southern nave of 4th bay (right) (Bourgeois, 2013).	
Figure 3.17. Deformation survey of the south façade (the deformed shape is in black and the theoretical undeformed shape is in red, displacement values are in cm) (González and Roca, 2003-2008).	105
Figure 3.18. Locations of the GPR profiles and seismic tomography: P1–P10: GPR profiles in walls and in some columns; C1–C14: single GPR vertical profiles columns; C3, C4 and C10: columns analyzed with GPR profiles in each side and with seismic tomography (Pérez-Gracia et al., 2013).	106
Figure 3.19. GPR inspection: radargram of clerestory wall with red lines showing possible distribution of stones (left); and radargram of a buttress with inner filling surrounded by a red closed shape (right) (Roca et al., 2008).	107
Figure 3.20. Reconstruction of columns internal structure using GPR inspection: distribution of blocks in elevation (most left); two cross sections (center); and 3D reconstruction of columns (most right) (Pérez-Gracia et al., 2013; González et al., 2008).	107
Figure 3.21. High, medium and low velocity (m/s) zones: C3 (left); C4 (center); and C10 (right).	108
Figure 3.22. Distribution of limestone varieties used in Mallorca cathedral using different grey tones based on chemical analysis (Roca et al., 2008).	109
Figure 3.23. Previous dynamic identification of Mallorca cathedral: sensor location on a transversal section (left); and plan view of sensors locations (right) (Martínez et al., 2006).	109
Figure 3.24. Different profiles and drilling points on plan (Ss: boreholes, Gs: GPR, Rs: ERT, Ms: ReMi profiles) and the division of the soil into three zones (adapted from Pérez-Gracia et al., 2009).	110
Figure 3.25. The soil formation under: (a) the west façade; (b) the north façade; and (c) the south façade (adapted from Martínez, 2007).	111
Figure 3.26. Measured shear wave velocity in each of the soil zones (Pérez-Gracia et al., 2009).	112
Figure 3.27. Static-graphic analysis of Rubió (1912).	114
Figure 3.28. Photo-elasticity analysis of Mark (1982).	115
Figure 3.29. Automatic static-graphics of Maynou (2001): thrust lines (in red) giving the maximum eccentricities at the base of the column.	116
Figure 3.30. The collapse mechanisms studied by Coutinho (2010).	118
Figure 3.31. Nonlinear analysis of a typical bay under self weight: (a) compressive stresses using theoretical undeformed geometry (left) and actual deformed geometry (right); (b) tensile stresses using theoretical undeformed geometry (left) and actual deformed geometry (right); (c) compressive and tensile stresses using GMF method; and (d) stresses plotted on deformed shape at collapse due to wind loads using GMF method (Salas, 2002).	120
Figure 3.32. Collapse mechanism of a typical bay under self weight: distributed damage model: tensile damage (left) and compressive damage (center); localized damage model (right) (Clemente, 2006).	122
Figure 3.33. Tensile damage of nonlinear analysis of a typical bay under self weight without considering the construction process (left); and considering the construction process (center and right) (Clemente, 2006).	122
Figure 3.34. Sensitivity analysis of tensile strength (top left); compressive strength (top right); and tensile fracture energy (bottom) (Clemente, 2006).	123
Figure 3.35. The macro elements studied by Martínez (2007): (a) typical bay; (b) transept bay; (c) triumphal arch; (d) west façade; and (e) longitudinal bay.	125
Figure 3.36. Tensile damage at collapse under gravity loads (left); and seismic loads	125

(right) (Das, 2008).	
Figure 3.37. The static monitoring system of Mallorca cathedral (González and Roca, 2003-2008).	127
Figure 3.38. The evolution in time of the mode 3.2 and the temperature (left); and the relation between the frequency and the temperature for the same mode (right) (Boromeo, 2010).	128
Figure 4.1. The first ten numerical mode shapes before model updating.	133
Figure 4.2. Measurement points depicted on the cathedral plan.	136
Figure 4.3. Photos during measurements of some points: (a) P6; (b) P14; (c) P16; and (d) P24.	137
Figure 4.4. The relative location between the cathedral and the station (adapted from Google Maps).	137
Figure 4.5. FDD method, identified modes from setup 10.	141
Figure 4.6. Stabilization diagram of setup 6 using maximum system order of 128 (top); and 600 (bottom).	143
Figure 4.7. One satisfactory identified mode from setup 9 using SSI-cov/ref method.	145
Figure 4.8. Estimated damping ratios for each mode in each setup using SSI-cov/ref method.	146
Figure 4.9. The well estimated modes from setup 12 using SSI-data/ref method.	147
Figure 4.10. Estimated damping ratios using SSI-data/ref for each mode in each setup.	147
Figure 4.11. One mode satisfactory estimated from setup 14 using pLSCF method.	149
Figure 4.12. Damping ratios for each mode in each setup using pLSCF method.	150
Figure 4.13. Comparison among identified damping ratios from different methods.	152
Figure 4.14. Schematic representation of the cathedral for mode shapes presentation.	153
Figure 4.15. First identified mode shape. Longitudinal movement for the three naves with clear bending movement for the south nave and slight bending of the north nave.	154
Figure 4.16. Second identified mode shape. Longitudinal movement for the three naves.	155
Figure 4.17. Third identified mode shape. Longitudinal movement for the three naves. This mode is very near to the previous one.	156
Figure 4.18. Fourth identified mode shape. Transversal movement for the three naves with clear bending of the south nave.	157
Figure 4.19. Fifth identified mode shape. Transversal movement for the main nave in the form of contraction and expansion.	158
Figure 4.20. Sixth identified mode shape. Contraction and expansion of the first west four bays and slight transversal movement for the remaining bays.	159
Figure 4.21. Seventh identified mode shape. Negligible movement for the north nave and bending movement for the south nave, the façade and the first two bays are moving longitudinally.	160
Figure 4.22. Eighth identified mode shape. Torsional mode.	161
Figure 4.23. Comparison of MAC values among the identified mode shapes from the different methods using all setups. cov = SSI-cov/ref, data = SSI-data/ref.	162
Figure 4.24. From (a) to (c) comparison of MPC, MP and MPD values respectively considering all setups set and selected setups set for each mode. cov = SSI-cov/ref, data = SSI-data/ref.	163
Figure 4.25. From (a) to (h) comparison between the MAC index considering all setups and selected setups. cov = SSI-cov/ref, data = SSI-data/ref.	167
Figure 4.26. Comparison between the max MAC index considering all setups and selected setups.	167

Figure 4.27. The setups that satisfactory estimate each mode using different identification methods. The setups ID's of transversally arranged roving sensors are highlighted in gray.	170
Figure 5.1. Investigated points for accommodating sensors (in blue) and the final chosen locations (in red).	174
Figure 5.2. The dynamic system in operation: S1 (left); 145 Station (middle); and Soil station (right).	175
Figure 5.3. Followed methodology in processing monitoring data.	176
Figure 5.4. Example of the spectrum of 145 station in NS direction for the day of 30-9-2012 at hour 20:00 and the peak picking.	176
Figure 5.5. Percentage of detection of each mode by each channel alone.	178
Figure 5.6. Evolution of the cathedral natural frequencies over time.	179
Figure 5.7. From (a) to (h): changes of the frequencies of the first eight modes with temperature.	186
Figure 5.8. Correlation between temperature and natural frequency for modes from 1 to 8. Linear and quadratic regression models are in solid and dashed lines, respectively.	187
Figure 5.9. Changes of frequencies with humidity: (a) mode 2; and (b) mode 8.	189
Figure 5.10. Correlation between humidity and natural frequency for mode 2 (left); and mode 8 (right). Linear, quadratic and cubic regression models are in blue, green and red are respectively.	189
Figure 5.11. Frequency distribution of wind direction (top); and wind velocity (bottom).	190
Figure 5.12. Exact orientation of the cathedral with respect to the main directions (adapted from Google maps). The red line points to the NE direction.	191
Figure 5.13. Correlation between wind velocity and the natural frequency for mode 1(left); and mode 7 (right). Linear and quadratic regression models are in solid and dashed lines, respectively.	192
Figure 5.14. Correlation between wind direction and natural frequency for mode 2(left); and mode 5 (right). Linear, quadratic and cubic regression models are in blue, green and red are respectively.	192
Figure 5.15. The percent of identification of each mode at each considered hour for processing the dynamic monitoring data.	193
Figure 5.16. Wind velocity frequency distribution at each of the four times of dynamic identification. From left to right and from top to bottom: hours: 06:00; 14:00; 20:00; and 24:00.	194
Figure 5.17. Scaled wind direction frequency distribution at each of the four times of dynamic identification. From left to right and from up to down: hours: 06:00; 14:00; 20:00; and 24:00.	195
Figure 5.18. Twelve hours spectrogram derived from channel 2, and wind parameters at 4/6/2012. Start time at 11:00.	195
Figure 5.19. Correlation coefficients of natural frequencies and environmental actions.	196
Figure 5.20. Spectrogram of the EW channel of Soil Station for Alagueña earthquake. Start time of the spectrogram is at 22:30:00 UTC.	197
Figure 5.21. Spectrogram of the EW component at 145 Station for Menorca earthquake.	200
Figure 5.22. Transfer function, coherence and power spectral densities of EW component between 145 Station and Soil-station for Menorca earthquake. Left: pre-earthquake with calm wind; center: pre-earthquake in windy condition; and right: during earthquake.	200
Figure 5.23. Processing of 13 consecutive hours of the 3rd of June 2012 (the start	201

time corresponds to 11:00 UTC and the end corresponds to 24:00 UTC): top two figures: accelerogram and spectrogram of NS component of Soil-station showing the arrival of two earthquakes; and bottom two figures: spectrogram of EW component of S1-station and the drops in mode 3.	
Figure 5.24. Mallorca cathedral thermography monitoring: (a) the red circle shows the IR camera position; (b) the IR camera during operation (inside the pulpit); and (c) the area covered by the IR camera.	202
Figure 5.25. Two examples of the thermography monitoring: on 2nd of July 2011 at 9:46 a.m. (top); and on 2nd of February 2011 at 13:15 (bottom). Temperature scale in (°C).	202
Figure 5.26. Selected samples from structural elements within the IR camera coverage area: clerestory walls and columns (top), arches, columns and vaults (bottom). Coverage area hatched in yellow.	204
Figure 5.27. Comparison between external, internal and stone surface temperatures in the summer period from 28/6/2011 to 13/7/2011.	205
Figure 5.28. Comparison between external and stone surface temperatures in the winter period from 27/1/2011 to 9/2/2011.	205
Figure 5.29. Comparison between external temperature for the summer and winter periods. The trend lines are also shown.	206
Figure 5.30. Changes of mode 4 with stone temperature: summer period (top); and winter period (bottom).	207
Figure 5.31. Summer period: comparison between coefficients of correlation of different temperatures with the first eight modes of the cathedral.	208
Figure 5.32. Winter period: comparison between coefficients of correlation of different temperatures with four of the cathedral modes.	208
Figure 6.1. Views of the FE model: complete model (top); plan showing filling above vaults in magenta (center); and longitudinal section (bottom).	213
Figure 6.2. View to the tower-buttress relation (left); and zoom to the separation (right).	214
Figure 6.3. Comparison between mode shapes of 1Num-2Exp (top); and 2Num-4Exp (bottom).	218
Figure 6.4. Followed procedure in updating the numerical model.	219
Figure 6.5. Mode 8: before adding the wall (left); and after adding it (right).	220
Figure 6.6. Comparison between 1Num-2Exp mode shape before (top) and after (bottom) adding the longitudinal wall between buttresses.	221
Figure 6.7. The effect of lateral chapels' vaults: (a) on frequencies; and (b) on Df.	222
Figure 6.8. Finding the optimized ratio for reducing elasticity modulus of the buttresses.	224
Figure 6.9. Effect of changing the average spring stiffness in the filling zone on: (a) Df; and (b) MAC.	225
Figure 6.10. Photos for the crack between third arch and fourth vault. In the left photo a zoom is made to the static monitoring sensor.	226
Figure 6.11. The numerical modeling of the crack by doubling the nodes. Before simulating the crack (top); and after simulating the crack (bottom).	227
Figure 6.12. Zoom at the crack location in the first mode (left); and the second mode (right).	227
Figure 6.13. The first ten mode shapes after updating. In parentheses MAC value between the initial and the final models.	230
Figure 6.14. Comparison between the experimental frequencies and the frequencies of the initial and the final models, the MAC values are shown beside the dots.	231
Figure 6.15. The changes in Df (top); and MAC (bottom) with the updating steps.	231
Figure 7.1. Representation of (a) tension cut-off and (b) tension softening (DIANA,	237

2009).	
Figure 7.2. The elastic response spectrum S_e (g) using the Eurocode 8 (EC8) and the Spanish code NCSE-02.	239
Figure 7.3. Capacity curve for the seismic analysis in (+X) direction. The control point (Max-D) is shown in circle.	241
Figure 7.4. Progress of damage in the two typical resisting frames: lower clerestory wall supported on buttresses (left); and upper clerestory wall supported on columns (right). Contour of maximum principal strain plotted on deformed mesh. Case of (+X).	242
Figure 7.5. Cracking pattern of vaults at collapse load. Contour of maximum principal strain plotted on deformed mesh. In red cracked areas. Case of (+X).	243
Figure 7.6. Damage experienced by the west façade at collapse load. Case of (+X). From outside the cathedral (left) and from inside the cathedral (right). Contour of maximum principal strain plotted on deformed mesh.	244
Figure 7.7. Capacity curve for the seismic analysis in (-X) direction. The control point (Max-D) is shown in circle.	245
Figure 7.8. Progress of damage in the two typical resisting frames: lower clerestory walls supported on buttresses (left); and upper clerestory walls supported on columns (right) Contour of maximum principal strain plotted on deformed mesh. Case of (-X).	246
Figure 7.9. Damage experienced by the east façade at collapse load. From outside the cathedral (left); and from inside the cathedral (right). Contour of maximum principal strain plotted on deformed mesh.	246
Figure 7.10. Crack survey of north (top) and south (bottom) clerestory walls. Red cracks are wider than blue ones. Photos for cracks surrounded by circles are shown in the next figure.	248
Figure 7.11. Photos from inside the cathedral for some of the cracks of the previous figure.	249
Figure 7.12. Capacity curve for the seismic analysis in (+Y) direction. The control point (Max-D) is shown in plan.	250
Figure 7.13. Capacity curves for the seven typical frames. The control point is shown in circle. Case of pushover in +Y direction.	250
Figure 7.14. From (1) to (8): arising cracking (in circle) and the associated seismic load factor. Cracking pattern in red plotted on deformed mesh.	252
Figure 7.15. Cracking pattern at collapse with sequence of cracking (left); and the seismic load factor of initiation of each crack (right).	253
Figure 7.16. Cracking pattern in red plotted on deformed mesh at collapse of the east facade.	253
Figure 7.17. Capacity curve for the seismic analysis in (-Y) direction. The control point (Max-D) is shown in circle.	254
Figure 7.18. Comparing deformations at collapse of case of +Y (left) with case of -Y (right).	255
Figure 7.19. Capacity curves for the seven typical frames. The control point is shown in circle.	255
Figure 7.20. From (1) to (8): arising cracking (in circle) and the associated seismic load factor. Cracking pattern in red plotted on deformed mesh.	256
Figure 7.21. Cracking pattern at collapse with sequence of cracking (left); and the seismic load factor of initiation of each crack (right).	257
Figure 7.22. Examples of damage possibly related to seismic events: (a) cracking around the middle rose window of the east façade; and (b) cracking at the south buttress of frame 3.	258
Figure 7.23. Damage pattern from seismic analysis of a typical bay. Distributed	259

damage model (left), localized damage model with (right). Source: Roca et al. (2013).	
Figure 7.24. Capacity curves varying f_t (left); and change of the capacity with the change of f_t ratio from the reference value (right).	260
Figure 7.25. Capacity curves varying f_c (Left); and change of the capacity with the change of f_c ratio from the reference value (right).	261
Figure 7.26. Capacity curves varying ε_{ucr} (left); and change of the capacity with the change of ε_{ucr} ratio from the reference value (right).	262
Figure 7.27. Capacity curves varying the modulus of elasticity E (left); and change of the capacity with the change of E ratio from the reference value (right).	263
Figure 7.28: (a) The west façade mechanism. The east façade mechanism: (b) cracked areas at collapse (in red) as deduced from the pushover analysis; (c) red circles show locations of hinges; and (d) lever arms for the macro-block weights and the seismic forces.	264
Figure 7.29. Artificial time-histories compatible with: (a) EC-08 (475 years); (b) EC-08 (975 years); (c) NCSE-02 (475 years); and (d) NCSE-02 (975 years).	267
Figure 7.30. Comparison between artificial time-histories of considered codes and return periods: average PGA (left) and significant duration (right).	268
Figure 7.31. Spectra of the four cases using SeismoArtif : (a) Eurocode 8 (475 years); (b) Eurocode 8 (975 years); (c) NCSE-02 (475 years); and (d) NCSE-02 (975 years).	269
Figure 7.32. The average PGA of each combination of real records compatible with each code and return period.	270
Figure 7.33. Examples of the real records mentioned in table 1.12 :(a) Gulf of Akaba (y-ST2898); (b) Izmit (x-ST766); (c) Almiros aftershock (x- ST1300); and (d) Umbria Marche aftershock (y-ST265).	271
Figure 7.34. Spectra of the four cases using REXEL: (a) Eurocode 8 (475 years); (b) Eurocode 8 (975 years); (c) NCSE-02 (475 years); and (d) NCSE-02 (975 years).	272
Figure 7.35. Comparing spectra of the artificial and the real records: (a) Eurocode 8 (475 years); (b) Eurocode 8 (975 years); (c) NCSE-02 (475 years); and (d) NCSE-02 (975 years).	273
Figure 7.36. Comparison between the average PGA (g) of the artificial and the real records.	273
Figure 7.37. Distribution of Rayleigh damping along the cathedral modes.	275
Figure 7.38. Time histories of the displacements of the considered control points.	276
Figure 7.39. Damage pattern in the two typical resisting frames. Contour of maximum principal strain plotted on deformed mesh.	276
Figure 7.40. Relation between seismic load multiplier and displacements of control points: (a) CG-cathedral; (b) CG-roof; (c) Top & Max-D of +X; and (d) Max-D of -X.	277
Figure 7.41. Time history of the displacements of the considered control points.	278
Figure 7.42. Damage pattern in a typical frame (frame 2). Contour of maximum principal strain plotted on deformed mesh: (left) damage pattern at the maximum negative displacement, point “a” in Figure 7.41, (right) Damage pattern at the maximum positive displacement (point “b” in Figure 7.41).	279
Figure 7.43. Relation between seismic load multiplier and displacements of control points: (a) CG-cathedral; (b) CG-roof ; (c) Top; and (d) Max-D of +Y and Max-D of -Y.	280
Figure 7.44. Application of the N2 method to the control point of CG-cathedral (case of +X direction) and EC-08 (return period of 975 years): (a) The elastic response spectrum in AD (acceleration –displacement) format; and (b) the performance point.	281
Figure 7.45. Evaluation of seismic safety in terms of displacements: ratios between maximum displacements and performance displacements.	282
Figure 7.46. Evaluation of seismic safety in terms of load multipliers: ratios between	283

collapse load multipliers and performance load multipliers.	
Figure 8.1. Global approach for structural assessment of historical structures.	287
Figure 8.2. Approach for dynamic identification of historical structures.	290
Figure 8.3. Approach for dynamic monitoring of historical structures.	293
Figure 8.4. Approach for historical construction model updating.	298
Figure 8.5. Approach for the seismic assessment of historical structures.	300

LIST OF TABLES

Table 2.1. AVT versus FVT (adapted from Dai et al., 2013).	13
Table 2.2. Multiplier factor for the estimation of the modulus of elasticity from the compressive strength of masonry adopted by modern codes of design.	63
Table 2.3. The relationship between the modulus of elasticity and the compressive strength of masonry found by several researchers.	63
Table 2.4. Pushover analysis versus nonlinear dynamic analysis (adapted from Elnashai, 2002).	71
Table 3.1. Dates of the important failures and reconstruction works of the cathedral in the three centuries after construction.	92
Table 3.2 Comparing main dimensions of some of the largest Gothic cathedrals in the world (Salas, 2001).	96
Table 3.3. Some of the characteristics of the four types of stone used in Mallorca cathedral (Alonso et al., 1996).	109
Table 3.4. Identified modes from AVT of Mallorca cathedral (Martínez, 2007).	110
Table 3.5. Properties of materials used in the structural analysis by Clemente (2006).	122
Table 3.6. Updating the moduli of elasticity (MPa) of different materials of the cathedral (Martínez, 2007).	124
Table 3.7 The cumulative trends measured by the static monitoring system (Godde, 2009).	127
Table 3.8. Statistical study on the identified modes during ten months (Boromeo, 2010).	129
Table 4.1. Frequencies and participation factors for the first ten numerical modes.	134
Table 4.2. Configuration of each setup (p16 is measured in all setups).	135
Table 4.3. Circumstances of each setup.	138
Table 4.4. Values of the RMS of the measured accelerations (mg*) in each setup.	139
Table 4.5. Average of RMS (mg) of all channels in each day.	140
Table 4.6. Detected natural frequencies (Hz) with the FDD.	142
Table 4.7. Estimated natural frequencies (Hz) of modes using the SSI-cov/ref method.	145
Table 4.8. Estimated natural frequencies (Hz) of modes with the method of SSI-data/ref.	148
Table 4.9. The identified modes with the application of pLSCF technique.	149
Table 4.10. Set of “selected setups” for each mode in each identification method.	151
Table 4.11. Identified natural frequencies (Hz) using all setups and selected setups sets.	151
Table 4.12. Comparison using selected setups set between the mode shapes of the modes 2 and 3.	168
Table 4.13. Judgment of the quality of identification process of Mallorca cathedral. P=poor, G= good.	171
Table 5.1. First two points of maximum normalized modal displacements in each direction.	174
Table 5.2. Summary of statistical variation of detected natural frequencies (Hz).	180
Table 5.3. Correlation coefficients between temperature and cathedral frequencies.	182
Table 5.4. Correlation coefficients between humidity and the frequencies (all values are negative).	189
Table 5.5. Correlation coefficients between wind velocity (WV) and wind direction (WD) and the cathedral natural frequencies.	192
Table 5.6. Environmental conditions at each considered time for processing the dynamic monitoring data.	193

Table 5.7. Details of the captured seismic events.	198
Table 5.8. Comparison between recorded accelerations (mg) under different conditions.	199
Table 5.9. Statistical variations in the cathedral frequencies in the summer and winter periods.	208
Table 6.1. Properties of different materials in the FE model.	214
Table 6.2. D_f values for correlation of initial FE model with experimental frequencies.	216
Table 6.3. MAC values for correlation of initial FE model with experimental modes.	216
Table 6.4. Best correlated numerical and experimental modes and corresponding D_f and MAC values.	217
Table 6.5. Comparison between initial FE model frequencies and mean frequencies obtained from the dynamic monitoring system.	217
Table 6.6. Comparing the numerical and experimental modes after adding the longitudinal wall.	220
Table 6.7. Comparing the numerical and experimental modes after considering the effect of the lateral chapels' vaults.	222
Table 6.8. Comparing the numerical and experimental modes after connecting tower with full height of adjacent buttresses.	223
Table 6.9. Comparing the numerical and experimental modes after reducing the modulus of elasticity of the buttresses.	224
Table 6.10. Comparing the numerical and experimental modes after using elastic foundations.	226
Table 6.11. Comparing the numerical frequencies with the dynamic tests and the dynamic monitoring frequencies.	228
Table 6.12. Confirmation of the initial correlation using D_f values.	232
Table 6.13. Confirmation of the initial correlation using MAC values.	232
Table 7.1. Properties of the different materials in the FE model.	237
Table 7.2. Chosen values for the sensitivity analysis*.	260
Table 7.3. Weights, lever arms and virtual displacements of the west and east facades mechanisms.	265
Table 7.4. The calculated parameters for the two mechanisms.	265
Table 7.5. Details of the combination of earthquake records compatible with the spectrum of each code and return period.	270
Table 7.6. The number of considered modes and the corresponding cumulative mass participation (%).	274
Table 7.7. Control points displacements from pushover ($\pm X$) and nonlinear dynamic analyses.	276
Table 7.8. Control points displacements from pushover ($\pm Y$) and nonlinear dynamic analyses.	278
Table 7.9. The performance displacements D_p (cm) and the performance load multiplier LM_p (a (g)) for the different control points.	281

CHAPTER 1

INTRODUCTION

1.1 Introduction

Historical structures are very important elements of the world heritage as cultural resources involving important artistic, spiritual, technical and scientific merits. They contribute to the identity of cultures and countries and provide valuable documents on the great achievements from the past. Moreover, they represent important economic resources. For these reasons and many others, modern societies allocate great technical and economical effort to the conservation of their architectural heritage. Nevertheless, the preservation of the architectural heritage faces significant challenges ranging from the difficulty in understanding the historical construction materials to the complexity of possible actions influencing on it. It is needless to say that adopted criteria in modern codes are hardly applicable to such class of buildings.

When assessing the safety of a historical structure, the first problem to face, in many cases, is the limited information available about the different aspects of the structure (construction history, used construction techniques, collapses due to previous seismic events, etc.). In order to overcome these limitations, a successful assessment approach should be based on combining and making use of the different investigation activities that may increase the level of knowledge about the historical structure. These activities include, among other possibilities, the historical investigation, the inspection (including laboratory and in-situ experiments), the monitoring and the structural analysis.

This research aimed at contributing to the seismic assessment of large masonry historical structures through the application of a methodology in which a number of investigation activities are employed in an integrated way. The cathedral of Mallorca, as a good example of large and interesting historical buildings, has been studied as a real case.

1.2 Motivations

Nowadays, the cultural heritage, including monuments and historical centers, is a powerful attractor for cultural tourism and can contribute very significantly to economic development. For instance, in 2012 the tourists that visited Spain generated an income of about 55608 million € (Ministry of industry, energy and tourism, 2012). It is interesting to find that more than the half of those tourists came for cultural interests (Ministry of industry, energy and tourism, 2012). More specifically, in the same year and, for the region of Andalusia (south of Spain), known for its rich cultural heritage, the income from cultural tourism was around 3000 million € (Government of Andalusia, 2013). In the same year, an

important monument, the Alhambra of Granada, produced alone about 25 million € (Board of the Alhambra and Generalife, 2012).

Conservation of historical structures faces the challenge meant by the fact that a large part of the world heritage is located in seismic regions, including Italy, Greece, Turkey, and China, among other countries with abundant architectural heritage. A large number of master pieces of human heritage structures have been destroyed by catastrophic earthquakes. Due to the earthquake of Lisbon 1755, the two thirds of the city became uninhabitable, and about 35 churches, 65 convents, 33 palaces, the Royal library, the Patriarchal Palace and the Arsenal were ruined (Pereira, 2009). More recently, the inspections carried out immediately after the L'Aquila 2009 earthquake revealed that more than 50% of the cultural heritage buildings were in critical conditions and could not be used (Dolce, 2009). Obviously, historical structures need to be seismically assessed and protected in order to ascertain its survival in the long term. In specific for large historical masonry structures, even when they are located in low to moderate seismic intensity zones, their vulnerability is of concern because of their extraordinary dimensions and, in some cases, their audacious structural design characterized by long span roofing elements and very slender vertical supporting elements.

Currently, the usage of numerical models to assess the seismic safety of historical structures is gaining increasing interest. However, these models need a significant amount of information for their preparation. The use of inspection techniques such as coring, flat jack tests, thermovision, sonic tomography, etc. is not enough, in some cases, to obtain all the desirable information due to the variability of the materials and the influence of previous alterations and repairs. In general and especially when the information gathered to build the model is judged too limited, the models have to be validated, at the global level, by comparison with experimental evidence. This validation can be carried out by comparing the predictions of the model with results obtained related to the performance of the structure under known mechanical or environmental actions.

In addition to the local inspection techniques, monitoring may be useful for the calibration and validation of models due to its ability to provide empirical information on the response of the structure. Among the monitoring techniques that can be used for this purpose are the dynamic identification tests, carried out punctually, and the static or dynamic monitoring systems, oriented to record the response of the structure during a certain period of time. The rapidly increasing advances in the technological aspects of these monitoring techniques have made them very attractive as a tool for the study of

historical structures. In fact, and prior to their application to historical structures, these techniques have been utilized for long time in modern civil engineering structures and especially in bridges and other important infrastructures.

The joint application of numerical modeling and monitoring requires for procedures and criteria allowing combining both of them into an integrated methodological approach. Such integrated approaches are intended to base the structural assessment on a sufficient knowledge of the historical structure. In turn, a detailed knowledge of the structure and the causes of its damage are essential in order to define possible repair or strengthening interventions granting the structural performance required while causing the minimum alteration to it, as required by modern conservation principle. The present research has been developed aiming at contributing to this topic.

1.3 Objectives

1.3.1 General objectives

The overall objective of this research is to evaluate the applicability of a general methodology for the seismic assessment of large historical masonry structures based on the combined use of experimental and numerical approaches. The methodology adopted is composed of a number of integrated investigation activities encompassing inspection, monitoring, numerical modeling and seismic analysis. The reliability and applicability of the methodology investigated is evaluated through its application to Mallorca cathedral, one of the largest built medieval structures in Europe, as an example of a large and complex historical construction.

1.3.2 Specific objectives

To achieve the general objective of the research, the following specific objectives have been considered:

- to review the state-of-the-art about dynamic identification and monitoring of historical structures, modal parameters identification, infrared thermography, numerical models updating, historical masonry properties, seismic assessment of historical structures and the applications of the previously mentioned items to real case studies;
- to select and validate technologies and strategies for dynamic identification and monitoring of large masonry historical structures including types of response

transducers, locations of measurements, parameters to be measured and other variables;

- to investigate the possibilities and utility of continuous dynamic monitoring in the study of large masonry historical structures;
- to study the influence of environmental effects on the modal parameters of historical structures. In particular, to investigate the influence of temperature on the dynamic properties of the historical structure;
- to show the application of numerical models in decision taking regarding dynamic identification and monitoring strategies;
- to propose an approach for model updating using information acquired from dynamic investigations;
- to transfer the experience gained from the above objectives into methodological considerations that could be applied to other historical structures;
- to draw conclusions on the investigated methodology regarding its real applicability to the assessment of large historical structures.

1.4 Outline of the thesis

The thesis is organized into the following chapters:

- **Chapter 1** introduces the research and presents its general and specific objectives;
- **Chapter 2** presents a literature review carried on different subjects relevant to the current research. The reviewed items are the dynamic identification of historical structures, the dynamic monitoring of historical structures, the modal parameters identification, the infrared thermography, the updating of finite element models of historical construction, the historical masonry properties and finally the seismic assessment of historical structures;
- **Chapter 3** reports the previous studies that have been carried out on Mallorca cathedral. These studies have addressed aspects such as the history of construction, the seismic assessment, the investigation of the soil underneath the cathedral and previous static and dynamic monitoring programs, among others;
- **Chapter 4** discusses the dynamic identification of Mallorca cathedral. Different aspects of the process including the design of the tests, the processing of the tests' data and the obtained results are presented;
- **Chapter 5** addresses the results of the dynamic and thermography monitoring systems installed in Mallorca cathedral. The relation between the environmental actions and the

modal parameters of the structure are discussed. The integration between the two systems is addressed;

- **Chapter 6** describes the validation and updating of the numerical model of the cathedral based on the results of the two previous chapters;
- **Chapter 7** presents the seismic assessment of the cathedral using the updated numerical model. The results of the nonlinear static and dynamic analyses as well the kinematic limit analysis are shown. The seismic safety of the structure is discussed;
- **Chapter 8** offers a set of methodological considerations derived from the study of Mallorca cathedral and the application of dynamic investigations, model updating and seismic assessment;
- **Chapter 9** presents the main conclusions emerged from the research and possible suggestions for future lines of investigation.

CHAPTER 2

STATE-OF-THE-ART

2.1 Introduction

This chapter presents the literature review carried out to cover the current state-of-the-art of the different topics relevant for the present research. The covered topics are: the dynamic investigation of historical structures which includes the dynamic identification tests and the dynamic monitoring, the modal parameters identification with the classical and the advanced techniques like the peak picking and the stochastic subspace identification, the application of the infrared thermography technique to heritage buildings, the updating of the numerical models of historical structures, some of the properties of materials of the historical masonry and the seismic assessment of historical structures.

2.2 Dynamic identification of historical construction

2.2.1 Motivations

Dynamic investigation of structures, whether modern or historic, includes two interconnected activities: dynamic identification and dynamic monitoring. Usually before installing a dynamic monitoring system in a structure, dynamic identification tests are first carried out. In some cases, due to economic reasons for instance, only the first activity is performed and can provide acceptable insight about the dynamic characteristics of the structure under study. The dynamic investigation of modern civil engineering structures started long time before the systematic investigation on historical structures. Therefore, a brief about the motivations for dynamic investigation of this type of structures is first given. Then, the objectives of performing dynamic identification of historical structures are discussed. In a following section, the dynamic monitoring of historical structures is discussed.

In recent decades, interest in the dynamic performance of civil engineering structures has increased significantly with the inevitable trend towards taller, longer, more slender, and more light weight structures that are increasingly vulnerable to dynamic excitation. Such excitation can arise from a wide variety of sources, such as earthquakes, wind, traffic, and human activities. Also, it is becoming increasingly important to guarantee that the structure dynamic response is adequate for many reasons like improving comfort for human occupants under the effect of wind oscillations in service, or ascertaining a satisfactory strength performance under the effect of earthquakes and hurricane wind. As a result, there is a clear need to carry out dynamic

investigations of a wide range of structures to characterize accurately their inherent structural dynamic properties and to understand better their response to real-world actions. So far, the key reasons for dynamic investigation of modern structures seem to be the following: to test and/or monitor existing structures to find out whether their performance falls within particular criteria (performance evaluation); to monitor existing structures to detect signs of damage or deterioration (structural health monitoring); to carry out testing/monitoring on a research basis to understand better the dynamic properties and performance and consequently propose guidance for improved future modeling and/or design; and to troubleshoot existing structures that have shown to be problematic. (Reynolds, 2008)

When moving to historical structures, dynamic identification tests are carried out to achieve some or all of the following aims (D10.4-NIKER, 2012):

- to obtain information on the global dynamic behavior of the structure, including natural frequencies, mode shapes and damping coefficients,
- to validate and update a structure's numerical model by comparing experimental and numerical natural frequencies and mode shapes,
- to assess the level of connection between different parts. In specific, assess the level of connection between parts partially separated by cracks,
- to identify weak structural features,
- to appraise the influence of major damage on the structural response,
- to evaluate the effect of possible repair and strengthening solutions by comparing the dynamic parameters before and after the intervention and hence improving the design for future applications in other similar structures,
- to allow monitoring before (diagnosis phase) and after the intervention (post-intervention control phase) by repeating periodically the dynamic tests and comparing the results, and
- to help in the optimal selection of strategic locations of sensors for the following activity, if needed, of dynamic monitoring.

2.2.2 Testing methods

To experimentally identify the dynamic characteristics of a structure, two methods are available: Forced Vibration Testing (FVT) and Ambient Vibration Testing (AVT) (Cantieni, 2005). In this section, the two methods are referred and a comparison between both is provided.

2.2.2.1 Forced vibration testing (FVT)

In Forced Vibration Testing (FVT) the structure is artificially excited with a forcing function $x_i(t)$ in a point (i) and its response $y_k(t)$ at point (k) to this excitation is measured together with the forcing function, Figure 2.1 (a). Transformation of these time (t) signals into the frequency (ω) domain and calculation of all Frequency Response Functions (FRF's) between the response and the forcing function time signals yields the Frequency Response Matrix (H), Figure 2.1(b). This matrix contains all the information necessary to determine the dynamic natural properties of the structure (natural frequencies, mode shapes and damping coefficients). The test can be done by keeping the excitation point constant and rove the response points over the structure or vice versa. Because it is not so easy to move the excitors used in civil engineering investigations, the first method is preferred. In mechanical engineering, where the structures to be tested are comparatively smaller and easy to excite, e.g. with a hammer, the second method is more common. (Cantieni, 2005)

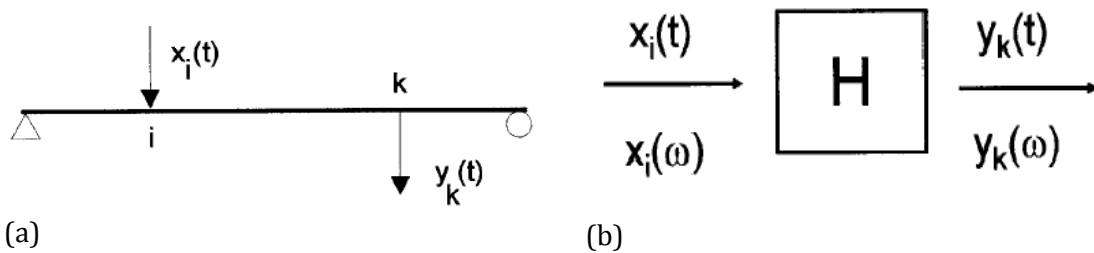


Figure 2.1. Basics of FVT: (a) testing scheme; and (b) calculation of the Frequency Response Matrix (H) (Cantieni, 2005).

Since the first practical applications until now, the testing equipment and the algorithms for data processing have evolved significantly. As a result, it is currently a well-established field founded on solid theoretical bases extensively documented in reference books and largely used in practice, particularly in aerospace and automotive industries. A lot of relevant applications are documented in the issues of the Mechanical System and Signal Processing Journal (MSSP) published during the last 25 years and in the proceedings of the International Modal Analysis Conference (IMAC), an annual conference organized since 1982 (Magalhães and Cunha, 2011). For more about FVT, interested reader may refer to Heylen and Sas (2006); Ewins (2000a); Ewins (2000b); Maia and Silva, (1997); McConnell and Varoto (1995).

2.2.2.2 Ambient vibration testing (AVT)

No artificial excitation is used in Ambient Vibration Testing (AVT). Instead, the response of the structure to ambient excitation is measured. For civil engineering structures, ambient excitation can be wind, traffic, seismic micro-tremors, etc. The more broad-band the ambient excitation, the better the results. Otherwise, there is some risk that not all natural frequencies of the structure are excited. Compared with the FVT, the information resulting from the force input signal $x_i(t)$ with FVT method is replaced with the information resulting from the response signal $y_R(t)$ measured in a reference point R then the matrix H is calculated, Figure 2.2 (a). Concerning response measurement requirements, the same basic rules apply as for FVT investigations. It is wise to use more than one reference point unless the structure to be tested is very simple. If response measurements are three-dimensional, at least one 3D-point has to be chosen as a reference. The risk of the reference point sitting in the node of a mode can be reduced significantly by choosing more than one reference point. As a rule of thumb, the length of the time windows acquired should be 1000 to 2000 times the structure's fundamental period. (Cantieni, 2005)

AVT permits the dynamic assessment of structures without disturbing their normal operation. Furthermore, as structures are characterized using real operation conditions, in case of existence of nonlinear behavior, the obtained results are associated with realistic levels of vibration and not with artificially generated vibrations, as it is the case when FVT is used. Nevertheless, as the level of excitation is low, very sensitive sensors with very low noise levels have to be used and even so, one should expect much lower signal to noise ratios than the ones observed in FVT. (Magalhães and Cunha, 2011)

In AVT the modal information is derived from structural responses (outputs) while the structure is in operation. Therefore, this identification process is usually called operational modal analysis (OMA) or output-only modal analysis. As the knowledge of the input is replaced by the assumption that the input is a realization of a stochastic process (white noise), the determination of a model that fits the measured data is also named stochastic system identification (Magalhães and Cunha, 2011). The first software package to extract modal parameters from AVT investigations was developed in the early nineties of the last century. Today, there are several packages on the market making use of the frequency domain procedures shown schematically in Figure 2.2(b). However, the most recent signal processing tools are not based on an analysis in the frequency domain but alternatively in the time domain. Stochastic Subspace Identification (SSI) is a method working completely in the time domain. Basically, a multi-order model is looked for which

synthesizes the measured time signals in an optimum way. This method has especially been developed for AVT investigations (Cantieni, 2005). Detailed information about identification of structure modal parameters is given in section 2.4.

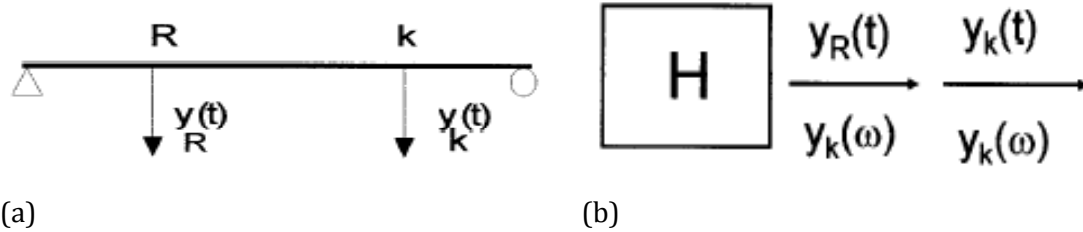


Figure 2.2. Basics of AVT: (a) testing scheme (R is a reference point and k is a moving point); and (b) calculation of the cross relationship between R and k signals (Cantieni, 2005).

2.2.2.3 FVT versus AVT

The main advantage of FVT is the fact that this method provides scaled results. Because the input force is measured, information on the mass and stiffness matrices of the structure is gathered. In AVT, modal masses are not estimated, or mode shapes are not scaled in absolute sense, unless additional tests with extra masses over the structure are performed (Cantieni, 2005 and Parloo et al., 2002). This allows automated updating of finite element models in case of FVT, whereas; model updating using the results of an AVT investigation is possible with manual techniques only (Cantieni, 2005). AVT has a disadvantage that the frequency content of the excitation may not cover the whole frequency band of interest, especially in the case of very stiff structures with high natural frequencies (Parloo et al., 2002). In AVT, the expected range of acceleration values is $10^{-7}g$ to $10^{-4}g$ and this low level of excitation only gives relevant information on the elastic behavior of the structure (Michel et al., 2008). Also, in AVT ambient excitation being non-controllable usually results in a lack of stationarity. This may lead to problems due to the non-linearity of the structure. In case of the excitation amplitude being significantly different for each of the setups, a certain scatter in the results may occur. This is not the case for FVT where the structural vibrations induced can be kept stationary (Cantieni, 2005). In historical masonry structures, the existence of cracks is an important source of non-linearity in dynamic behavior even under low excitation levels.

The main advantage of AVT is the fact that no artificial excitation is necessary. This makes such tests comparatively cheap. In addition, AVT investigations can be performed without embarrassing the normal user. This fact is very important for certain structures like highway bridges. In AVT, the excitation is of the so-called multiple-input type. Wind, traffic, micro-tremors, etc are acting on many points of a structure at the same time. In the

contrary, a forced vibration is usually of the single-input type. For small structures, this difference is not important. For large and complex structures, AVT has hence an advantage on the excitation side (Cantieni, 2005). See also Brincker et al. (2003a) for advantages of AVT. Summarizing, Table 2.1 provides a comparison between the pros and cons of the two methods: AVT and FVT.

Table 2.1. AVT versus FVT (adapted from Dai et al., 2013).

Method	Advantages	Limitations
AVT	<ul style="list-style-type: none"> – Few equipments and operators – Quick and cheap – Tests realized while structure is in service 	<ul style="list-style-type: none"> – Excitation input unknown – Insufficient excitation of modes – Stationary white noise excitation assumption – Heavy noise treatment in data processing
FVT	<ul style="list-style-type: none"> – Better signal to noise ratio – Control of input – Excitation of many modes – More accurate results 	<ul style="list-style-type: none"> – Heavy equipment – Expensive – Time consuming

2.2.3 Equipments

2.2.3.1 Excitation Mechanisms

In small and medium-size structures, the excitation can be induced by an impulse hammer similar to those currently used in mechanical engineering, Figure 2.3(a). This device has the advantage of providing a wide-band input that is able to stimulate different modes of vibration. The main drawbacks are the lack of energy to excite some relevant modes of vibration and the relatively low frequency resolution of the spectral estimates which can preclude the accurate estimation of modal damping factors. As a result and specifically designed to excite bridges, some laboratories have built special impulse devices, Figure 2.3(b). An alternative, derived from mechanical engineering, is the use of large electrodynamic shakers (Figure 2.3(c)), which can apply a large variety of input signals (random, multi-sine, etc.). The shakers have the capacity to excite structures in a lower frequency range and higher frequency resolution. The possibility of applying sinusoidal forces allows for the excitation of the structure at resonance frequencies and, consequently, for a direct identification of mode shapes. (Cunha and Caetano, 2006)

For large civil engineering structures, the controlled excitation requires the use of heavy excitation equipment. One option frequently used in the past in dynamic testing of dams was the eccentric mass vibrator (Figure 2.3(d)), which enables the application of sinusoidal forces with variable frequency and amplitude. The main drawbacks of this technique are low force amplitude induced at low frequencies, some difficulty in measuring the applied force, and restraining relative movement of the vibrator with regard to the structure. A better option, in terms of providing a wide-band excitation over the most interesting frequency range for large civil structures, is the use of servo-hydraulic shakers. For example, in Figure 2.4 two shakers of this type built at EMPA (Swiss Federal Laboratories for Materials Testing and Research for Industry, Construction and Commerce) are shown, they are used to excite bridges or dams vertically and laterally. (Cunha and Caetano, 2006)

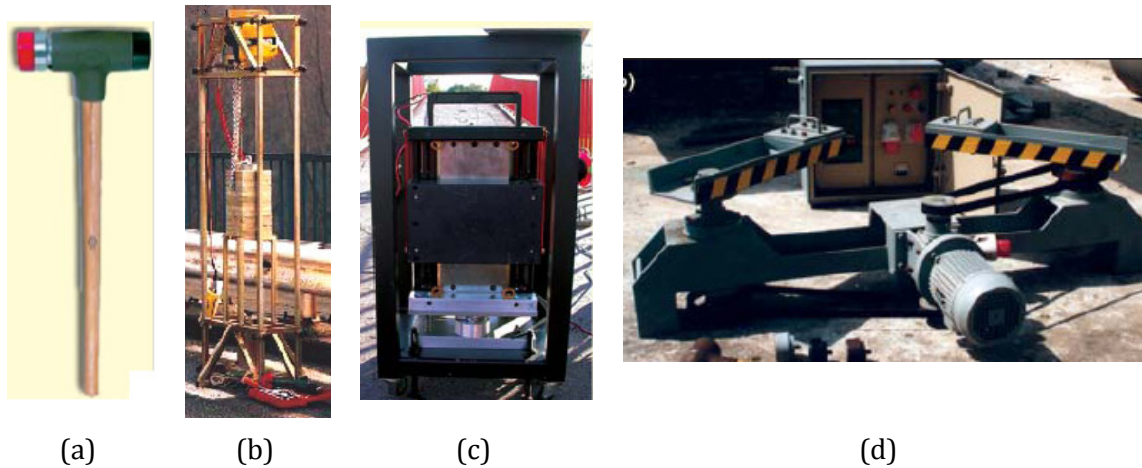


Figure 2.3. Excitation mechanisms: (a) Impulse hammer; (b) impulse excitation device for bridges (K.U. Leuven); (c) electrodynamic shaker over three load cells; and (d) eccentric mass vibrator (adapted from Cunha and Caetano, 2006).

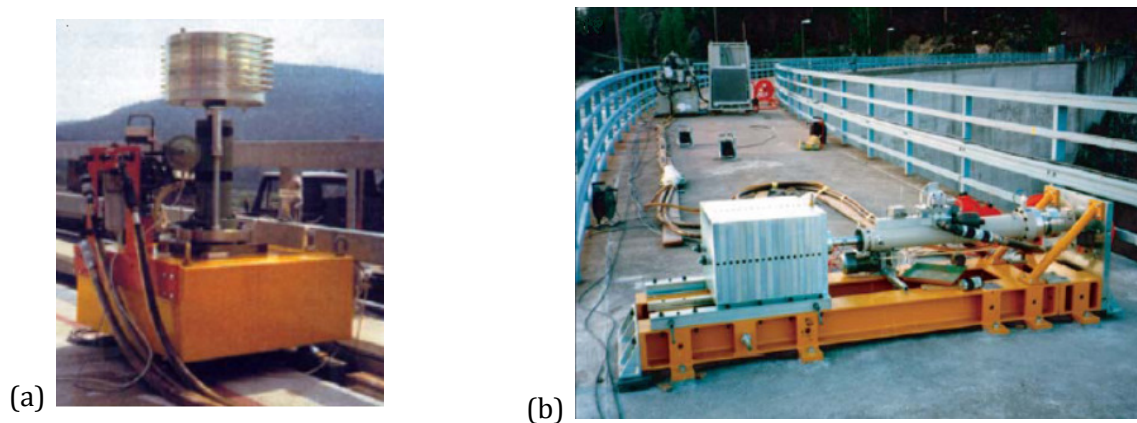


Figure 2.4. Servo-hydraulic shakers to excite: (a) bridges (vertically); and (b) dams (laterally) (EMPA) (adapted from Cunha and Caetano, 2006).

Some of other references that give more details on the subject are Pusey (2008) who follows the development of excitation mechanisms since the 50's; Carne and Stasiunas (2006) examine some common and not so common excitation techniques like projectile impacts, explosive inputs, step relaxation, and base excitation; De Silva (2007) provides a guiding on how to choose a shaker for a certain application; Underwood and Keller (2008a; 2008b) discuss newly developed multi shaker for testing large structures and Salawu and Williams (1995) reviews the state-of-the-art on the excitation techniques of bridges.

2.2.3.2 Accelerometers

a) Basics

Accelerometers are specific types of sensors. A sensor is a device that converts the physical variable input, like acceleration in case of accelerometers, into a signal variable output, like current, voltage, light, etc. The output signal variables can be manipulated in a transmission system (electrical or mechanical circuit) and then transmitted to a recording device (data acquisition system). (Eren, 1999)

Generally, accelerometers are preferred over displacement and velocity sensors for many reasons. First, they have a wide frequency range from zero to very high values and therefore, steady accelerations can easily be measured. Second, Acceleration is frequently needed since destructive actions (earthquakes for instance) are often related to acceleration rather than to velocity or displacement. Third, Measurement of transients and shocks can readily be made, easier than with displacement or velocity sensing. Fourth, displacement and velocity can be obtained by simple integration of acceleration by electronic circuitry; integration is preferred over differentiation (Eren, 1999). Nevertheless, for low frequency response cases (for example, civil engineering structures) measuring displacements may be better, while for higher frequency components (for example, machinery) acceleration measurements are more adequate. In specific for civil engineering structures, measuring displacements requests all sensors to be related to an external reference point, however, it is frequently costly to do it (Caetano, 2000; Ramos, 2007). Therefore, accelerometers are usually preferred to measure the dynamic response due to their relatively low cost and high sensitivity (Cunha and Caetano, 2006).

b) Types

Accelerometers can be classified in a number of ways, for instance, deflection or null-balance types, mechanical or electrical types, dynamic or kinematic types. A large

number of practical accelerometers, in specific those used in vibration and shock measurements, are deflection types. The general configuration of this type is shown in Figure 2.5. As can be seen, the seismic mass is suspended by a spring or cantilever inside a rigid frame which is connected to the vibrating structure. When vibrations take place, the mass tends to remain fixed so that relative displacements can be measured. They are manufactured in many different types and sizes and they exhibit diverse characteristics. Although their principles of operation are similar, they only vary in minor details, such as the spring elements used, types of damping provided, and types of relative motion transducers employed. (Eren, 1999)

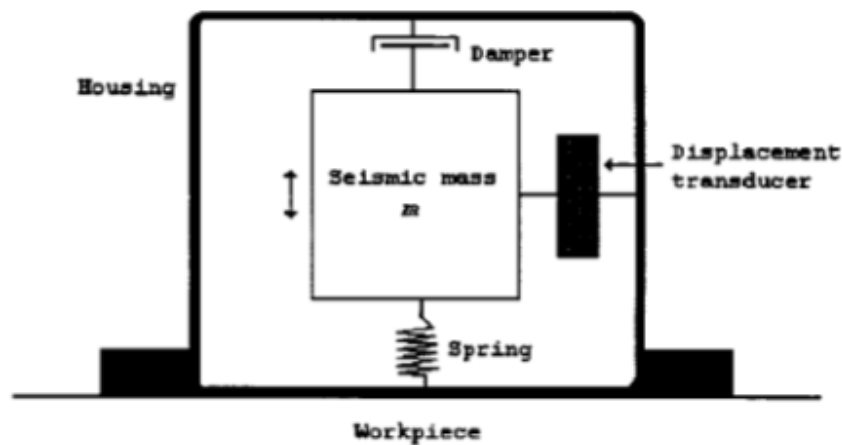


Figure 2.5. A typical deflection-type seismic accelerometer (adapted from Eren, 1999).

Eren (1999) detailed nine types of accelerometers. Those are: electromechanical force-balance; piezoelectric; piezoresistive; differential-capacitance; seismic; strain-gage; inertial; micro accelerometers and electrostatic force feedback accelerometers. Interesting information about the history of evolution of some of these accelerometers is given by Walter (1997, 1999 and 2002). In the following, some of these types are referred because either they are the ones used in the present experimental work, or they have been already used in the dynamic identification of historical construction.

Electromechanical force-balance accelerometers: they depend on the principle of feedback. An acceleration-sensitive mass is kept very near to a neutral position or zero displacement point by sensing the displacement and then feeding back this displacement. When the mass is displaced from the neutral position, a proportional magnetic force is generated to oppose the motion, thus restoring neutral position — just as a mechanical spring in a conventional accelerometer would do, see Figure 2.6. The advantages of this

approach are the better linearity and elimination of hysteresis effects as compared to mechanical springs. Also, in some cases, electric damping can be provided. (Eren, 1999)

Electrostatic force feedback accelerometers: the aim in this type is to counteract the effect of the ground motion inertial force by producing another force that acts on the accelerometer mass to keep it still. This controlled external force changes in intensity and direction. Figure 2.7 shows a schematic configuration of this accelerometer. In the figure, the force is produced by electronically controlled (via a control circuitry) force transducer. The displacement transducer feeds the position of the mass to the control circuitry which in turn adjusts the force produced by the force transducer to move the mass back to its equilibrium position.

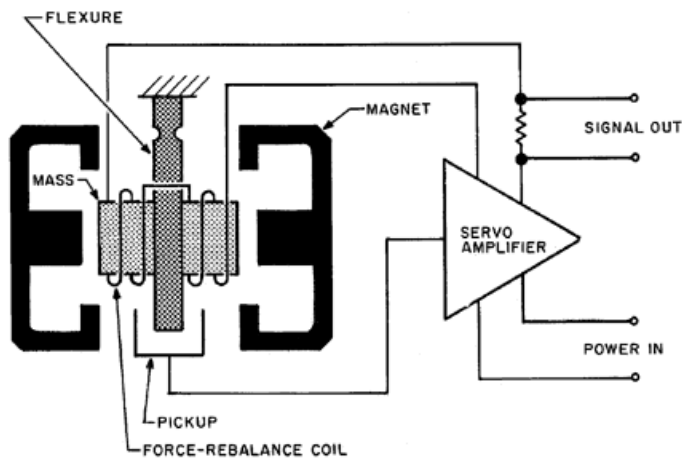


Figure 2.6. Left: schematic of the force-balance accelerometer (Wilson, 1999a). Right: Titan force-balance accelerometer (www.nanometrics.ca).

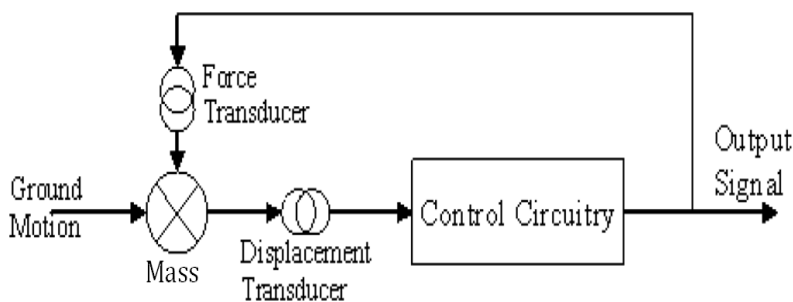


Figure 2.7. Left: the general force feedback control system (Stuart-Watson, 2006). Right: CMG-5T feedback accelerometer (www.guralp.com).

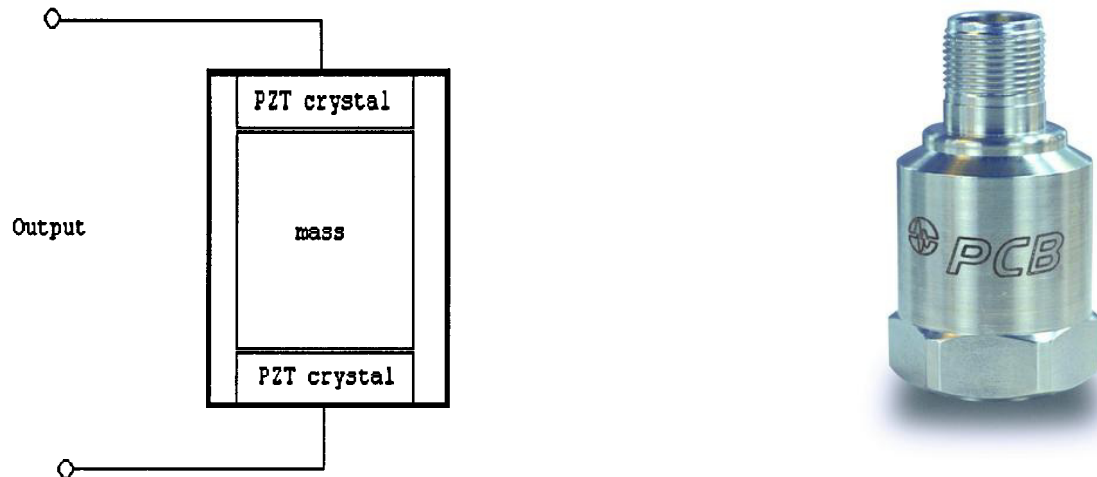


Figure 2.8. Left: A compression-type piezoelectric accelerometer (Eren, 1999). Right: 393B12 piezoelectric accelerometer (www.pcb.com).

By monitoring the electronic control signal of the force transducer, a measurement can be obtained which indicates how much force is required to balance the inertial force. The inertial force on the mass is a good indication of the ground motion and the electronic control signal is a good indication of the inertial force. Therefore, the electronic control signal can effectively be used as a measure of the ground motion. (Stuart-Watson, 2006)

Piezoelectric accelerometers: these devices use a mass in direct contact with the piezoelectric component, or crystal, as shown in Figure 2.8. The crystal is under compression at all times, either by a mass or mass and spring arrangement. When a varying motion is applied to the accelerometer, the crystal experiences a varying force excitation resulting in a proportional electric charge to be developed across it. The electric charge is developed because the crystal has a regular crystalline molecular structure with a net charge distribution that changes when strained. These accelerometers have the advantage of being small in size and self-generating (do not require an external power source for operation); however, they demonstrate poor performance at low frequencies (Eren, 1999; Chu, 1987).

c) Selection criteria of an accelerometer for a certain application

For real-life applications, accelerometers can be classified into two main groups. The first group is for the general-purpose accelerometers. The second group is for the accelerometers that have characteristics targeted toward a particular application. In deciding the application type (general or special purpose) and the accelerometer to be used, the following characteristics should be considered. (Eren, 1999)

The frequency range: it is the range in which the accelerometer is useful for vibration measurement (Sinha, 2005). As a rule of thumb, the upper frequency limit for

the measurement can be set to 1/3 of the accelerometer's resonance frequency such that the measured vibrations will be less than 1 dB in linearity (Eren, 1999). Linearity is defined as the accuracy of the measured acceleration amplitude in the measuring frequency range (Sinha, 2005). The lower measuring frequency limit is determined by the low-frequency cut-off of the associated preamplifiers, and the effect of ambient temperature fluctuations to which the accelerometer would be sensitive (Eren, 1999). The accelerometers specifications sheet should have a typical frequency response curve illustrating how the accelerometer's accuracy varies over a specified frequency range (Lent, 2009).

The dynamic range: it is the difference between the smallest and largest accelerations that can reliably be measured by the accelerometer. The dynamic range of the accelerometer should match the high or low acceleration levels of the tested/monitored structures. (Eren, 1999)

The sensitivity: it relates the electrical signal (often in Voltage (V)) to the amplitude of vibration in acceleration (Sinha, 2005). Ideally, the higher the accelerometer sensitivity, the better; but trade-offs might have to be made for sensitivity versus mass (Eren, 1999). Higher sensitivity is achieved by using a softer mass-spring system that generates greater output at lower accelerations levels, nevertheless; the cost is having a lower resonance frequency. If the softer system is accomplished by increasing the mass, the accelerometer will be heavier. Higher sensitivity accelerometers tend to be unacceptably nonlinear at higher levels of acceleration because of the higher stresses on the sensor (Wilson, 1999b). As a general rule, the accelerometer mass should not be greater than 1/10 the effective mass of the part or the structure that is mounted onto for dynamic testing. This is because the accelerometer should not load the tested part, since additional mass can significantly change the levels and frequency presence at measuring points and invalidate the results, (Eren, 1999). Higher sensitivity can also be achieved by amplifying the signal from a low sensitivity sensor, but because the noise is also amplified, the signal-to-noise ratio is not improved (Wilson, 1999b).

Environmental conditions, such as temperature ranges need to be considered. Operating temperature affects sensitivity and the manufacturer's data should address this concern. The effect of temperature on the sensitivity of the accelerometer is called temperature sensitivity error or temperature response; some refer to it as temperature coefficients. Since most manufacturers do not supply individual temperature response

information with their accelerometers, separate calibration should be requested if this characteristic is critical for the application. (Wilson, 1999b)

2.2.3.3 Data acquisition systems

The task of a data acquisition (DAQ) system is the measuring and recording of a physical signal after it has been converted into the corresponding electrical signal by a transducer. A continuous time signal is also called an analog signal because its waveform is often analogous to that of the physical variable. On the other side, a discrete time signal with its amplitudes coded in binary form is called a digital signal. Although our real world is an analog one, many signals are now processed digitally because of many advantages of digital technique over analog technique. Therefore a main component of a DAQ system is the Analog-to-Digital Converter (ADC). (Chen, 2010; Vermariën et al., 1999)

A mathematical relationship conveniently shows how the number of bits an ADC handles determines its specific theoretical resolution: An n -bit ADC has a resolution of one part in 2^n . For example, a 12-bit ADC has a resolution of one part in 4,096, where $2^{12} = 4,096$. Thus, a 12-bit ADC with a maximum input of 10 V can resolve the measurement into $10 \text{ V}/4096 = 0.00244 \text{ V} = 2.44 \text{ mV}$. The resolution is usually specified with respect to the full-range reading of the ADC, not with respect to the measured value at any particular instant. (MC, 2005)

Signals need to be conditioned by some signal-conditioning components before they are converted to digital information. These components may be one or more of the following: amplifiers, filters, nonlinear analog functions, analog multiplexers, and sample-holds. In Figure 2.9, the interaction between all DAQ system components is shown. This is probably the most commonly used DAS configuration. The input to the system is a physical parameter, like acceleration, which is an analog quantity. This parameter is first converted into an electrical signal by means of a transducer, like accelerometer. After, the amplifier boosts the amplitude of the transducer output signal to a useful level for further processing. The output signals of a transducer may be of the level of microvolt or millivolt which is then amplified to 1 to 10V levels. The amplifier is frequently followed by a low-pass active filter that reduces high-frequency signal components, unwanted electrical interference noise, or electronic noise from the signal. The processed analog signal next goes to an analog multiplexer which switches sequentially between a number of different analog input channels. Each input is in turn connected to the output of the multiplexer for a specified period of time by the multiplexer switch. During this connection time, a

sample-and-hold circuit acquires the signal voltage and then holds its value while an ADC converts the value into digital form. The resultant digital word goes to a computer data bus or to the input of a digital circuit. Thus the analog multiplexer, together with the sample-and-hold, time shares the ADC with a number of analog input channels. The timing and control of the complete DAQ system is done by a digital circuit called a programmer sequencer, which in turn is under the control of the computer. (Sydenham and Thorn, 2005)

Finally, it should be noticed that frequently, only a plug-in DAQ board is considered in the data acquisition system; nevertheless, a board is only one of the components in the system. A complete DAQ system consists of transducers, signal conditioning, interface hardware, and software. (Vermariën et al., 1999)

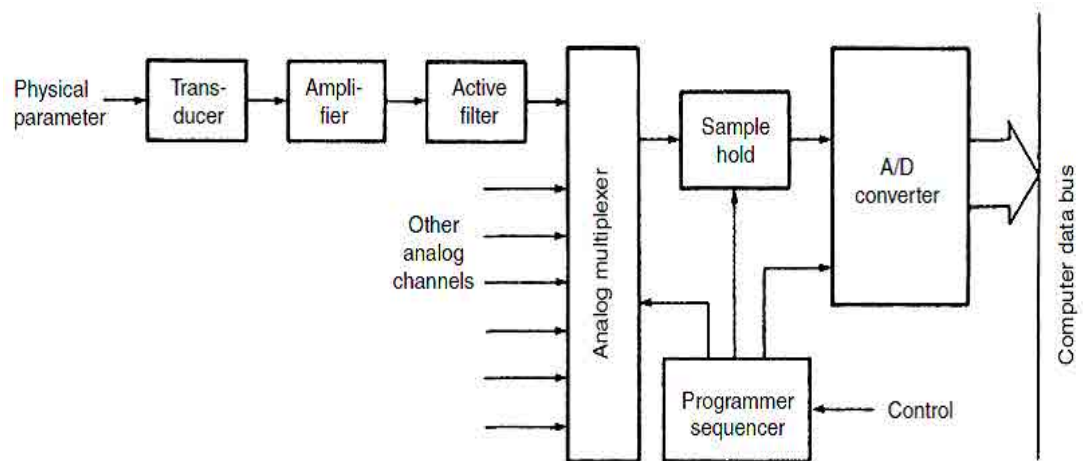


Figure 2.9. Data acquisition system (Sydenham, 1983).

2.2.4 Applications: from modern to historical structures

2.2.4.1 Pioneering studies on modern structures and future challenges

Ivanovic et al. (2000) presented a comprehensive review of AVT from its early applications in USA up till the end of the 90's. The following are very few examples from this review aimed at showing the development of application of this technique and the interested reader is referred to Ivanovic et al. (2000) for more details. In the early 1930's, the United States Coast and Geodetic Survey started measuring the fundamental periods of structures by AVT. In a period of about 4 years, AVT's were carried out on more than 340 structures in California and Montana. Some of these structures, like the Golden Gate Bridge, were being measured from time to time during construction. In Carder (1936a; 1936b; 1937), the found results and derived conclusions are discussed. Some 30 years later, Crawford and Ward (1964) and Ward and Crawford (1966) revived the interest in

this method and showed that it can be used to determine the lowest frequencies and modes of vibration of full-scale structures. Around 1970, reports about testing of full-scale structures by the AVT began to appear regularly, with about 75% of all contributions devoted to the experiments of buildings, dams, chimneys and silos, and about 25% devoted to bridges testing. For instance, Trifunac (1970a, 1970b) used wind and micro-tremor induced vibrations to test a twenty-two and a thirty-nine story steel frame buildings. Two years later, the same author compared the results of FVT on the same two buildings with the results of AVT and found that the results of both tests were consistent and comparable (Trifunac, 1972). Throughout the 1970's and the 1980's, AVT and FVT were used to compare small amplitude with larger amplitude response and to find the pre- and post-earthquake apparent frequencies of full-scale structures (Mulhern and Maley, 1973). Also, they were used to identify the three-dimensional nature of deformations accompanying the apparent frequencies of response (Moslem and Trifunac, 1986). During the 1990's, AVT's continued to contribute to in-depth studies of the changes in structural properties (Mendoza et al., 1991) and towards further development of structural identification methods (Kadakal and Yuzugullu, 1996).

In the last decade up till now, the AVT is attracting more interest and hundreds of publications are available yearly on the subject. Despite the already long history of AVT, there are still several issues that need further research. The use of sophisticated parametric system identification algorithms in civil engineering structures is recent and still needs to become more mature throughout the performance of more practical applications. In addition, the developments of the acquisition hardware have permitted to obtain with little effort large databases that have to be processed in an efficient way. Therefore, there is the need to develop and test processing methodologies suitable to deal with large quantities of data. (Magalhães, 2010)

2.2.4.2 Applications to historical construction

Applications of dynamic identification in the field of historical construction started decades after its use for modern structures. Next, some of the pioneering studies are first referred and then more recent studies are discussed.

a) Early studies in the 90's

Chiostrini et al. (1991 and 1992) tested a typical Florentine masonry building that was about to be demolished. They used FVT employing a vibrodine. The amplitude of excitation was raised until structural damage and partial collapse of some elements were

produced. The first four experimental natural frequencies were determined and used to update a FE model of the structure. In the beginning of the 90's Aya Sofya in Istanbul was tested using AVT method (Durukal, 1992; Erdik et al., 1993). The tests were carried out using four uniaxial Kinematics SS-1 seismometers in 15 setups with measurement time about 1 to 2 minutes for each. The first 11 natural frequencies and mode shapes were identified using basic spectral analysis calculations. Tzenov and Dimova (1992) carried out AVT on a Bulgarian church from the 6th century that had suffered several structural problems along its history, in specific, developed alarming cracks in the columns. The AV was caused by a car passing over an obstacle. They used 7 Kinematics SS-1 velocimeters and performed 7 setups. The sensors were placed in meaningful measurement points based on preliminary investigation and building particularities. They concluded from the obtained mode shapes that (1) the connections between bearing walls were not sufficient; (2) the cracks had clear influence on the dynamic behavior; (3) the foundation characteristics were not identical under the different parts of the church.

Modena et al. (1997) carried out the dynamic identification of the roman amphitheatre (Arena) of Verona using FVT beside AVT. The overall structural behavior of the wing, and particularly its interaction with the main body of the amphitheatre was analyzed. Using FVT, it was possible to identify the first eight natural frequencies. For AVT, however, the authors found that electrical resonance of the acquisition system, which is not negligible for low intensity signals, makes unfortunately unreliable the frequency responses. Nevertheless, it was shown that at least qualitative comparison between theoretical and experimental responses were possible. They commented that although the FVT results were more accurate than the AVT, the application of FVT is rather difficult and costly because of the need of installing and removing of appropriate scaffolding to access the excitation points. Some years later, using only AVT the Arena wing was tested again by Lorenzoni et al. (2013). The average error in identified natural frequencies between the old and the new tests were found to be not more than 7,3%. It should be commented on this case study that the today available data acquisition technology can overcome the encountered problem in the tests of 1997 because this new technology is characterized by ultra-low self noise performance.

Some other examples of pioneering studies include masonry buildings (Capecchi et al., 1990; Angotti et al., 1992; Salstan and Foissner, 1995; Vestroni et al., 1996; Genovese and Vestroni, 1998; Sigmund and Herman, 1998); masonry bridges (Armstrong et al., 1995; Bensalem et al., 1995; Roca and Molins, 1997; Bensalem et al., 1998; Nasser, 2001);

stone masonry pinnacles (Ellis, 1998) and stone masonry columns (Llorens et al., 2001; Araiza, 2003).

b) Recent studies

With more advances in sensors technology and dynamic identification techniques, vibration testing is attracting more attention as a powerful tool in the investigation stage of historical structures and more research results are being published. Next, some of the recent studies are discussed.

The Gothic church of Fossanova in Italy was tested by AVT (De Matteis and Mazzolani, 2010; De Matteis et al., 2008). These tests were one of several investigation campaigns employed to study the structure and assess its seismic behavior. The DAQ system composed of three uniaxial seismometers, four channels signal conditioner system, and a two-channels frequency analyzer for processing recorded signals in frequency domain to obtain Fourier amplitude spectra. In total 25 points were selected for different setups, from which one point was selected as a reference for all setups. The measurements were taken on three typical bays of the church: R0, R4 and R7. On the central bay (R4) measurements were taken on both sides at four levels. On the other two bays (R0 and R7) data were acquired on one side only, see Figure 2.10. The two global mode shapes in the longitudinal and transversal directions, in addition to, the first torsional mode were successfully identified. The damping ratios were found between 5.5% and 7.5% of critical damping.

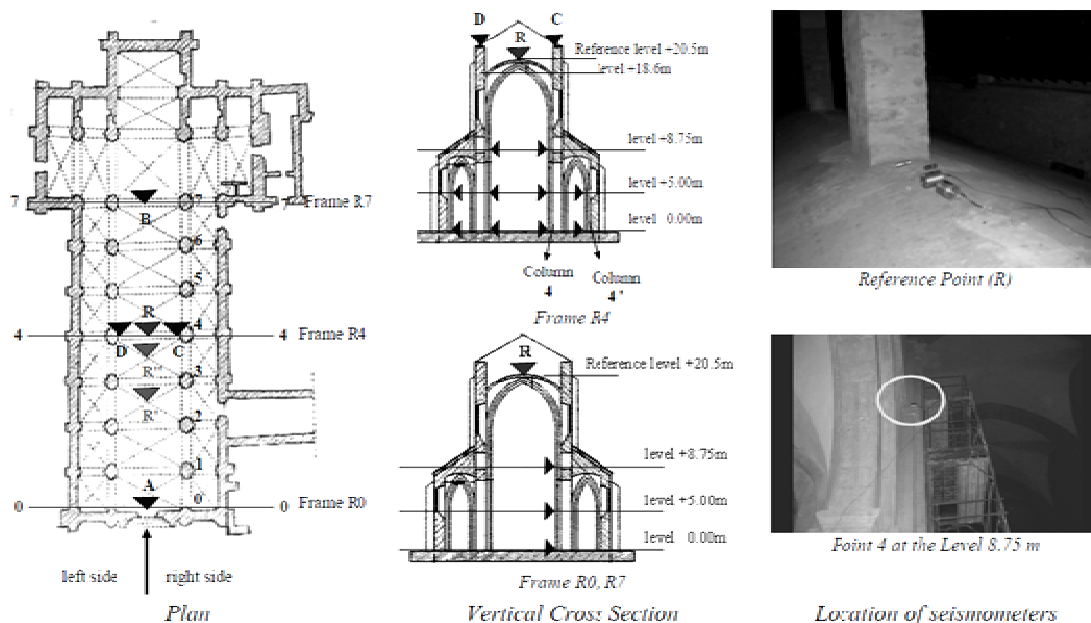


Figure 2.10. Setups of AVT of Fossanova church. Solid arrows show measurement points (De Matteis et al., 2007a).

Atamturktur et al. (2009) discussed FVT's conducted on five Gothic churches in UK, USA and Italy. The general objective of the research was to give recommendations for FVT of vaults of typical bays of such structures. The preliminary FE models showed that the vaults mode shapes were composed of diagonal symmetry and bending. The diagonal symmetry modes constituted vertical movements of the crown, while the bending modes primarily constituted symmetric movements of diagonal and orthogonal axes, Figure 2.11 (a). Therefore, a number of measurement points were selected at every one-third length on the main axes of the quadripartite vaults, Figure 2.11 (b). The excitation points were selected where the highest responses were expected, Figure 2.11 (b) and (d). In the planning phase of tests, the frequency range of the first 10-15 modes of the vaults were observed to be between 3.5-30 Hz. Therefore, an accelerometer with sensitivity of 1V/g was selected to be able to measure frequencies as low as 2-3 Hz, Figure 2.11 (c). Three different excitation mechanisms were used: the instrumented impact hammer (Figure 2.11 (d)), electrodynamic shaker, and heel-drop on instrumented force plate excitations.

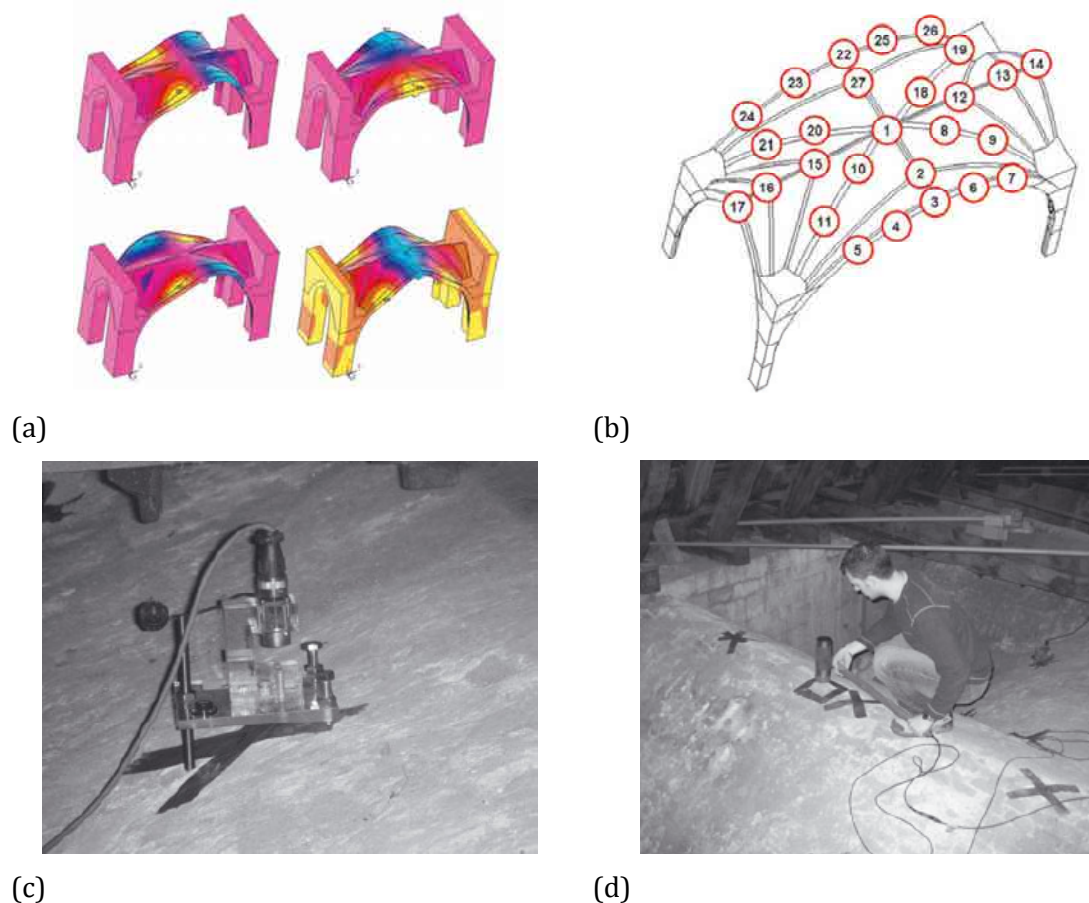


Figure 2.11. FVT of Gothic vaults: (a) preliminary FE mode shapes; (b) measurement and excitation points (1,3,12,18); (c) vertical positioning of accelerometers by adjustable screws of mounting cases; and (d) applying the hammer at excitation points (Atamturktur et al., 2009).

The authors discussed a number of quality checks to be completed on the immediate findings of the FVT which included: immediate repeatability check, linearity check and reciprocity check. The first was used to diagnose the effects of the ambient vibration on the FRF measurements. It was found that due to the massiveness of these structures, the different sources of ambient vibration were insignificant. The second and third checks aimed at discovering if the assumption of linear elasticity holds for the tested structures. The authors found that the second and third checks were satisfied as long as the excitation force is kept consistent throughout the test. For the tests setups, they commented that exciting the ribs is preferred to exciting the webbing because it reduced the difficulties in system identification due to the dominant local modes which occur when the webbing is excited.

Ramos et al. (2010a) carried out the dynamic identification of the main nave of the Gothic Monastery of Jerónimos in Lisbon. Two triaxial force balance accelerometers were used; one was a reference and the other was roving. 29 setups were carried in which the measurement points were located on strategic places to measure the nave boundaries and the global dynamic response of the structure. The Enhanced Frequency Domain Decomposition (EFDD) and the Stochastic Subspace Identification (SSI) methods were used and a comparison between both was made. No significant differences were found between the two methods as far as the natural frequencies were concerned. For the damping coefficients, differences up to 140% were observed due to the noise in the signals and the low excitation levels. The Modal Assurance Criteria (MAC) values were higher than 0,95 only for the first two mode shapes as a consequence of the difficulty in exciting this heavy structure. However, the authors commented that this modal identification was accepted because of the structural complexity of this structure. Also, the usage of two identification methods helped them in the validation and discussion of results.

The modal parameters of the historical large scale Reggio Emilia cathedral were identified using the AVT (Casarin and Modena, 2008; Casarin and Modena, 2006; Casarin, 2006). The identified mode shapes and natural frequencies were used then in updating a FE model and carrying out seismic assessment analysis. The measurements were taken at the structure's elements that were considered most characteristic from a dynamic point of view. Those are the dome, the facade dome lantern, and the upper part of the main nave. The acquisition system was composed of a compact unit with 24-bit digital acquisition modules, connected to piezoelectric uniaxial acceleration transducers. The acquisition time was about 11 minutes at a sample rate of 100 Hz which was appropriate because the

significant structural frequencies are between 0–10 Hz, i.e. the selected sampling times is about 10 times the highest frequency to be measured. The FDD method was used to extract the modal parameters. It was found that although several peaks appeared in the PSD, only few structural modes were satisfactorily detectable with coherence in the range of 0.8–0.9.

The famous Colosseum of Rome was tested by Pau and Vestroni (2008). The aim was to investigate the traffic effect on the safety of the structure and also to update its preliminary FE model. Based on initial FE modal analysis, the authors decided about the used instruments, their location and the parameters for data acquisition. Two setups of ambient vibration recordings were performed. In the first setup, 5 triaxial accelerometers were used with sampling rate of 500 Hz and measurement time of 20 min and the accelerations were measured in radial, circumferential and vertical directions. In the second setup, only radial recordings were measured using 6 uniaxial accelerometers with sampling rate of 200 Hz and 40 min of measurement. In addition, Impact vibration tests were carried out on the columns using an instrumented hammer. For the entire structure, the first six natural frequencies were satisfactory identified, whereas, only the first two mode shapes were satisfactory estimated.

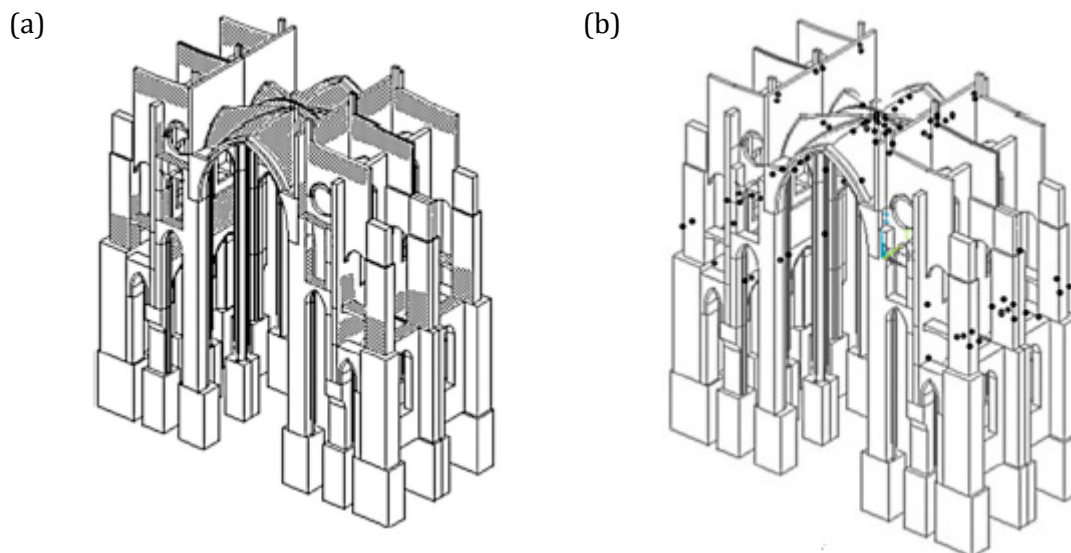


Figure 2.12. Choosing optimum sensor locations in Gothic cathedrals: (a) candidate locations are shaded; and (b) optimum locations as dots (Prabhu and Atamturktur, 2013).

An interesting research aimed at providing a methodology for choosing the optimum locations of sensors in dynamic identification tests of Gothic cathedrals with the application to St. John the Divine cathedral in Washington was presented by Prabhu and Atamturktur (2013) and Prabhu (2011). Optimal sensor locations were determined by

using a validated FE model of the cathedral's nave and a modified version of the Effective Independence Method (EIM) developed by Kammer (1991). In this methodology the following steps were applied: 1) a number of candidate locations were selected based on practical considerations like the easy access to these locations, Figure 2.12(a); 2) the global mode shapes that desired to be identified experimentally were selected from a modal analysis carried out using the validated FE model of the cathedral. The model was validated against the modal parameters deduced from FVT of one vault of the main nave and also by checking its capability to reproduce some visible cracks in the cathedral that are believed to be resulted from gravity loading only; 3) the candidate locations are reduced to an optimum number of sensor locations using the EIM after being modified by introducing a distance-based criterion so that the final optimal set of sensors is not clustered, Figure 2.12(b). The authors believe that their research presents a number of optimum regions suitable for sensor placement for similar Gothic cathedrals, and the use of these recommended locations is anticipated to reduce the necessary resources and to expedite the modal testing of similar structures.

In addition to the previously discussed case studies of dynamic testing of historic structures, some additional cases can be mentioned. These include the AVT carried on a historical basilica in Rome (Pau and Vestroni, 2013), a fortress in L'Aquila damaged by Abruzzo 2009 earthquake (Lorenzoni, 2013), a church in Portugal (Alaboz, 2009) and many historic buildings in Cyprus including a Gothic cathedral, a Byzantine church, ruins of a church and some schools (Votsis et al., 2013; Votsis et al., 2012; Lourenço et al., 2012a; Chrysostomou et al., 2013).

Finally, it is worthy to comment that the dynamic tests (also the identification process and the numerical model updating) are easier to carry out on some types of masonry historic structures. Those are the structures characterized by one predominant dimension, as for instance, arch bridges in which the longitudinal dimension is predominant and tall structures like bell towers in which the vertical direction is predominant. The dynamic behavior of these structures is simple compared to other types of structures like churches and large complex Gothic cathedrals. For case studies of dynamic identification of historical arch bridges, refer to Sena-Cruz et al. (2013); Pau and Vestroni (2011). For tall structures, see Corbi et al., (2013); Bayraktar et al. (2011); Aoki et al., (2008) ; Gentile and Saisi (2013) and Ivorra et al. (2011).

2.3 Dynamic monitoring of historical construction

2.3.1 Motivations

Similar to the dynamic identification, dynamic monitoring is carried out to achieve the following two objectives: to obtain information on the global dynamic behavior of a historical structure and to validate and update a historical structure's numerical model. In addition, dynamic monitoring may also aim at achieving the following purposes (D10.4-NIKER, 2012; D9.4-NIKER, 2012):

- to study the evolution of modal parameters in time, thus evaluating quantitatively the progression of the damage pattern (structural health monitoring),
- to study the influence of environmental climatic effects (temperature, humidity, etc.) on the dynamic parameters,
- to capture the dynamic response in the occasion of possible seismic events. The measured accelerations in this case are expected to be higher than those measured in AVT by several orders of magnitude. Thus, it helps to better characterizing the structure's modal parameters that may be unattainable from AVT like the damping ratios and the higher modes of vibration which are difficult to obtain under ambient vibrations only.
- to verify the effectiveness of any possible intervention. Before the execution, the dynamic monitoring can work as an early warning system to detect the need for any urgent intervention. During the execution, it can provide warning procedures contributing to the safety of the personnel involved. After the execution, by comparing the dynamic parameters before and after the intervention, it is possible to evaluate its effectiveness. In addition, it can be used to perform verification and long term control within a long-term maintenance program. This purpose is shown schematically in Figure 2.13. In the figure, the diagnosis reveals that the structure doesn't have the required seismic capacity. Therefore, an intervention is undertaken to increase the seismic capacity. The capacity may include some distinct increments if the intervention is applied incrementally. An evaluation phase follows to verify the efficiency of the intervention. The last and longest phase is the maintenance one during which the structure is monitored to verify the maintenance of the expected seismic capacity. Possible correction actions may be required if it decreases below the tolerable limit. At the end of the maintenance period, a new seismic assessment, with a possible new intervention, may be necessary.

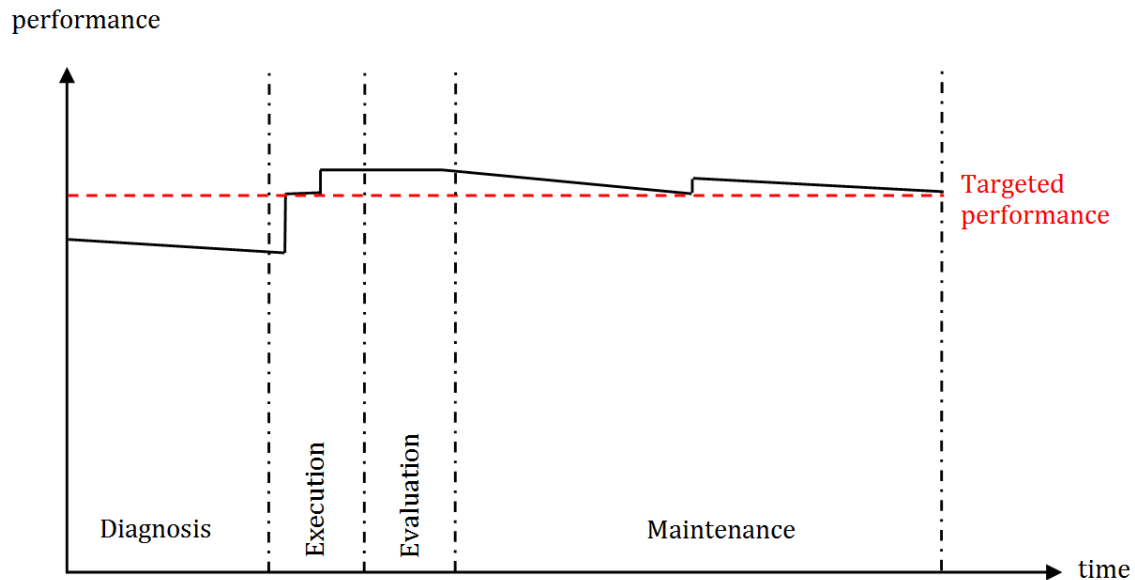


Figure 2.13. Different monitoring phases across the study of a cultural heritage building, intervention and maintenance (D9.4-NIKER, 2012).

2.3.2 Types of dynamic monitoring systems

According to the types of instruments involved, the dynamic monitoring systems can be classified in two groups: conventional wired based systems and wireless based systems, Figure 2.14. The first system is composed by measurement sensors, DAQ system and in some cases remote connection system. These systems are still widely in use, in principal, for three reasons: 1) there are a lot of commercial solutions that need just to be placed in the structure; 2) there are several types of measurement sensors and DAQ systems with high sensitivity and resolution; and 3) there is well known commercial software available for the dynamic identification of modal parameters. However, they possess two important drawbacks: high costs of these equipments due to the need of high sensitive sensors for measuring the low amplitude vibrations, and architectural limitations for the deployment of the equipments. As a result to the previously mentioned limitations of wired systems, there is an increasing interest for wireless monitoring systems as a low cost, easy to install alternative. A typical wireless system is composed by measurement units, base station and in some cases remote connection system. The measurement units are formed by MEMS (Micro Electro-Mechanical Systems) as measurement sensors, and autonomous DAQ platforms that collect the data and send them wirelessly to a base station. The base station is formed by a DAQ platform coupled with an interface board in charge on data transferring to a local computer. The remote

connection is in charge on data transferring from the local computer to a central “brain” station. (Aguilar, 2010)

According to the activation regime of the recording devices, three different systems can be distinguished. The first is the dynamic monitoring system with threshold. In this system, the recording devices are automatically activated when the amplitude caused by the excitation (for instance, an earthquake) surpasses some predefined threshold. Thus, only the strong motion experience during meaningful episodes is captured. The second is the periodical dynamic monitoring in which the recording devices works constantly, capturing a sufficiently dense input, during some given intervals activated in a periodic way according to a predefined program. The third is the continuous dynamic monitoring. This system records continuously the vibrations experienced by the historical structure. In the post processing of saved data, meaningful episodes involving earthquakes, micro-tremors or wind can be extracted. (D10.4-NIKER, 2012)

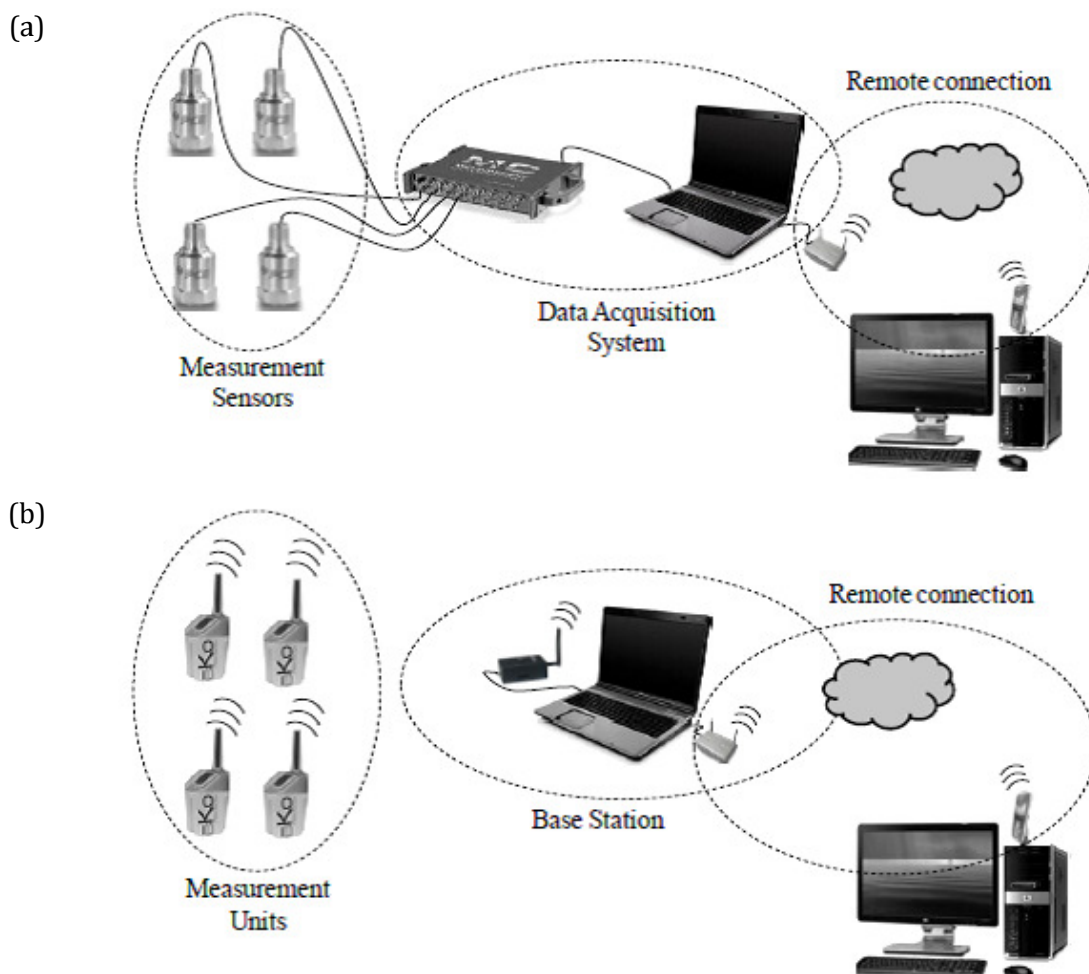


Figure 2.14. Types of dynamic monitoring systems: (a) conventional wired based systems; and (b) wireless based systems (Aguilar, 2010).

2.3.3 Applications of dynamic monitoring to cultural heritage buildings

A pioneering study of the dynamic monitoring of large scale historical construction was the one carried out by Erdik et al. (1993). The authors instrumented the Aya Sofya in Istanbul with 9 triaxial strong motion accelerometers. The system was triggered with a previously defined threshold. The system captured a seismic event of $M_b=4.8$ and 105 km epicenter far from the structure. Although the event had a low-amplitude, about 12% decrease was observed in the frequencies of the first two modes during the event when compared to those identified under ambient vibration levels.

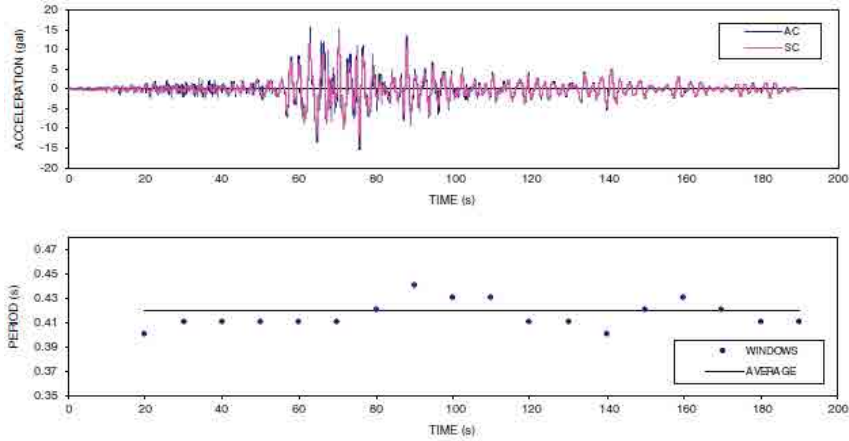
A dynamic monitoring system was installed in the Roman Arena of Verona by the end of 2011 and is still in operation (Lorenzoni et al., 2013). It is a conventional wired system including 16 uniaxial accelerometers and a remote connection. Due to the interest in the safety of the Arena wing, it was instrumented with 6 accelerometers and the remaining ones were distributed all around the amphitheatre. For the dynamic measurements, two strategies are being used. The first is periodical each 24 hours for a time of about 22 minutes at a sampling rate of 100 Hz to allow daily dynamic identification with the change of the environmental conditions. The second is with threshold for duration of about 4 minutes at a sampling rate of 100 Hz to capture any possible seismic events. During the period from December 5, 2011 to May 31, 2013, the system was used to identify the modal parameters of the first seven modes of the Arena wing using the periodical measurements. The values of the coefficient of variation of the natural frequencies showed that the environmental conditions have a clear influence on these modal parameters, with a variation over the frequencies from about 2 to 6% were found. A bilinear relation between the temperature and the frequencies was observed. The mode shapes were not found to be sensitive to the changes in environmental actions. For the damping ratios, it was noticed that they present a high scatter due to the fact that their estimation is always affected by some uncertainty. However, the variation of modal damping ratios for two modes was noticed to be somehow correlated with temperature, with a clear tendency to increase with low temperatures. Damping coefficients for the other modes are not influenced by temperature and keep constant. The structural response was also registered during two seismic events of magnitudes of 4,2 and 5,8 with epicenters at 11 (near-field) and 70 (far-field) Km from the city of Verona, respectively. It was observed that the near-field event induced higher absolute vibrations on the structures due to the closer distance of the epicenter. Nevertheless, the far-field event produced a significant higher structural amplification both on the amphitheater itself and

on the Arena's wing due to the different frequency contents of the inputs. The data collected during the near-field earthquake were used to carry out a dynamic identification before, during and after the event to evaluate possible changes in modal parameters. A significant decrease (from 16% to 30%) of all natural frequencies was observed during the earthquake. Modal damping ratios showed significant increase during the earthquake meaning that the dissipation mechanisms of the construction have been fully activated. After the earthquake, both modal parameters showed slight permanent decrement, however, no damage was observed in the structure after a careful inspection after the earthquake. The authors concluded that capturing moderate or even low intensity earthquakes helped in evaluating the structural response in detail and understanding much better than under operational conditions only the dynamic properties and the seismic behavior of the historical structure.

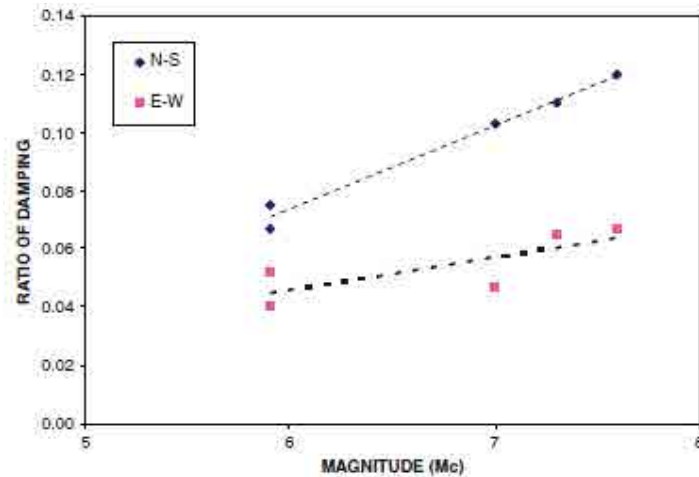
Russo (2013a) discussed the results of a 2-year dynamic monitoring system of a historical church damaged by the earthquake of L'Aquila (Italy) in 2009. After the earthquake, the remaining parts of the church were kept in place using emergency safety measures including the usage of steel ties for confinement. A wired system with threshold consisting of 20 piezoelectric accelerometers was used. The accelerometers were distributed all over the church so that each group of them could control the dynamic behavior of a macro element of the structure. Five macro elements were individuated: the dome, the façade, the southern east and the northern west walls of the transept and the apse. The objective was to study the dynamic behavior of each of the macro elements alone and also the full behavior of the strengthened construction under the effect of the after-shock events. Six events were captured and analyzed. Two of them occurred before the full strengthening measures were completed. The author compared between the full church's dynamic response before and after the complete execution of the safety measures. It was noticed that the dynamic behavior clearly improved because of the strengthening measures, which caused an increase of the natural frequencies and damping ratios.

A dynamic monitoring system was installed in a masonry tower after its repair intervention with the objective to evaluate the environmental effects (temperature and relative air humidity) on the dynamic behavior and to detect any possible damage (Ramos and Lourenço, 2011; Ramos et al., 2010a; Ramos et al., 2008a; Ramos et al., 2008b; Ramos, 2007). A wired system with three piezoelectric accelerometers was used. The system recorded periodically ten minutes of ambient vibrations each one hour with no threshold

specified. It was found that the environmental effects significantly change the dynamic response of the structure. In specific, the water absorption of the walls in the beginning of the raining seasons changed the frequencies about 4%.



(a)



(b)

Figure 2.15. Recorded dynamic behavior of Mexico City cathedral during a seismic event: (a) variation of the period; and (b) variation of the damping ratio (Rivera et al., 2008).

The seismic response of the Mexico City Cathedral was investigated by dynamic monitoring system during several earthquakes occurred between 1997 and 2003 by Meli et al. (2001) and Rivera et al. (2008). The network was composed 1 accelerometer located at ground level 10m outside the cathedral's foundation, 3 accelerometers placed at the foundation level and 4 accelerometers were located on the roof. The system was a wired one of a triggered-based type. Around 20 events were captured that had epicenters at least 100 km away from the building. For the comparison between the measurements at the roof and at the foundation level, it was noticed that the maximum recorded ground acceleration was about 0,015g whereas the maximum acceleration recorded on the cathedral roof, for the same event, was about 0,018g. This indicted that the cathedral moved like a rigid body with a very small amplification. Important findings were obtained

Integrated monitoring and structural analysis strategies for the study of large historical construction. Application to Mallorca cathedral

for the fundamental periods and the damping ratios of the cathedral in the two horizontal directions (E-W and N-S). First, the fundamental period increased in the zone of maximum intensity of an earthquake and decreased later on, returning at the end of the record close to its initial value, Figure 2.15 (a).

This indicated a significant nonlinear behavior during the event which could be related to the existing cracking in the masonry and that no additional damage has been produced by the studied event. Second, the obtained damping coefficients varied clearly with the magnitude of the earthquake. In Figure 2.15 (b) it is shown that the damping ratios increased from 4 to 6% for the transverse direction (E-W) and from 7 to 12% for the longitudinal direction (N-S). In average, damping was 50% greater for a magnitude 7.6 than for a magnitude 5.9 earthquake. This again was attributed to early nonlinear behavior due to cracking. Two of the accelerograms were then removed from the cathedral and placed on one of the bell towers to study its local seismic response. It was observed that the maximum recorded acceleration at the tower top level was 7.5 times greater than that at the basement level. This suggested that the towers vibrated with the façade as a structure almost independent from the rest of the building. This assumption was consistent with the presence of a wide transverse crack crossing the whole span of the nave in its first nave.

The following is a number of studies on dynamic monitoring of cultural heritage that are briefly discussed. Cabboi (2014) proposed a methodology for automatic processing of permanent dynamic monitoring data and applied it to a historic iron arch bridge and a historic masonry tower. The automatic procedure is based on the Covariance-Driven Stochastic Subspace Identification method (see section 2.4.2.3 about this technique). In his methodology, he gave some recommendations on the selection of some input parameters of this method. For the masonry tower, he observed that the dynamic behavior exhibit a high variance in time. All the identified frequencies tended to increase with the temperature increase. Other publications related to this research can be consulted at Cabboi et al., 2014; Cabboi et al., 2013a; Cabboi et al., 2013b and Gentile et al., 2012. Ramos et al. (2013b) introduced an algorithm for automatic processing of dynamic monitoring measurements for the identification of modal parameters. The algorithm is based on the Data-Driven Stochastic Subspace Identification method (see section 2.4.2.4 about this method) and was applied to a Portuguese church. One of the important findings was the clear scatter in the identified damping ratios for all identified modes during the whole monitoring period. Lorenzoni (2013) proposed an algorithm for automatic dynamic

monitoring and applied it to four case studies in Italy. His algorithm is based on polyreference Least Square Complex Frequency domain (see section 2.4.2.5 about this identification technique). He found (similar to Ramos et al., 2013b) that the identified damping ratios manifested a high scatter. An example of using the dynamic monitoring as a tool for controlling intervention can be found at Lorenzoni (2013) and Gaudini et al. (2008) who presented the results of a dynamic monitoring system installed in the stone tomb of *Cansignorio della Scala* in Verona. One of the important results in this case study is the effect of the removal of scaffolding that was installed temporary for carrying out some interventions. By processing the monitoring data, it was clearly noticed a decrease in the identified natural frequencies after scaffolding removal. The captured seismic responses of two instrumented mosques in Turkey were presented by Erdik and Durukal (1996).

Contrary to the large available number of publications on dynamic identification of historic structures, only few publications exist for dynamic monitoring studies. Only 6 years ago, Rivera et al. (2008) commented that “*only a handful of historic buildings have been instrumented worldwide*”. This fact can be confirmed by reviewing the number of publications on the subject in the series of the conferences on *Structural Analysis of Historical Constructions (SAHC)*. In the 8 editions of this conference, less than 1% of the published papers were dedicated to the dynamic monitoring. The situation is similar also regarding the number of publication in international journals.

2.4 Modal parameters identification

2.4.1 Introduction

The acquired signals via the previously discussed dynamic investigation activities are processed by identification techniques in order to identify the modal parameters of a historical building. In any of these techniques, the signal processing is an essential step. Therefore, this part first gives some important concepts in signal processing like sampling, spectral analysis, Fast Fourier Transform, aliasing, etc. Following, a number of modal parameters identification techniques that have been used in this research are presented.

2.4.2 Concepts in signal processing

2.4.2.1 Signal, system and signal processing

A signal is a description of how one parameter varies with another parameter, for instance, voltage changing over time in an electronic circuit (Smith, 2002). Mathematically, a signal is a real (or complex) valued function of one or more real variable(s) (Sharma, *Integrated monitoring and structural analysis strategies for the study of large historical construction. Application to Mallorca cathedral*

2014). A system is any process that produces an output signal in response to an input signal. Continuous systems input and output continuous signals, such as in analog electronics. Discrete systems input and output discrete signals, such as computer programs that manipulate the values stored in arrays (Smith, 2002).

Signal processing means to operate in some fashion on a signal to extract some useful information, e.g. manipulate or combine various signals, extract information, or otherwise process the signal (Sharma, 2014; Kulkarni, 2014). Signal processing can be implemented in two different ways: analog (or continuous time method) and digital (or discrete time method). The analog approach uses analog circuit elements such as resistors and transistors, and was dominant for many years. The analog signal processing is based on the ability of the analog system to solve differential equations that describe a physical system. Nowadays with the advent of digital computers and microprocessors, the digital signal processing has become dominant. The digital signal processing relies on numerical calculations. (Sharma, 2014)

2.4.2.2 Sampling

Sampling is the process of picking one value of a signal to represent the signal for some interval of time. The Nyquist sampling theorem provides a quantitative answer to the question of how to choose the sampling time interval which must be small enough so that signal variations that occur between samples are not lost. It states that *“if a signal only contains frequencies less than cut off frequency f_c all the information in the signal can be captured by sampling it at a minimum frequency of $2f_c$ ”*. Therefore, two conditions must be met. First, the signal $x(t)$ must be band-limited, i.e., its frequency spectrum must be limited to contain frequencies up to some maximum frequency f_{max} and no frequencies beyond that. Second, the sampling rate f_s which represents the density of samples per unit time and is measured in units of samples/sec or Hertz (Hz) must be chosen to be at least twice the maximum frequency f_{max} , that is $f_s \geq 2f_{max}$. The minimum allowed sampling rate is called the Nyquist rate. For the second condition, nevertheless, common practice dictates that while working in the frequency domain, the sampling rate must be set more than twice and preferably between five and ten times the signal's highest frequency component. (Loewenstein, 1999; MC, 2005; Antonelli et al., 1999; Orfanidis, 1996)

2.4.2.3 Noise and white noise

Desired signals are subject to various types of degradation in many applications. This degradation can arise from a variety of sources such as limitations of the response

transducers, random and/or un-modeled fluctuations of underlying physical processes, or environmental conditions during sensing, transmission, reception, or storage of the data. Thus, the term noise is typically used to describe a wide range of degradation. (Kulkarni, 2014)

White noise is a basic concept underlying the modeling of random disturbances, such as sensor noise and environmental disturbances. In contrast to continuous time, white noise is straightforward to characterize in discrete time. The noise signal said to be white if (Reist, 2013) (1) it has zero mean and unit variance, (2) it is independent from sample to sample, i.e. not correlated in time.

2.4.2.4 Signal conditioning

Commonly, signals measured by a sensor do not have acceptable characteristics for display, recording, transmission, or further processing. For instance, they may lack the amplitude, power, level, or bandwidth required. Also, they may have superimposed interference that may mask the required information. Signal conditioning aims at adapting sensor's signals to the requirement of the receiver they are connected - whether a circuit or equipment (Pallas-Areny, 1999). In the following, a number of common signal conditioning functions are briefly discussed, mainly stressing the concept behind.

a) Aliasing

Aliasing occurs when input signals are sampled at less than the Nyquist rate. As a result, ambiguous signals that are much lower in frequency than the signal being sampled can appear in the time domain. For instance, Figure 2.16 (a) shows a 1 kHz sine wave sampled at 800 Hz. The reconstructed frequency of the sampled wave is much too low and is not a true reproduction of the original frequency. Alternatively, Figure 2.16 (b) shows the same signal sampled at more than twice the input frequency or 5 kHz. Consequently, the sampled wave now appears closer to the original one. To prevent aliases, a low-pass, anti-aliasing filter is used. Although the filter eliminates the aliases, it also prevents any other signals from passing if their frequencies are above the stop band of the filter. Therefore, the DAQ system should be selected so that the sampling frequency per channel is more than twice (at least) the highest frequency intended to be measured as previously discussed in section 2.4.2.2. (MC, 2005)

b) Leakage and windows

The leakage error occurs when transforming a signal from the time domain to the frequency domain using the Fast Fourier Transform (FFT, see section 2.4.2.5 (c)). The FFT

can produce a proper representation of the data in the frequency domain if the sampled data consist of either a complete representation of the measured data for all time or alternatively contain a periodic repetition of the measured data. When any of these are not satisfied, then leakage will occur causing a serious distortion of the data in the frequency domain. To minimize this effect, weighting functions called windows are applied to the measured data to force it to better satisfy the periodicity requirements of the FFT. An example of these functions, the exponentially decaying window, is shown in Figure 2.17 (a). Some other common window functions are Hanning, Hamming, Blackman, Figure 2.17(b).

c) Filters

Distortions in the data that reside in a frequency band that can be separated from the frequency band of interest can be removed by filtering the data. Filters are commonly classified according to the filter function they perform, Figure 2.18. In this figure, it is shown the basic filtering functions: low-pass, high-pass, band-pass, and band-stop. A low-pass filter passes frequencies from zero to its cutoff frequency Ω_c and stops all frequencies higher than the cutoff frequencies. On the contrary, a high-pass filter stops all frequencies below its cutoff frequency and passes all frequencies above it. A band-pass filter passes frequencies from Ω_1 to Ω_2 and stops all other frequencies. Oppositely, a band-stop filter stops frequencies from Ω_1 to Ω_2 and passes all other frequencies. (Jamal and Steer, 1999; Verhaegen and Verdult, 2007)

d) Decimation

When the sampling frequency is too high with respect to the bandwidth of interest of the tested structure, one may resample the data by selecting every j^{th} sample from the original data sequences. If the original sampling frequency was f_s , the so-called down-sampled or decimated data sequence is sampled with a frequency of f_s / j . This is carried out because a too high sampling frequency results in high-frequency disturbance in the data above the frequency band of interest. Before decimation, a digital anti-aliasing filter with a cut-off frequency of $f_s / 2j$ must be applied to prevent aliasing. (Verhaegen and Verdult, 2007)

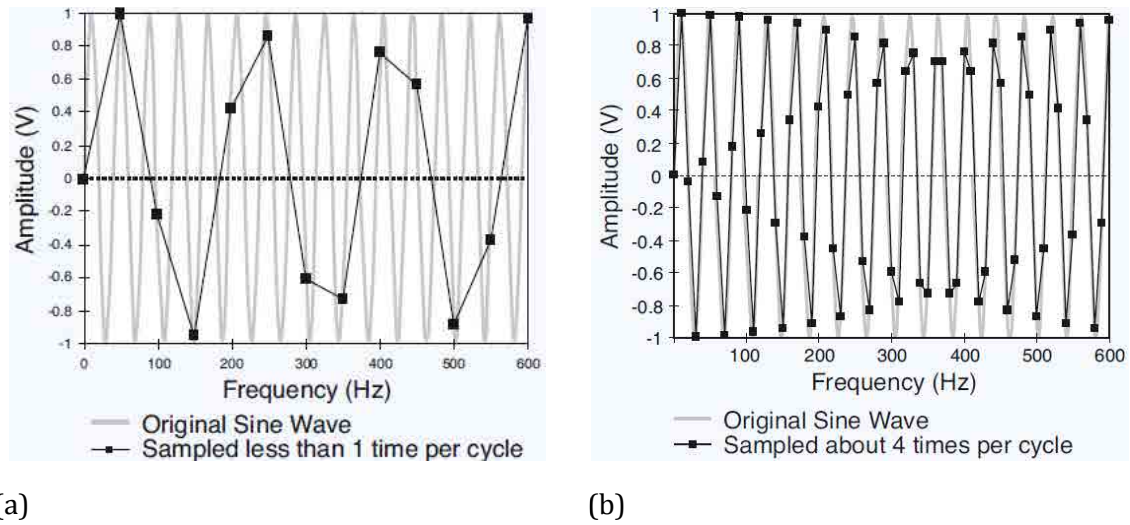


Figure 2.16. Aliasing: (a) inadequate Nyquist sampling rate; and (b) acceptable Nyquist sampling rate (MC, 2005).

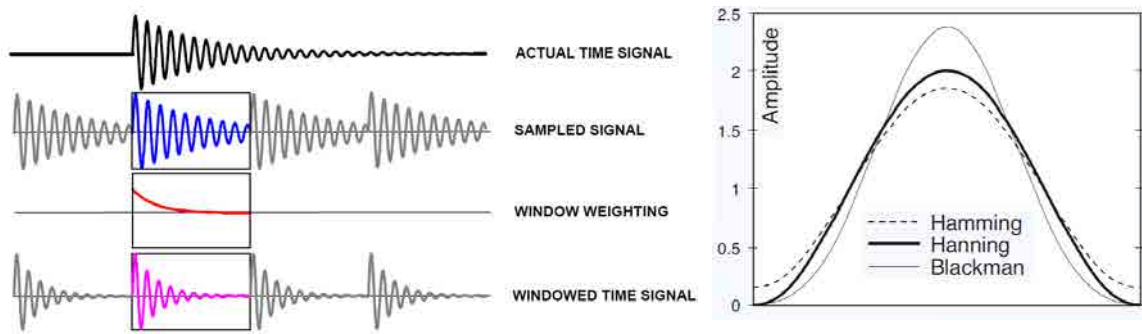


Figure 2.17. (a) Minimizing the leakage effect using the exponentially decaying window (Avitabile, 2001); and (b) Hamming, Hanning, and Blackman window functions (adapted from MC, 2005).

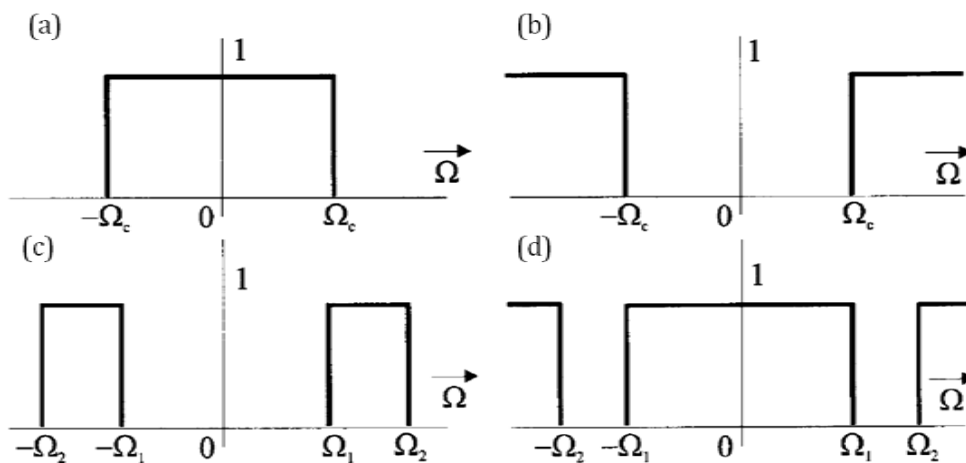


Figure 2.18. Filters types: (a) low-pass; (b) high-pass; (c) band-pass; and (d) stop-band. Note that the magnitude function of an ideal filter is 1 in the pass-band and 0 in the stop-band (adapted from Jamal and Steer, 1999).

2.4.3 Modal parameters identification methods

The methods developed from extraction of modal parameters for FVT are based on employing the FRF's derived in frequency domain or on the equivalent Impulse Response Functions (IRF's) in time domain. These methods are generally classified as frequency domain or time domain approaches. Some of the frequency domain methods are the Peak-Picking (PP) method, the Complex Mode Indicator Function (CMIF) method and the polyreference Least Squares Complex Frequency (pLSCF) method. Some of the time domain methods are the Least-Squares Complex Exponential (LSCE) method, the Poly Reference Complex Exponential (PRCE) method, the Multiple Reference Ibrahim Time Domain (MRITD) method and the Eigen-system Realization Algorithm (ERA) method. For AVT, the proposing of Natural Excitation Technique (NExT) by James et al. (1992) was a milestone step that allowed the adaptation of FVT identification methods to be used in AVT. The idea behind the NExT technique is that Correlation Functions (COR's) between the responses can be expressed as a sum of decaying sinusoids. Each decaying sinusoid has a damped natural frequency and damping ratio that is identical to the one of the corresponding structural mode. Consequently, COR's can be employed as IRF's to estimate modal parameters. For instance, in the frequency domain, the FDD and the PolyMAX methods were developed by Brincker et al. (2000a) and Peeters et al. (2004), respectively, by replacing the FRF's matrix with the output spectral matrix assuming that the input is white noise. Similarly, in the time domain, by replacing IRF's with COR's, the Covariance driven Stochastic Subspace Identification (SSI-COV) method was developed by Peeters (2000). (Hu, 2012)

For more about classification of dynamic identification techniques, the interested reader can refer to Cunha et al. (2013); Hu et al. (2010); Masjedian and Keshmiri (2009), De Stefano and Ceravolo (2007); Cunha et al. (2006); Zhang et al. (2005); Ren and Zong (2004); Peeters and De Roeck (2001); Maia and Silva (2001); Maia and Silva (1997). In the following, four methods that have been used in this research are discussed to show their theoretical background, advantages and limitations. These methods are: PP, FDD, SSI-Cov driven SSI-Data driven and polyreference least square complex frequency domain (pLSCF).

2.4.3.1 Peak picking (PP)

The Peak Picking (PP) method is the simplest known method for identifying the modal parameters of structures tested by AVT. It is a frequency domain based

identification technique and is also called Basic Frequency Domain (BFD). It is based on simple signal processing using the DFT. It depends on the fact that well separated modes can be estimated directly from the Power Spectral Density matrix (PSD) at the peak as proposed by Bendat and Piersol (1993). There is other implementations of that make use of the coherence between channels as proposed by Felber (1993). (Brincker et al., 2001a; Brincker et al., 2000a; Brincker et al., 2000b; Andersen et al., 1999)

Frequency domain algorithms are most popular mainly due to their simplicity and processing speed. In the context of FVT, the PP is based on the fact that the FRF reaches extreme values around the natural frequencies; therefore, the frequency at which this extreme occurs is a good estimate for the frequency of the structure. In the context of AVT, the FRF is only replaced by the auto spectra of the ambient outputs. In such a way the natural frequencies are simply determined from the observation of the peaks on the graphs of the averaged normalized power spectral densities (ANPSD's). The ANPSDs are basically obtained by converting the measured accelerations to the frequency domain by DFT.

Even though the input excitation is not measured in AVT, this problem has often been solved by adopting a derived modal parameter identification technique where the reference sensor signal is used as an input and the FRF's and coherence functions are calculated for each measurement point with respect to this reference sensor. The coherence function calculated for two simultaneously recorded output signals has values close to one at the resonance frequencies because of the high signal-to-noise ratio at these frequencies. Accordingly, inspecting the coherence function helps in selecting the natural frequencies of the structure. This method also yields the operational shapes that are not the mode shapes, but almost always correspond to them. The components of the mode shapes are determined by the values of the transfer functions at the natural frequencies. In the context of AVT, transfer function means the ratio of response measured by a roving sensor over response measured by a reference sensor. So, every transfer function yields a mode shape component relative to the reference sensor. Here it is assumed that the dynamic response at resonance is only dominated by one mode. The validity of this assumption increases as the modes are better separated and as the damping in the structure is lower. (Ren and Zong, 2004)

Advantages and drawbacks The main advantages is that the PP is faster, much more user friendly, simpler to use and gives the user a feeling of the data he is dealing with. Because the user works directly with the spectral density functions, this helps him in

figuring out what is structural just by looking at the spectral density functions. This strengthens the user understanding of the physics, hence provides a valuable tool for a meaningful identification. Also, the PP gives a clear indication of harmonic components in the response signals. The PP technique has some drawbacks: picking the peaks is always a subjective task; operational deflection shapes are obtained instead of mode shapes; only real modes or proportionally damped structures can be deduced by the method; and damping estimates are unreliable. In spite of these drawbacks many civil engineering cases exist where the PP technique is successfully applied. (Ren and Zong, 2004; Brincker et al., 2000a;; Peetres and De Roeck, 1999)

2.4.3.2 Frequency domain decomposition (FDD)

The Frequency Domain Decomposition (FDD) method was firstly presented by Brincker et al. (2000a, 2000b; 2001a). Nevertheless, the concepts behind the method had already been used in the analysis of structures subjected to AV by Prevosto (1982) and Correa and Costa (1992), and on the identification of modal parameters from FRF (Shih et al., 1988b) (Magalhães and Cunha, 2011). In the FDD, it is shown that taking the Singular Value Decomposition (SVD) of the spectral matrix, the spectral matrix is decomposed into a set of auto spectral density functions, each corresponding to a single degree of freedom (SDOF) system (Brincker et al., 2000a; 2000b; 2001a).

Advantages and drawbacks The FDD aims to be a simple and user-friendly technique allowing at the same time the accurate separation of closely spaced modes which is not achievable by the PP technique (Magalhães and Cunha, 2011). The FDD results are exact provided that the excitation is white noise, the structure is lightly damped and the mode shapes of closely spaced modes are geometrically orthogonal. If these assumptions are not satisfied, the decomposition into SDOF systems is approximate, but still the results are significantly more accurate than the results of the PP method (Brincker et al., 2000a; 2000b; 2001a). Like the PP technique, the FDD cannot estimate the damping ratios; therefore, a new method was developed by Brincker et al. (2001b), called the Enhanced FDD or EFDD, to overcome this drawback.

2.4.3.3 Stochastic subspace identification methods

Stochastic Subspace Identification (SSI) modal estimation algorithms have been around for about two decades by now. The real break-through of the SSI algorithms was introduced by Van Overschee and De Moor (1996). In this book, it was showed that the SSI algorithms were a strong and efficient tool for natural input modal analysis. Because of the

immediate acceptance of the effectiveness of the algorithms the mathematical framework described in the book where accepted as a de facto standard for SSI algorithms. (Brincker and Andersen, 2006)

The SSI methods perform the identification of modal parameters using a stochastic state-space model. This model in its discrete form and assuming the excitation as a white noise is represented by:

$$\begin{aligned}x_{k+1} &= A x_k + w_k \\ y_k &= C x_k + v_k\end{aligned}\tag{Equation 2.1}$$

Where x_k is the discrete-time state vector at time instant k , y_k is the vector with the sampled outputs, A is the discrete state matrix, C is the discrete output matrix and w_k , v_k are vectors that represent the noise due to disturbances and modeling inaccuracies and the measurement noise due to sensor inaccuracy. If the Identification of matrices A and C is performed from the measured time series, the method is called Data-driven Stochastic Subspace Identification (SSI-DATA), and if performed from the correlations of the time series, it is called Covariance-driven Stochastic Subspace Identification (SSI-COV). Both methods are based on the properties of stochastic systems (Van Overschee and Moor, 1996) and involve singular value decomposition and the resolution of a least-squares equation (Peeters, 2000). The quality of the results obtained by both methods is similar. But, the SSI-COV method is faster and requires less memory, because the time series are compressed in covariance matrices. After the identification of the state-space model, modal parameters are extracted from matrices A and C . (Magalhaes et al., 2010; Magalhaes et al., 2009)

Peeters and De Roeck (1999) introduced a modified version of classical SSI-COV called SSI-COV/ref. In this method the modification consisted of reformulating the algorithm so that it only needed the covariances between the outputs and a limited set of reference outputs instead of the covariances between all outputs. In the same publication they proposed also a modified version of SSI-DATA called SSI-DATA/ref. In this new method the idea was to take instead of all past outputs only the past reference outputs when projecting the future output into the past outputs.

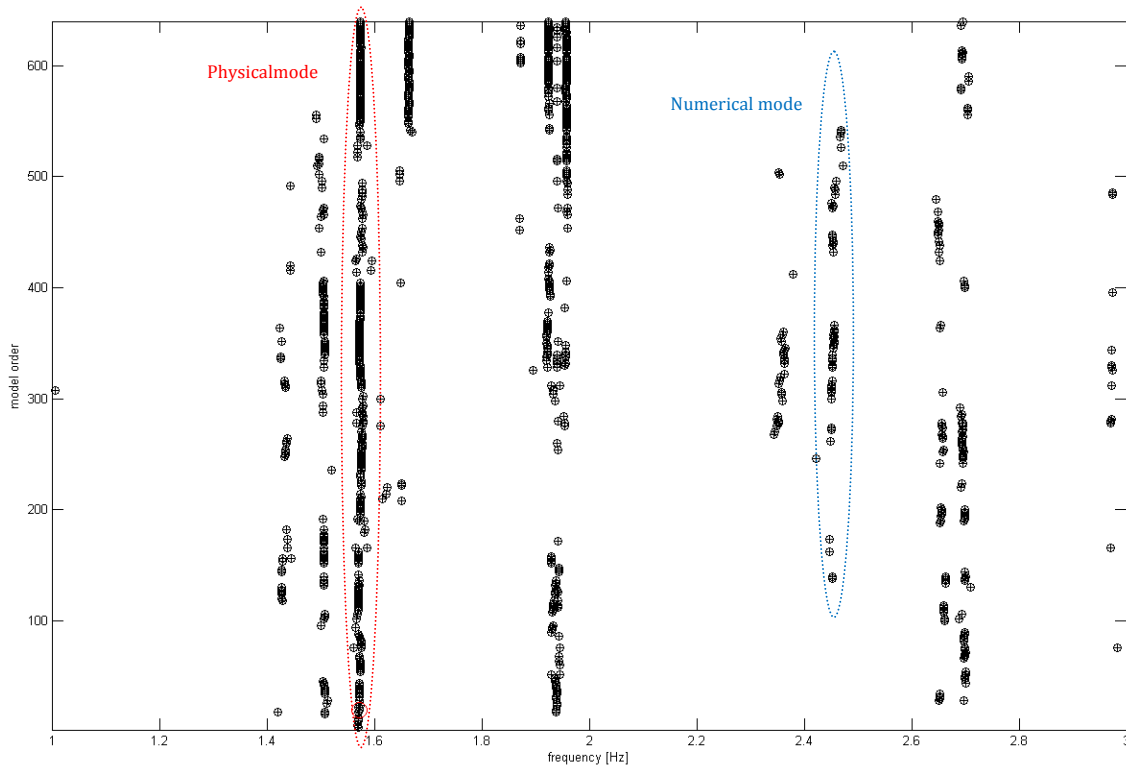


Figure 2.19. Example of a stabilization diagram showing the difference between physical and numerical modes. Source: the dynamic identification tests of the current research.

Stabilization diagram The identification of the state-space model requires the definition of the model order. Nevertheless, it is not possible to predict the model order that better fits the experimental data and realistically characterizes the dynamic behavior of the tested structure. Therefore, the estimation of the modal parameters is carried out using models with an order within an interval defined in a conservative way. The identified modal parameters are then represented in a stabilization diagram that allows the distinction of parameters that are stable for models of increasing orders (points over the same vertical alignment), and these are the ones with structural significance (Figure 2.19). The others are just associated with numerical modes, which are important to model the noise that exists always in measured data (Figure 2.19). In other words, the frequencies indicating a structural mode appear in a stable vertical alignment of identified poles; instead, the frequencies indicating spurious poles appear randomly scattered in the diagram. (Magalhaes et al., 2010; Cabboi, 2014)

Advantages and drawbacks The SSI methods are time domain based techniques that directly works with time data, without the need to convert them to correlations or spectra. However, and common to all system identification methods for AVT, it is not possible to obtain an absolute scaling of the identified mode shapes (e.g. mass

normalization) because the input remains unknown (Ren and Zong, 2004). Some proposals to overcome these limitations can be found at Brincker and Andersen (2003b); Bernal (2003); Bernal and Gunes (2002) and Parloo et al. (2002). In specific for SSI/ref methods, the prediction errors are higher for channels that do not belong to the reference channels because these channels are partially omitted in the identification process. However, there is a clear reduction in the dimensions of the problem and the computation time (Peetres and De Roeck, 1999).

2.4.3.4 Polyreference least square complex frequency domain (pLSCF)

In Zhang et al. (2005) a tracking of the development of pLSCF method from the FVT to the AVT can be found, a summery is presented here. Guillaume et al (1998) used the Least Squares Complex Frequency-domain (LSCF) estimation method to find initial values for the iterative maximum likelihood method which was proposed for modal identification from FRF in FVT context. It was found that these initial values resulted in accurate modal parameters with small computational effort; nevertheless, LSCF had two limitations. First, the mode shapes are difficult to obtain using the SVD. Second, the closely spaced modes are difficult to separate. Therefore, Guillaume et al (2003) presented a polyreference version of the LSCF method, based on right matrix-fraction model to overcome the above limitations and short time after Peetres and Van der Auweraer (2005) presented the polyreference Least Square Complex Frequency domain (pLSCF) for AVT.

Advantages and drawbacks The main advantages of the pLSCF are (1) it is fast; (2) it yields a very clear stabilization diagram; (3) the numerical stability of the algorithm allows for a large-bandwidth and high-model order analysis and makes it suitable both for lowly- and highly-damped structures. The main drawback is that the damping estimates associated with some stable poles decrease with increasing noise levels and this situation becomes worth for poorly excited modes. (El-Kafafy et al.,2013; Peetres et al., 2012; Peetres, 2000)

2.5 Infrared thermography

2.5.1 Theoretical background

Most materials absorb infrared radiation (IR) over a wide range of wavelengths which results in an increase in their temperature. When an object has a temperature greater than absolute zero it emits IR energy. IR thermography is a nondestructive inspection technique which converts the emitted IR radiation pattern into a visual image

by the usage of an IR camera. An IR camera measures, calculates and displays the emitted IR radiation from an object. The radiation measured by an IR camera does not depend only on the object surface temperature but is also a function of the emissivity which is a measure of the efficiency of a surface to act as a radiator. According to the Stefan-Boltzmann law, the equation of the radiation of an object is given by:

$$E = \epsilon \sigma T^4 \quad \text{Equation 2.2}$$

where E is the radiation (W/m^2), ϵ is the emissivity, σ is the Stefan-Boltzmann constant ($5,67 \times 10^{-8} \text{ W}/\text{m}^2 \text{ K}^4$) and T is the temperature (K). It should be noticed that there are three methods of heat transfer: conduction, convection and radiation, and an IR camera only records the amount of radiated heat (Clark et al., 2003). For further reading on the subject, the reader is referred to (Ibarra-Castanedo et al., 2007; Walker and Nowicki, 2005; Hellier, 2003; Avdelidis and Moropoulou, 2003; Maldague and Moore, 2001).

2.5.2 Practical considerations

2.5.2.1 Approaches

There are two approaches in IR thermography: passive and active. In the passive approach the object under investigation is naturally at a higher or lower temperature than the background. This approach can be applied only if the object is subjected to sufficient exposure of sun light, so that it can emit IR radiation. In the active approach, an energy source is required to produce a thermal contrast between the object and the background to allow for a transient heat transfer phenomena to occur. (Ibarra-Castanedo et al., 2007; Olivito and Zuccarello, 2009)

2.5.2.2 Advantages and disadvantages

The main advantages of IR thermography are:

- remote sensing: no direct contact between the camera and the object under investigation is required,
- large monitoring capacity: an IR camera can monitor temperature at many different points within a scene simultaneously,
- range of measurement: typical temperature ranges are of the order of -20 to 1600 °C,
- fast response rate: IR cameras can detect rapid temperature fluctuations to an accuracy of $\pm 0,08$ °C,
- portability: IR cameras are lightweight and can be easily transported,

- easy data manipulation: the recorded data can be processed on standard PC using dedicated imaging software. (Clark et al., 2003)

The main disadvantages of IR thermography are:

- as previously mentioned, the radiation measured by an IR camera is not only a function of the object temperature but also of its emissivity and since emissivity varies from material to material, the brightness of different objects within a scene do not necessarily give a clear indication of their relative temperatures,
- material with emissivity less than one reflects radiation from surrounding objects as well as emits its own radiation. As a result, the temperature obtained for an object may be influenced by other objects in the surrounding area,
- the obtained results are affected by the attenuation of radiation in the atmosphere caused by the absorption of energy by suspended particles and subsequent re-radiation in random directions. In case of small distance between the object and the IR camera these effects can be neglected. (Clark et al., 2003)

2.5.3 Infrared thermography in historical construction: case studies

In the following some case studies on the use of IR thermography in the inspection of architectural heritage buildings are presented. There are numerous case studies in the literature and the following are only some selected cases.

The IR thermography was used extensively in the inspection activities carried out on the church of Nativity in Bethlehem (Faella et al., 2012). The IR thermography showed: 1) moisture problems to rainwater seepage and re-climbing moisture presence in several masonry walls; 2) the plugging of some openings; 3) nearly homogenous materials used in the roof except one area in which different materials were used; 4) the narthex roof had great seepages of rainwater since there was no efficient waste disposal system for drainage.

Binda et al. (2011a) used the IR thermography as one of the inspection techniques applied to the Spanish Fortress damaged by L'Aquila earthquake. Because the masonry was hidden by thick plaster, the IR thermography was used to reveal its texture which helped in identifying the most representative areas where to place local tests like flat-jack. The active approach was used in which the parts subjected to the test were previously heated for one hour. They discovered the presence of a non homogeneous masonry texture under the plaster of some walls (Figure 2.20, top) and the peculiar presence of bricks and large stones at the base of the vault arches (Figure 2.20, bottom). In Figure 2.20

(bottom) the yellow and blue colored area at the basis of the vault was identified as a discontinuity in the stone masonry. After removing some parts of the plaster brick masonry was found. Moreover, underneath the spring of the vault large blocks of rather regularly cut stones were found. These stones formed a sort of built-in stronger column collecting the higher stresses coming from the vault spring.

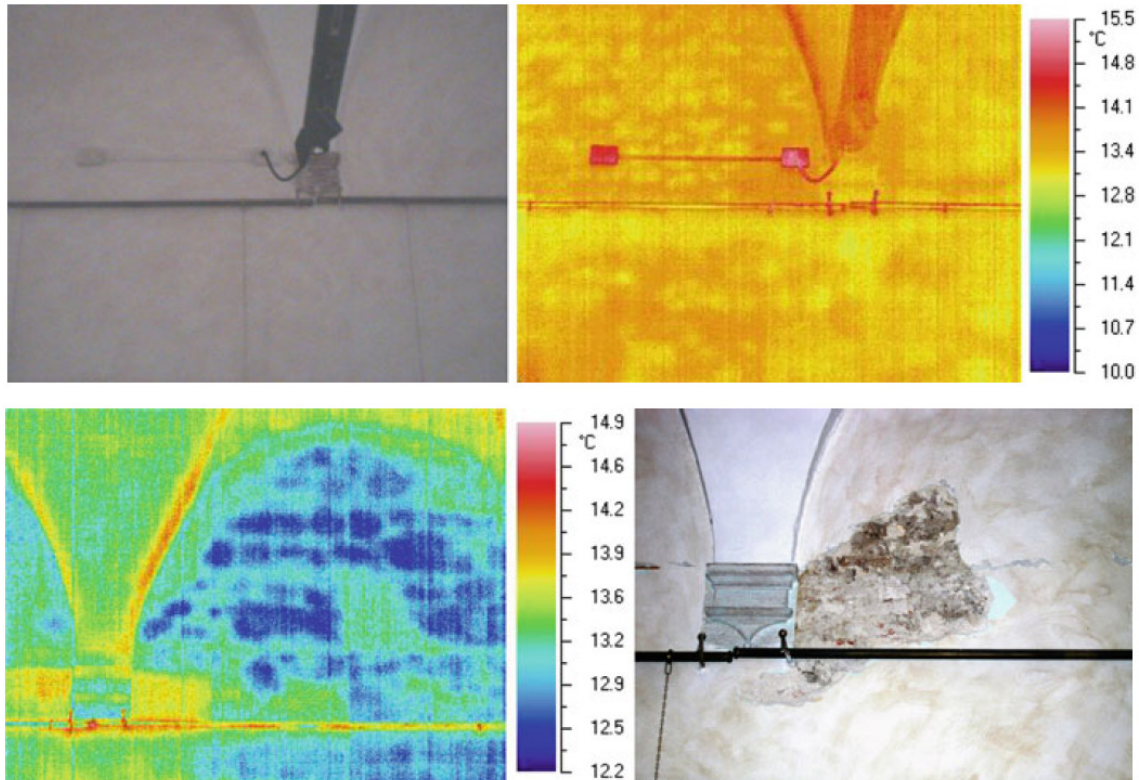


Figure 2.20. Examples of IR thermography applied to two walls of the Spanish Fortress in L'Aquila: top: first wall, bottom: second wall (Binda et al., 2011).

Tavukçuoğlu et al. (2010) used the IR thermography in NDT of a 16th century historical mosque. The IR thermography was used beside ultrasonic testing technique. The aim was to discover the activeness of observed structural cracks. The active IR approach was used. It was noticed that the superficial and deep cracks had different thermal responses to exposed conditions which made them easily distinguishable. The results of IR thermal monitoring were useful in assessment of the thermal behavior characteristics of masonry structural cracks in relation to depth, moisture content and exposure conditions. Also, some of the non-visible cracks by eye were discovered. The depth of cracks was estimated by the ultrasonic.

Grinzato et al. (2002a) showed the application of the IR thermography for several purposes in the monitoring of the historical Arsenal of Venice. Villegas et al. (2009) used IR thermography as one of the several employed NDT and MDT of a 19th century large

scale building. Bosiljkov et al. (2010) used thermography technique for investigating the condition of the pointing mortar. Thermography was used in testing the Fresco artwork by Giotto in the Scrovegni chapel in Padova by Grinzato et al. (2002b). The technique was applied successfully for the knowledge of wall bonding, moisture mapping and the measure of the thermal diffusivity of bricks and plaster. The IR thermography technique can be used as quality assurance test as recommended by Italian guidelines (CNR-DT 200, 2004) and was utilized by Olivito and Zuccarello (2009) for estimating the efficiency of the FRP strengthening of masonry structures. Other norms related to the usage of IR thermography are ASTM C1060 (ASTM, 2011) and RESNET (RESNET, 2012). It is well known that water infiltrations represent a mean source of deterioration for historical structures if not dealt with caution. For this purpose, thermography can detect damp areas in the structures due to their different temperature compared with the dry ones (Gayo and de Frutos, 1997; Sandrolini and Franzoni, 2006).

Other studies involving the use of thermography in ancient structures are those by Jo and Lee (2014); Alves et al. (2014); Bagavathiappan et al. (2013); Martínez et al. (2013); Kordatos et al. (2013); Paoletti, et al. (2013); Moropoulo et al. (2013); Cotic et al. (2013); Barreira et al. (2013); Binda et al. (2011b); Kandemir-Yucel et al. (2007); Avdelidis and Moropoulou (2004); Xavier and Patrick (2001).

2.6 Updating of finite element models of historical construction

2.6.1 Introduction

Finite element (FE) method is nowadays widely used to model historical construction. Many relevant references can be found for this method, among them (Rao, 2005; Entwistle, 2001; Huebner, 2001; Zienkiewicz and Taylor, 2000). The method has large capabilities in modeling complex geometries and different materials constitutive models and to perform nonlinear analyses whether static or dynamic. However, creating a reliable FE model of a historical structure is a difficult task due to the challenges usually involved in this class of structures. These challenges are related to different aspects like geometry, construction materials, boundary conditions, existing damage and previous repairs. Therefore, there is a need to update (calibrate) the historical construction FE model against possible modeling inaccuracies and uncertainties. The process of calibration by matching the FE model outputs with the experimentally measured data is called model updating. The experimental data can be obtained from static load tests, dynamic identification tests or a combination of both. This section discusses the different

approaches of FE model updating. Some case studies of updating FE models of historical construction based on results of dynamic identification tests are then given and critically reviewed.

2.6.2 Philosophy of FE model updating

When creating a FE model it is usual to make some simplifying assumptions. Likewise, boundary conditions and connections between different structural parts are not modeled with complete certainty. In addition, the FE method is based upon the material properties (Young's modulus, mass density, etc.) and the physical dimensions of the system under test. The shape function of the chosen elements determines the distribution of the mass and stiffness properties, so that the terms in the mass and stiffness matrices can be understood physically. However, alternative elements are available with different shape functions and for that reason the FE models are meaningful but non-unique. Consequently, the analyst may need to examine the sensitivity of the FE model results to changes in the mesh configuration and/or boundary constraints. Ultimately, he settles for a model which will be likely to provide acceptable results according to his engineering judgment. Limitations and errors are associated also with experimental testing. For instance: electronic systems can generally introduce low levels of instrument noise, piezoelectric accelerometers lack linearity at low frequencies, and noise can arise from accelerometer cables. In addition, test measurements usually contain fewer modes than the order of the identified model and therefore are said to be incomplete. Therefore, when comparing experimental and theoretical vibration mode shapes, the latter generally contain more points than those available from the former. The problems introduced by incompleteness are clear in large structures where it is expensive to take measurements at a large number of locations and to process large volumes of data. (Mottershead and Friswell, 1993)

The rule of the model updating process is to modify the mass, stiffness and damping parameters of the FE model to obtain better agreement between numerical results and experimental data. One important aspect of FE model updating is that there exists more confidence in the experimental dynamic data than in the FE model itself. It is clear that the improved agreement in results should be achieved by correcting the inaccurate modeling assumptions and not by making other physically meaningless alterations to the model. Several techniques have been developed whereby FE models of structures are altered so that their dynamic characteristics become a closer match of experimentally determined behavior. At the most simple, it is very common to make a small number of changes to the

overall properties of a FE model in a number of iterations. This type of process involves a large amount of intervention from an engineer to assess the level of improvement in the dynamic predictions of the FE model. (Mottershead and Friswell, 1993; Greening, 1999)

2.6.3 Methods of FE model updating

The FE model updating methods can be divided into direct methods and indirect (iterative) methods (Ewins, 2000c). In the following, these methods are briefly presented. For a more in-depth review, the reader is referred to several available publications on the subject like those of Mottershead and Friswell (1993), Friswell and Mottershead (1995) and Rad (1997). In their specific state-of-the-art research on the applications of FE model updating to the masonry monuments, Atamturktur (2009), Atamturktur et al. (2010) and Atamturktur and Laman (2012) classify the updating approaches into deterministic and stochastic. The deterministic approach is subdivided to manual and automated methods. These are also presented hereinafter.

2.6.3.1 Direct methods

Direct methods depend on adjusting individual elements in the structure mass and stiffness matrices by direct comparison between measured data and initial predictions of the FE model (Ewins, 2000c). Some examples for the direct methods are: the matrix mixing method (Ross, 1971), the Lagrange multiplier method (Baruch and Bar Itzhac, 1978), and the error matrix method (Sidhu and Ewins, 1984). The main advantages of these methods are: assured convergence, less computational time compared with indirect methods and exact reproducing of the reference data set (Rad, 1997). On the other hand, there are two main disadvantages. First, a reduction in the number of DOF of the FE model has to be made because the measured DOF (measurement points) are usually less than the numerical ones. Second, the updating of the structure matrices is performed without involving a physical meaning of the resulting state, and it's difficult to control the results because changes are not directly related to structural parameters (Jiménez-Alonso and Sáez, 2011).

2.6.3.2 Indirect (iterative) methods

In these methods changes are made to specific physical or elemental properties in the FE model searching for an adjustment which makes measured and predicted data closer. These methods are more acceptable than the direct methods because the parameters which they adjust are physically realizable quantities (Ewins, 2000c). Some of

the indirect methods are the minimum variance method (Collins and Young, 1972), the inverse eigen sensitivity method (Collins et al, 1974) and the eigen dynamic constraint method (Ibrahim et al., 1989; Lin, 1991). The advantages of indirect methods are that both measured data and FE model data can be weighted, a feature which can accommodate engineering judgment; and that a wide range of parameters can be updated simultaneously (Rad, 1997). The main disadvantages are that the experimental and theoretical modes must be paired from the beginning of the updating process and a faced problem here is that there is no guarantee that all modes can be matched; the FE and identified mode shapes should be scaled correctly because the mass distribution of the FE model and that of the actual structure may be different (Rad, 1997).

2.6.3.3 Deterministic model updating approach

This approach assumes that both FE model and dynamic investigation measurements are deterministic. It aims at determining the most probable values for uncertain input parameters by comparing FE solutions against in situ measurements. The bridge between FE solutions and measurements are comparative features (like modal parameters: natural frequencies and mode shapes). The model updating is an inverse problem in which ill conditioning is a potential problem if the quality or quantity of the comparative features is insufficient. The success of FE model updating depends not only on selecting the right comparative features but also in updating the right parameters. The updating parameters must be selected according to the combined effects of parameter uncertainty and parameter sensitivity. Parameter uncertainty can be determined from a prior knowledge of the historical structure or from laboratory testing of some specimens taken from it. The sensitivity of the FE model parameters can be determined by a sensitivity analysis which aims at measuring the changes in the model outcomes due to a unit change in the model input. After identifying the comparative features and calibration parameters, the model updating is a matter of changing the updating parameters based on the functional relationships between the measured and calculated comparative features. The FE model inherent properties that can be calibrated are directly related to the quantity, quality and type of comparative features. Successfully and widely used comparative features are the modal parameters because they contain global information about the structure mass and stiffness. Deterministic methods can be classified into manual or automated ones as discussed in the following paragraphs. (Atamturktur, 2009a; Atamturktur et al., 2010; Atamturktur and Laman, 2012)

a) Manual

Manual FE model updating is a trial-and-error based approach which calibrates selected parameter values based on engineering judgment. This approach can be justified when the initial model is a close representation of reality. In this case, usually after calibration the parameters are only minimally adjusted and they maintain their physical meaning. It is an appealing and convenient approach for calibrating FE model parameters because it incorporates engineering judgment into the updating process. Thus, it keeps the updated model from converging to an unrealistic model. Manual FE model updating proved to be successful when deficiencies arising from imprecise parameters are independent and uncorrelated. However, it is possible that, using manual updating, the existing hidden dependencies between input parameters can be revealed. If these dependencies are strong, this will raise the problem that updating one parameter compensates for imprecision in another. Also, due to its nature, manual updating cannot include uncertainties. As a result, in the presence of several sources of uncertainty, manual updating of material properties will likely compensate for the errors introduced by an inappropriate boundary condition. (Atamturktur, 2009a; Atamturktur et al., 2010; Atamturktur and Laman, 2012)

b) Automated

In this approach the FE model updating is carried out by constructing a series of loops based on optimization procedures or Bayesian inference (Atamturktur, 2009a; Atamturktur et al., 2010; Atamturktur and Laman, 2012). An optimization scheme is used through which a number of updating parameters are modified to minimize an objective function. The objective function is a formulation of the differences in dynamic behavior between the experimental data and the FE model. This is recalculated at each stage of the iteration. The method is iterative with changes made to the FE model at each step. Limitations upon the amount of information available from dynamic tests reduce the number of updatable parameters (Greening, 1999).

2.6.3.4 Stochastic model updating approach

This approach is more realistic than the deterministic approach because a FE model contains uncertainty in its input parameters (material properties, dimensions of cross sections, boundary conditions, etc.). Also, dynamic identification tests contain uncertainty in their measurements. The concept of this approach is to reach a statistical correlation between the FE model and dynamic measurements by formulating the FE model input

parameters and FE model output response probabilistically (Atamturktur, 2009a; Atamturktur et al., 2010; Atamturktur and Laman, 2012). In general, the treatment of uncertainty and quantification of errors is a two-step process. In the first step, the identification of all uncertainty and error sources is carried out. In the second step, the assessment and propagation of the most significant uncertainties and errors is carried out to obtain the predicted response quantities (Mares et al., 2006). More information about the theoretical background of this advanced technique can be consulted at Beck and Katafygiotis (1998).

2.6.4 Experimental and numerical data correlation techniques

Correlation techniques are a mixture of visual and numerical means to identify the differences between experimental and numerical modal parameters, in specific natural frequencies and mode shapes. Whereas numerical correlation techniques return a numerical value, visual means of correlation are subjective and of qualitative nature. Some of the basic correlation tools include simple tabulation or plotting of measured and predicted natural frequencies. When plotting the relation between experimental and numerical natural frequencies, perfectly matched numerical frequencies should lie on a 45° line. On the other hand, in case that the points scatter around the 45° line, this means lower matching. (Grafe, 1999). In numerical terms, for the mode number (i), the frequency discrepancy (D_f) between the experimental frequency (f_i^e) and the numerical frequency (f_i^n) can be defined as (Gentile et al., 2009; Gentile and Saisi, 2007; Beconcini et al., 2006):

$$D_f (\%) = 100 \left| \frac{f_i^e - f_i^n}{f_i^e} \right| \quad \text{Equation 2.3}$$

For mode shape vectors correlation, the Modal Assurance Criterion (MAC) (Allemang and Brown, 1982) is most widely used:

$$MAC = \frac{\left| \sum_{i=1}^n \varphi_i^e \varphi_i^n \right|^2}{\sum_{i=1}^n (\varphi_i^e)^2 \sum_{i=1}^n (\varphi_i^n)^2} \quad \text{Equation 2.4}$$

where: φ_i^e is the experimental mode shape vector and φ_i^n is the numerical mode shape vector.

Some other assurance criteria include the coordinate modal assurance criterion (COMAC), the frequency response assurance criterion (FRAC), coordinate orthogonality check (CORTHOG), frequency scaled modal assurance criterion (FMAC), partial modal assurance criterion (PMAC), scaled modal assurance criterion (SMAC), and modal assurance criterion using reciprocal modal vectors (MACRV) (Allemang, 2003).

2.6.5 Case studies using different updating approaches

There are many case studies in literature about model updating of FE models of historical construction. The following paragraphs present a summary on some of these case studies.

2.6.5.1 Indirect (iterative) approach

Aoki et al. (2007) used the inverse eigen sensitivity method (IEM) to update a FE model of a historical masonry bridge based on the results of dynamic identification tests. Four experimentally identified modes were used in the updating process. In the first phase of model updating, the FE model was composed of 24 macro blocks to represent in detail the arches, spandrels, fill materials, buttresses, abutments, and piers, Figure 2.21(a). Two materials were used. The first was for the arch, the spandrel wall and the piers and the second was for the fill materials. Based on tested samples from the stone and the mortar, the Young's moduli for these materials were estimated. The updating parameters were the stiffness' of the macro blocks. In an iterative process, the stiffness' of the macro blocks were adjusted by applying correction factors (Figure 2.21(c)) to match the experimental and numerical frequencies and mode shapes (Figure 2.21(d)). This resulted in increasing the stiffness of the three arch stones and decreasing the stiffness of the two piers. For evaluating the stiffness correction with more detail and accuracy a second phase of model updating was considered. The arch of each bay was divided into four in length and three in width, the spandrels were divided into four according to length and the piers were divided into five along the height (Figure 2.21(b)).

As a result, FE model was divided into 83 macro blocks. No changes in material properties or boundary conditions were made. Again the correction factors were applied to the stiffness' of the macro blocks and after updating, the difference between the experimental and analytical frequencies was less than 0,96% for all the modes and the MAC values were more than 0,96 for the second to fourth modes. Some of the physical meanings for the updated stiffness' were the following: (1) to simulate the increased arch thickness that was not considered in the FE model, the stiffness of all macro blocks at the

arch stones was increased; (2) the stiffness' of the macro blocks of the piers were reduced perhaps due to the effect of bridge-soil interaction; (3) the stiffness' of the macro blocks of the spandrels near the second pier were reduced probably due to the effect of existing cracks; and (4) probably due to the effect of the boundary condition, the stiffness of the macro blocks at the abutments and spandrels near the abutments was reduced. These interpretations were supported by visual inspection and other testing methods applied to the bridge.

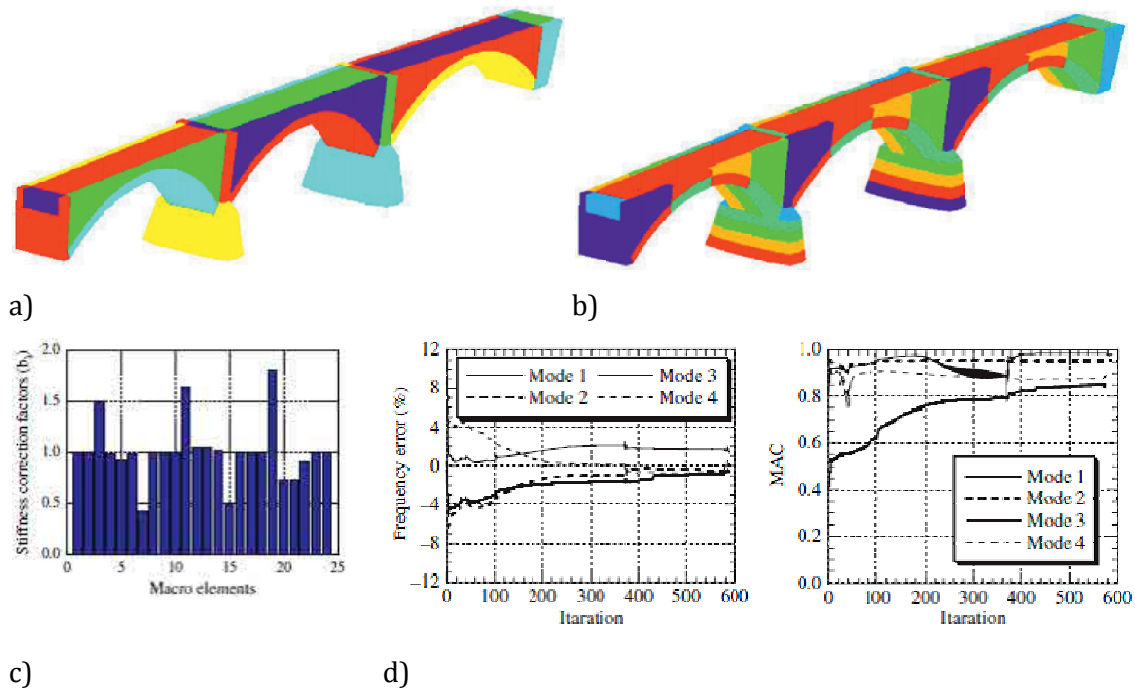


Figure 2.21. Using IEM in model updating of a masonry arch bridge: (a) 1st FE model; (b) 2nd FE model; (c) Stiffness correction coefficients obtained from model updating of the 1st FE model; and (d) iterative updating of the 1st FE model (Aoki et al., 2007).

The IEM method was used by Aoki et al. (2008) to update two FE models of a brick masonry chimney. Experimental dynamic analyses and various investigation tests were carried out to assess the structural stability of this chimney (Aoki and Sabia, 2005; Aoki and Sabia, 2006). The first three mode shapes in each main direction of the structure were identified experimentally. The FE models were built using solid, beam and truss elements. One model assumed fixed base and the other used more detailed modeling for foundations using truss elements to consider the rock behavior. For the two models, the updating parameters were the stiffness' of the finite elements. Two updating strategies were followed. The first considered only the natural frequencies and the second considered both of the natural frequencies and mode shapes. After updating the FE models by applying correction factors (as described in the previous case study) it was found that: (1)

the stiffness' of the elements at the base for the two FE models were reduced, probably due to the effect of chimney-soil interaction; (2) the stiffness' of some corner elements were increased to simulate the effect of four iron angles at the corners because they were not considered in the FE models; and (3) the influence of considering the mode shapes in the updating process is significant.

2.6.5.2 Manual approach

El-Borgi et al. (2005) carried out a manual updating of a FE model of a historical palace. To determine the compressive and tensile strengths of stone and mortar, some samples were extracted; however, it was allowed to take samples from damaged parts of the external walls only. This induced a bias, because data were based on rather altered materials, and relevant to only a selected part of the palace. Therefore, the estimated compressive strength of masonry was a doubtful parameter, and also the Young's modulus which was taken as 1000 times the compressive strength. AVT was carried out and the first five natural frequencies were identified. The frequencies of the first two modes were used to update the uncertain value of the Young's modulus. To update the model, it was observed that two values of Young's modulus should be used. The first was for the external wall and the second for the internal walls. The updated frequencies were 2.5% and 5.1% away from the experimental values for the first and second modes, respectively. The compressive strengths were then estimated from the updated values of Young's modulus.

El-Attar et al. (2005) updated a FE model of a minaret. The minaret was modeled in details by introducing the internal helical stair, and modeling both the external and the internal limestone walls in addition to the filling materials between them. The base was modeled using springs. The updating parameter was the spring stiffness which depends on the soil modulus of sub-grade reaction (K_s). Three values of K_s were tried: $1K_s$, $50K_s$, and $100K_s$. With the value of $50K_s$, three numerical natural frequencies were found to be in a good matching with the measured ones.

Manual FE model updating has been widely used for architectural heritage and many references can be seen about its application to historic buildings. These include, among many other, the studies performed on a historic church damaged by the earthquake of L'Aquila in 2009 (Casarin et al., 2011); two structures in Verona: the *Cansignorio* stone tomb and the *Arena* (Lorenzoni, 2013); two monuments in Cyprus, a

church from the 16th century (Votsis et al., 2012) and a cathedral from the 14th century (Votsis et al., 2013; Votsis et al., 2012).

2.6.5.3 Automated approach

The FE model of the church of San Torcato was updated using the automatic approach (Ramos et al., 2011; Alaboz, 2009). AVT tests were carried out and the first four modes were identified. Due to the structure complexity, it was not fully modeled. Interface elements were introduced to simulate the stiffness of the missed parts. The soil-structure interaction was defined with interface elements that reproduced the horizontal and the vertical stiffness properties of the soil. The numerical assumptions of the soil properties were based on a previous soil investigation results. The model updating procedure was carried out using four updating parameters; those are the masonry modulus of elasticity, the normal stiffness of the soil-structure interaction interface elements, the normal and shear stiffness of the interface elements of the unmodeled parts. Before the automatic model updating, the effect of each updating parameters on the calibration results were investigated manually. The effect of each parameter was studied independently from the other parameters. For the automatic updating analysis, the Douglas-Reid method (Douglas and Reid, 1982) was used. The lower and upper boundaries of the updating variables were defined based on first manual updating. Completing the updating process, it was found that the average D_f and MAC values were about 1,5% and 85%, respectively.

The automatic model updating using in specific the Douglas-Reid method (Douglas and Reid, 1982) was also used in the updating of the FE model of a masonry tower in Arcisate (Cabboi et al., 2014; Gentile and Saisi, 2007; Gentile and Saisi, 2004); a stone masonry church (Trujillo, 2009; Lourenço et al., 2012a); a stone tower subjected to AVT before and after repair interventions (Ramos et al., 2010a; Ramos, 2007); an Indian masonry minaret (Peña et al., 2010). Other examples of automatic model updating that can be checked at Pau and Vestroni (2013) and Rainieri et al. (2013).

2.6.5.4 Stochastic approach

Atamturktur (2009a and 2009b) performed this type of model updating to Washington National cathedral. She carried out FVT on a typical vault of the structure and identified the first four natural frequencies with the corresponding mode shapes. The uncertainty in experimental measurements was assessed from replicating the dynamic testing. FE model uncertainty was explored via computer experiments in which different values for material properties and springs used for simulating unmodeled parts were

tried. From the experimental measurements and the FE modal analyses, the natural frequencies and mode shapes were extracted probabilistically as mean and variance statistics. The uncertain parameters that were candidates for calibration were ranked based on the sensitivity of test-analysis comparative features using a Phenomenon Identification and Ranking Table (PIRT). Five parameters out of thirteen checked parameters were found to have high sensitivity on the matching process between the numerical and experimental results. Sensitivities of the first four frequencies to each one of the five calibration parameters were investigated. It was observed that the first two natural frequencies were highly sensitive to all of the five calibration parameters. The third natural frequency was sensitive to the modulus of elasticity of the lime stone—the cathedral construction material. The fourth frequency was sensitive to one the spring constants. At end, the five updating parameters were found not as a single deterministic value but as a mean value and standard deviation.

This model updating technique is not so common in the literature and only few examples can be found like Prabhu et al. (2014); Atamturktur et al. (2012); De Stefano and Ceravolo (2007); De Stefano (2007); De Stefano and Clemente (2005) and Sortis et al. (2005).

2.7 Historical masonry properties: literature review

2.7.1 Introduction

The results of any nonlinear analysis of a historical structure and consequently the derived conclusions depend significantly on the input materials properties. These properties are generally difficult to specify because taking samples from a historical structure is not usually allowed by responsible authorities to preserve the structure authenticity. And even when it is permitted, often due to economical restrictions, there are a limited number of tested samples which cannot cover the large variability usually contained within the construction materials of a historical structure. Moreover, some parameters, like the fracture energy, are experimentally difficult to characterize.

The following sections provide a literature review about the mechanical properties of historical masonry used in structural analysis of many case studies. This review is recalled in chapter 7 where a sensitivity analysis of used materials properties is carried out for the case study of the presented investigation. Some examples of references provide more information about in-situ characterization of historical masonry properties are: Mazzotti et al. (2014), Derakhshan et al. (2014), Quelhas et al (2014) and Andreini et al. *Integrated monitoring and structural analysis strategies for the study of large historical construction. Application to Mallorca cathedral*

(2014). Some other references for laboratory determination of masonry mechanical properties include Borri et al. (2014), Silva et al. (2014a), Silva et al. (2014b) and Milosevic et al. (2013).

2.7.2 Tensile strength

The tensile strength of historical masonry is difficult to determine. However, it is known that it takes very low values as masonry is a no-tension material due to the weak bond between units and mortar. As a rule, masonry tensile strength is not more than 10% of its compressive strength (Casati and Gálvez, 2009).

Brignola et al. (2008) proposed a methodology for the evaluation of the tensile strength of masonry f_t from the diagonal compression test (see for instance Calderini et al., 2010 for this test), with the following formula:

$$f_t = \alpha \frac{P}{A} \quad \text{Equation 2.5}$$

where, P is the applied diagonal load, A is the net area of the panel (taking into account only the percentage of the solid area of the unit) and α is a coefficient depends on masonry typology. The minimum value of α is 0,35 in cases of rubble masonry or hollow brick masonry with dry head joints. The maximum is 0,56 in cases of solid or quite solid brick with lime or cementitious mortar. In the same research, the authors critically reviewed the criteria given by ASTM (ASTM, 2002) and RILEM (RILEM, 1994), and concluded that the RILEM one, although more accurate than the ASTM, is not on the safe side for irregular masonry. FEMA 356 (FEMA, 2000) allows a lower-bound for masonry walls' tensile strength of 0,14; 0,07 and zero MPa for masonry in good, fair and poor conditions, respectively. The evaluation of the masonry condition is based on identification of some aspects of the masonry via visual inspection. Alternatively and more conservatively, the same guidelines recommends to neglect the tensile strength of older brick masonry walls constructed with lime mortar. Peña (2004) discussed the effect of the tensile strength on the collapse mechanism and the damage pattern for in-plane behavior of brick masonry construction using the rigid element method proposed by Casolo (2000).

To show how the tensile strength of historic masonry can be reasonably assumed, especially in the case of the absence of any experimental tests, in the following a literature review is given for some case studies. The first paragraph represents the first approach in which the tensile strength was set to zero or a very small value regardless the masonry

compressive strength. An alternative approach is presented in the second paragraph in which the tensile strength was taken as a ratio of the compressive strength.

Zero tensile strength was used successfully without having problems in numerical convergence in assessing the seismic capacity of the stone masonry “Pombaline” building typology in Portugal (Ramos and Lourenco, 2005; Ramos and Lourenco, 2004; Ramos and Lourenco, 2003; Ramos, 2002; Silva et al., 2001). For the structural assessment under self weight, a zero tensile strength was used for the stone masonry and the rubble infill of the church of the Monastery of Jerónimos in Portugal (Lourenco and Lança, 2010; Lourenco et al. 2007a; Lança, 2005; Lourenco and Krakowiak 2004). Again, null tensile strength was used for the regular and irregular stone masonry and brick masonry of a Portuguese church (Lourenco, 2005b; Lourenço et al., 2001).

Ceroni et al. (2009) used a tensile strength of 5% of the compressive strength in studying the seismic performance of a bell tower made from tuff stone masonry with thick mortar joints and from clay brick masonry, this ratio was in accordance with the recommendations given by the Italian code (O.P.C.M 3431, 2005) for these masonries. In the seismic analysis of a typical masonry building in Bosnia, the tensile strength was assumed as 5% of the compressive strength (Ademovic et al., 2013; Ademovic, 2011). The tensile strength was taken as 5% of the compressive strength in the studies on some stone masonry structures in Barcelona. Those are the church of the Poblet Monastery (Saloustros, 2013); a 19th century building (Potter, 2011); spire of Barcelona cathedral (Elyamani, 2009) and Santa Maria del Mar cathedral (Murcia, 2008). Pelá et al. (2009) studied the seismic vulnerability of two masonry arch bridges made from sandstone with lime mortar and a sensitivity analysis was carried out for the tensile strength trying ratios of 5, 7 and 10% of the compressive strength. For a minaret built with limestone, a tensile strength of 5% of the compressive strength was used based on experimental tests on similar masonries (Turk, 2013).

2.7.3 Modulus of elasticity

The modulus of elasticity of masonry E can be empirically estimated as a factor over the compressive strength f_c . According to modern codes for design of masonry structures, the factor takes a wide range of values depending on the type of the masonry and the compressive strength of the mortar, Table 2.2. For instance, PIET-70 (PIET-70, 1971) recommends a minimum value of 500 (natural stone masonry with dry joints) and a maximum of 3000 (ashlar masonry with mortar of a compressive strength of 16 MPa). The

Italian code (Circ. NTC08, 2009) follows a different methodology. This code gives explicitly the upper and lower values for the modulus of elasticity for a number of masonries typologies. For instance, the worst condition is for the irregular stone masonry for which the lower value is 0,69 GPa and the upper value is 1,05 GPa. The best condition is for the semisolid concrete block masonry for which the lower value is 2,40 GPa and the upper value is 3,52 GPa.

Several researchers conducted experimental tests and suggested different values for the factor in the range from 200 to 1670, Table 2.3 . The wide variability is related to the different types of used unites and mortars.

Table 2.2. Multiplier factor for the estimation of the modulus of elasticity from the compressive strength of masonry adopted by modern codes of design.

Eurocode 6 (CEN, 2005)	CSA (2004)	IBC (2003)	MSJC (2002)	FEMA (1999)	PIET-70 (1971)
1000	850	550	700 to 900	550	500 to 3000

Table 2.3. The relationship between the modulus of elasticity and the compressive strength of masonry found by several researchers.

Kaushik et al. (2007)	Tomazevic (1999)	Drysdale et al. (1994)	Paulay and Priestley (1992)
550	200 to 1000	210 to 1670	1000

For in-situ determination of the modulus of elasticity of historical masonry structures, the double flat jack test is a useful tool. The first application of this test in historical structures dates back to the beginning of the the 80's by Rossi (1982). Some code regulations can be consulted for this testing method like RILEM (2004a), RILEM (2004b), ASTM (2004a) and ASTM (2004b). Two new approaches for this test were proposed by Gutermann and Knaack (2008) and Ramos et al. (2013a).

In the literature, different approaches can be found for assumming reasonable values for the modulus of elasticity for historicmasonry. The following are some case studies to show the methodologies followed in determing and/or assumming the modulus of elasticity for a number of historical structures.

Ceroni et al. (2009) applied the double flat jack test to a bell tower made of tuff and clay brick masonries. They found values of 530 and 850 MPa for the modulus of elasticity of tuff masonry and clay brick masonry, respectively. The authors also conducted dynamic identification tests on the tower and used it to calibratea FE model of the tower. They found that the moduli of elasticity had to increase significantly to 900 MPa (instead of 530) and 1200 MPa (instead of 850) to find good correlation between experimental and

numerical modal parameters. The new values are related to the dynamic moduli that may be significantly higher than the static ones.

Saloustros (2013) assumed the modulus of elasticity as 500 times the compressive strength in a structural study of the seismic behavior of a stone masonry monastery. He then carried out a sensitivity analysis by using three other ratios of 250, 650 and 850 and found significant effect on both of the seismic capacity and the displacement capacity. Increasing the modulus of elasticity increased the load capacity and in the same time decreased the displacement capacity. Turk and Cosgun (2012) carried out the seismic analysis of a minaret built from a limestone called *Kufeki* that had been widely used by *Mimar Sinan* in many historical structures in Istanbul. Based on extensive experimental studies on this type of stone, it was found that the modulus of elasticity was 720 times the compressive strength. El-Borgi et al. (2005) found the compressive strength of the masonry of a historical palace by testing some samples. They assumed the modulus of elasticity as 1000 the compressive strength. With this assumption, good matching was found between the numerical and the experimental frequencies found by dynamic identification tests.

Another aspect about the modulus of the elasticity of historical structures that can be rarely found in the literature is the dynamic modulus of elasticity. Few researchers considered the found modulus of elasticity by means of dynamic identification tests is a dynamic modulus and used a reduction factor of 2 to find the static modulus which was then used in pushover analysis. Pelá et al. (2009) on their study on a historical bridge, after carrying out dynamic tests and FE model updating, considered the found modulus as a dynamic one and divided it by 2 to get the static modulus which was then used in nonlinear static seismic analysis. Similarly, De Mattis et al. (2007) firstly assumed the modulus of elasticity using the recommendations of the Italian seismic codes (OPCM-3274, 2003 and OPCM-3431, 2005), then to calibrate the FE model using the dynamic tests results, they had to double the code value, i.e. they applied a dynamic factor of 2.

2.7.4 Fracture energy

The fracture energy is defined as “*the amount of energy necessary to create one unit of area of a crack*” (Petersson, 1982). The concept of fracture energy was introduced by Hillerborg et al. (1976) to define the softening behavior. Softening is “*a gradual decrease of mechanical resistance resulting from a continuous increase of deformation imposed on a material specimen or structure*” (Lourenço et al., 2005b). Softening is a prominent feature

of quasi-brittle materials like brick and mortar that fail due to a process of progressive internal crack growth. This mechanical behavior is usually due to the heterogeneity of the material that results from the existence of different phases and material defects, like flaws and voids. For instance, prior to loading, mortar contains microcracks due to the shrinkage during curing and the presence of the aggregate. Initially, the microcracks are stable which means that they grow only when the load is increased. Around peak load an increase of crack formation takes place and the formation of macrocracks starts. The macrocracks are unstable, which means that the load has to decrease to avoid an uncontrolled growth. In a deformation controlled test the macrocrack growth results in softening and localization of cracking in a small zone while the rest of the specimen unloads (Lourenço, 1996).

The characteristics of stress(σ)-displacement(δ) diagrams for quasi-brittle materials in uniaxial tension and compression are shown in Figure 2.22. The inelastic behavior both in tension and compression can be described by the integral of the σ - δ diagram. These two quantities G_f and G_c are called fracture energy (or tensile fracture energy) and compressive fracture energy, respectively, and are assumed to be material properties (Lourenço, 1996). The testing configurations schematically represented in Figure 2.22 were used by Mohamed (2007), Lourenço et al. (2005a), Pluijm (1999) and Pluijm (1997) in determining G_f and G_c of solid and hollow bricks.

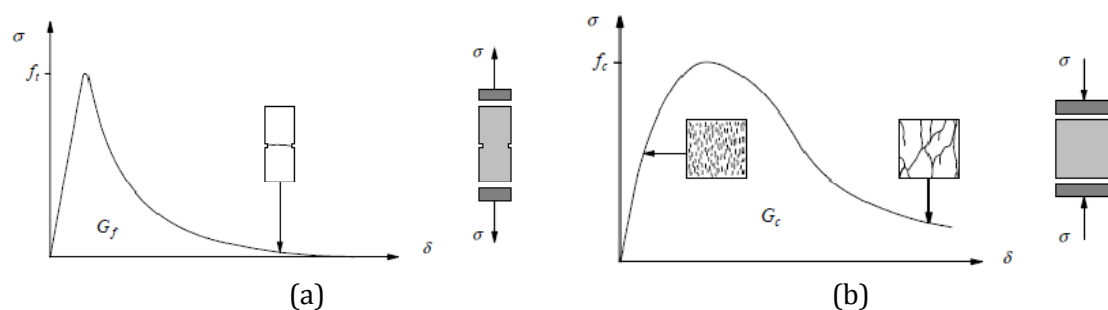


Figure 2.22. Typical behavior of quasi-brittle materials under uniaxial loading and definition of fracture energy: (a) tensile loading; and (b) compressive loading (Lourenço, 1996).

RILEM TC50- FMC (RILEM, 1985) proposed an experimental test to determine the fracture energy, it is a three-point-bending test on notched beams. Before the release of this method, Hillerborg (1983) discussed its validation through extensive experimental campaigns carried out in 9 different laboratories in Europe and Japan. Bocca et al. (1989) applied this test method on bricks sampled from 19th century historical structures. This test method was critically reviewed by Guinea et al. (1992), Planas et al. (1992) and Elices et al. (1992) and they proposed a correction method to derive the fracture energy without having the effects of bulk energy dissipation, experimental procedures and size effects.

However, some assumptions made in this method are doubtful and it is not clear if this method is also valid for different types of experiments (Schlangen, 1993). For compressive fracture energy of masonry, It is known that there is limited information on it and also that it depends on the experimental set-up and boundary conditions (Medeiros et al., 2013). In the following, some examples for the used tensile and compressive fracture energies in the seismic analysis of some historical structures are given.

2.8 Seismic assessment of historical construction

2.8.1 Introduction

In the recent years a number of catastrophic earthquakes occurred in Europe and resulted in significant damage to cultural heritage buildings. Some useful references that addressed the diastrophic effects of these earthquakes on historical structures are Romao et al. (2013), Paupério et al. (2012) and Feriche et al. (2012) who discussed the seismic damage to some churches after Lorca earthquake (Spain) in 11th May 2011. Brandonisio et al. (2013), Lagomarsino (2012), Ceci et al. (2011), Kaplan et al. (2010), Augenti and Parisi (2010), Ceci et al. (2010) showed the effects of L'Aquila earthquake (Italy) in 9th April 2009. Cattari et al. (2013), Sorrentino et al. (2013) and Bournas et al. (2013) discussed the performance of some types of structures affected by Emilia earthquake (Italy) in May 2012. Leite et al. (2013), Moon et al. (2012) and Dizhur et al. (2011) presented the damages resulted from the two recent earthquakes that hit New Zealand, those are Canterbury in 4th September 2010 and Christchurch in 22nd February 2011. The Van earthquake that struck eastern Turkey in 23rd October 2011 and the related damage was discussed in some publications like Akansel et al. (2013), Tapan et al. (2013), Korkmaz and Korkmaz (2013), Korkmaz (2013) and Ozturk (2013). Minarets, similar to other tall structures like bell-towers and spires, present very vulnerable architectural elements to earthquakes. Therefore, their seismic behavior and common collapse mechanisms are always of concern, and were discussed in some publications like Cakti et al. (2013), Oliveira et al. (2012), Sezen and Dogangun (2012), Dogangun and Sezen (2012), Dogangun (2008) and Dogangun et al. (2007). In Figure 2.23 some of the damage and collapses to historic structures are shown.

In the same context, it is clearly noted that modern societies are allocating great efforts to protect their culture heritage buildings from earthquakes. Europe, in particular, has carried out a number of research projects on the subject and closely related topics like in-situ investigation, structural monitoring and conservation of historical structures.

Among them are NIKER (NIKER, 2010-2012), PERPETUATE (PERPETUATE, 2010-2012), SMOOHS (SMOOHS, 2008-2011), SEVERES (SEVERES, 2010-2012), PROHITECH (PROHITECH, 2004-2008), EU-India (EU-India, 2004-2006), DIAS (DIAS, 2002-2005), ONSITEFORMASONRY (ONSITEFORMASONRY, 2001-2004), RISK-UE (RISK-UE, 2001-2004) and CHIME (CHIME, 2000-2003).



a) Collapse of the transept of Santiago church (Romao et al., 2013) b) Damage of Espolón tower (adapted from Feriche et al., 2012)



c) Collapse of the gable of San Biago church (Brandonisio et al., 2013) d) overturning of façade of San Paolo a Peltuinum church (Brandonisio et al., 2013)



e) Collapse of historic minarets in Van (Turkey) at the weaker section at balconies (Ozturk, 2013)

Figure 2.23. Some examples of damage to historical structures: (a) and (b) Lorca earthquake (Spain); (c) and (d) L'Aquila earthquake (Italy); and (e) Van earthquakes (Turkey).

Assessing this vulnerability can be carried out using several techniques varying in complexity and time and resources demands. Using more than calculation method is preferably required to cross check the results and increase the level of confidence on the results. In the following, three techniques are discussed: the FE nonlinear static and dynamic analyses and kinematic limit analysis. To assess the seismic safety, the N2 method is presented. Finally, some case studies are shown and discussed.

2.8.2 Nonlinear static (pushover) analysis

2.8.2.1 General

Pushover analysis is defined by ATC-40 (ATC, 1996) as *“an incremental static analysis used to determine the force-displacement relationship, or the capacity curve, for a structure or structural element. The analysis involves applying horizontal loads, in a prescribed pattern, to a computer model of the structure, incrementally; i.e. “pushing.” the structure; and plotting the total applied shear force and associated lateral displacement at each increment, until the structure reaches a limit state or collapse condition”*.

The nonlinear static (pushover) analysis is a relatively simple structural analysis technique that aims at evaluating the expected performance of a structure under earthquakes by estimating its strength and deformation capacities. It accounts in an approximate manner for the redistribution of internal forces occurring when the structure is subjected to inertia forces that no longer can be resisted within the elastic range of the structural behavior. It involves applying a predefined lateral load pattern which is distributed along the structure height. The lateral forces are then monotonically increased in constant proportion with a displacement control at the considered control point (usually at the top of the structure) until either the ultimate condition or a certain level of deformation is reached. The target top displacement may be the deformation expected in the design earthquake (in case of designing a new structure) or the drift corresponding to structural collapse (in case of assessing an existing structure). The pushover analysis can provide valuable information about the seismic response of existing structures which includes estimates of the deformation capacities of elements that have to deform in elastically to dissipate the seismic energy; consequences of the strength deterioration of individual elements on the global behavior of the structure; the realistic force capacity of potentially brittle elements; identification of the strength discontinuities that can lead to changes in the dynamic characteristics in the inelastic range; and verification of the completeness and adequacy of load path, considering all the elements of the structural

system, all the connections, and the foundation system. (Krawinkler and Seneviratna, 1998; Mwafy and Elnashai, 2001)

The pushover analysis has been developed and reviewed over the last four decades by Freeman et al. (1975), Saiidi and Sozen (1981), Kunnath et al. (1992), Lawson et al. (1994), Bracci et al. (1997), Krawinkler and Seneviratna (1998), Tso and Moghadam (1998), Kim and D'Amore (1999), Antoniou (2002), Themelis (2008) and Vijayakumar and Venkateshbabu (2011), among others.

The pushover analysis is described and proposed as an efficient analysis technique for design and assessment of structures by several modern codes among them: Eurocode 8 (CEN, 2004), the Spanish seismic code (NCSE-02, 2002), the Italian seismic codes (O.P.C.M 3274, 2004; O.P.C.M 3431, 2005; NTC, 2008), FEMA-273 (FEMA, 1997), FEMA-440 (FEMA, 2005), FEMA P440A (FEMA, 2009); ATC-40 (ATC, 1996), ATC-55 (ATC, 2002), IBC (IBC, 2000) and ASCE 41 (ASCE, 2007).

2.8.2.2 Lateral load patterns

The used lateral load patterns in pushover analysis are intended to represent and bound the distribution of inertia forces in a design earthquake. Clearly, the distribution of inertia forces will vary with the severity of the earthquake and with time within an earthquake. However, an invariant load pattern can be used assuming that the distribution of inertia forces will be reasonably constant throughout the earthquake and that the maximum deformations (obtained from this invariant load pattern) will be comparable to those expected in the design earthquake. The results are near to truth in case that the analyzed structure response is not importantly affected by higher modes of vibration and the structure has only a single load yielding mechanism that can be detected by an invariant load pattern. The use of at least two load patterns that are expected to bound inertia force distributions is recommended because no single load pattern can capture the variations in the local demands expected in a design earthquake. One should be a uniform load pattern that emphasizes the demands in lower elevations compared to the demands in upper elevations of the structure. The other could be a load pattern that accounts for higher modes effects. Nevertheless, none of these invariant load patterns can account for a redistribution of inertia forces occurs when a local mechanism forms and accordingly the dynamic properties of the structure change. Thus, it is attractive to utilize adaptive load patterns that follow more closely the time variant distribution of inertia forces. (Krawinkler and Seneviratna, 1998)

Some of the proposed adaptive load patterns which try to establish equivalent lateral load distribution based on a certain theoretical basis mentioned in Jingjiang et al. (2003) are: (1) distribution proportional to the product of the mass and fundamental mode shape, which is used initially until the first yielding takes place, then the lateral forces are determined based on the product of the current floor displacement and mass at each step (Fajfar and Fischinger, 1988); (2) the adaptive distribution, which is varied as the inter story resistance changes in each load step (Bracci et al. , 1997); (3) a distribution based on mode shapes derived from secant stiffness at each load step (Eberhard and Sozen, 1993). These load patterns, however, haven't demonstrated their superiority over the simple invariant load patterns.

For design codes, the Eurocode 8 (CEN, 2004) and FEMA-273 (FEMA, 1997), for instance, recommend using at least two load patterns. The first is a uniform pattern based on lateral forces proportional to mass regardless of elevation. The second is a modal pattern able to account for higher mode effects.

2.8.2.3 Limitations

The main limitations of this technique can be summarized as:

- it may not detect some important deformation modes of the structure when subjected to severe earthquakes and it may exaggerate others, i.e., if higher mode effects become important, nonlinear dynamic response may differ significantly from predictions based on invariant or adaptive static load patterns; (Krawinkler and Seneviratna, 1998) ;
- whatever load pattern is selected, it is likely to advocate certain deformation modes (triggered by the load pattern) and neglect others that are due to the ground motion and inelastic dynamic response characteristics of the structure (Krawinkler and Seneviratna, 1998);
- none of the invariant load patterns can account for the contributions of higher modes to response, or for a redistribution of inertia forces because of structural yielding and the associated changes in the dynamic characteristics of the structure (Chopra and Goel, 2001);
- it is unable to account for the progressive stiffness degradation, the change of modal characteristics and the period elongation of a structure subjected to monotonic loading (Antoniou and Pinho, 2004);

- it provides only a measure of the capacity and has to be combined with a demand measures using methods like capacity-spectrum and N2 to complete the assessment study (Elnashai, 2002).

2.8.3 Nonlinear time-history (dynamic) analysis

2.8.3.1 General

When properly implemented, the nonlinear dynamic analysis (also called nonlinear response-history analysis) provides a more accurate assessment of the structural response to strong ground shaking compared to the pushover analysis. Because the nonlinear dynamic analysis incorporates inelastic member behavior under cyclic earthquake ground motions, thus, it explicitly simulates hysteretic energy dissipation in the nonlinear range. Only the damping and other non-modeled energy dissipation need to be added as viscous damping. The analysis output is the dynamic response calculated for the input ground motions, resulting in response history data on the relevant demand parameters. Dynamic analyses for multiple ground motions are necessary because of the inherent variability in earthquake ground motions. Thus, it is possible to calculate statistically robust values of the demand parameters for a given ground motion intensity. The nonlinear dynamic analysis involves fewer assumptions than the pushover analysis; therefore, it is subject to fewer limitations. Nevertheless, the results accuracy depends on the details of the analysis model and the input ground motions, among other factors.

Table 2.4. Pushover analysis versus nonlinear dynamic analysis (adapted from Elnashai, 2002).

	Static Analysis	Dynamic Analysis
Damping representation required?	No	Yes
Mass representation required?	No*	Yes
Additional operators required?	No	Time integration operations
Input motion required?	No	Yes
Action distribution	Fixed*	Vary in time
Computational time	Usually faster than dynamic analysis	Usually slower than static analysis

* may not be the case for adaptive pushover analysis

This analysis technique poses several challenges such as the complexity of time-integration algorithms and the difficulties in damping representation which affect the results. In addition to the dependency of the results on the characteristics of the analyzed structure, they are affected also by the nature of each earthquake record which exhibits its

own peculiarities, dictated by frequency content, duration, sequence of peaks and their amplitude. The differences between the nonlinear static and dynamic analyses are summarized in Table 2.4. (Deierlein et al., 2010; Elnashai, 2002; Mwafy and Elnashai, 2001)

2.8.3.2 Input ground motions

The main important issues to consider when selecting the input ground motions for nonlinear dynamic analysis are (1) the target hazard spectra, (2) the source of ground motions, and (3) the number of ground motions. For the first issue, while the earthquake hazard is a continuum, codes typically define specific ground motion hazard levels for specific performance checks, i.e. the hazard is defined in terms of response spectral accelerations with a specified mean annual frequency of exceedance. For the second issue, there are three sources of ground motions (1) artificial accelerograms, (2) natural records of past earthquakes and (3) simulated accelerograms. (Deierlein et al., 2010)

Artificial accelerograms were used in the past because of the lack of natural records of past earthquakes and the need to have seismic input closely representing a specific scenario to match (Iervolino et al., 2009). It was found, however, that some types of artificial accelerograms have shown inadequacy in being a realistic representation of possible ground motions (Bazzurro and Luco, 2003). On the other hand, the recently increasing accessibility to data bases of natural accelerograms recorded during real earthquakes helped significantly in using natural records (Iervolino et al., 2009). Simulated accelerograms are spectrally matched ground motions created by manipulating the frequency content and intensity of natural records to match a specific hazard spectrum (Deierlein et al., 2010). For more information about the debatable subject of selecting and scaling natural records, the reader is referred to O'Donnell et al. (2011); Iervolino et al., (2009); De Luca et al. (2009); Iervolino et al.(2008); Luco and Bazzurro (2007); Iervolino and Cornell (2005); Cornell (2005); Bommer and Acevedo (2004). Regarding the number of ground motions, typical practice is to use seven motions; however, the accurate number of motions is still a topic that needs more research (Haselton et al., 2012).

The input ground motion is doubtlessly the most important variable (more than the analytical model parameters) affecting the results and the amount of uncertainty in seismic design or assessment using nonlinear dynamic analysis (O'Donnell et al., 2011). However, it is found that the recommendations given in seismic codes about selection of input ground motions are generally poor (Iervolino et al., 2008; Bommer and Ruggeri,

2002). Haselton et al. (2012) refers this to the fact that these recommendations are based, in large part, on research of analysis of seismically isolated structures from more than 20 years ago. This occurs, in part because research on the topic is developing fast and at least a few years are required by codes to take it in (Iervolino et al., 2008). The Eurocode 8 (CEN, 2003) regulations are discussed in (Iervolino et al., 2008). This code allows employment of all three kinds of input ground motions previously discussed. It asks for matching of the average spectral ordinates of the chosen set of records to the target code-based spectral shape. To find the mean of the structural response, the set has to consist of at least seven recordings. Otherwise, if the size of the set is from three to six, the maximum response to the records within the sets needs to be considered. Little, if any, prescriptions are given about other features of the input ground motion. It seems that the code requirements have been developed having only spectrum compatible records in mind (Iervolino et al., 2008). In short, there is no general agreement in the earthquake engineering community on how to appropriately select and scale earthquake ground motions for design and seismic performance assessment of structures using nonlinear dynamic analysis (Haselton et al., 2012).

2.8.3.3 Damping

a) General

Any structure has some energy-dissipating mechanisms. Inelastic hysteretic energy dissipation, radiation of kinetic energy through foundation, kinetic friction and viscosity in materials are examples of energy-dissipating mechanisms in structures. Such energy dissipation or capacity is called damping and it is usually assumed to be of viscous type because of its mathematical simplicity (Otani, 1980). However, it has been shown in the literature that the actual mechanism of energy dissipation in real structures is closer to the so-called hysteretic damping than to the viscous damping (Oliveto and Greco, 2002). Damping capacity is not a unique value of a structure, but it depends on the level of excitation (Otani, 1980). The state-of-the-art does not provide a method to determine the damping capacity based on the material properties and geometrical characteristics of a structure (Otani, 1980). On the other hand, since damping can result from many sources, it is difficult to describe analytically and in a thorough way the complex physical phenomena that determine the energy dissipation (Crandall, 1970).

For masonry historical structures, in specific, there is no information on the nature of inherent damping mechanisms. Since cracking always exists in this type of structures, their damping ratios would be different from those used for modern structures. Moreover,

cracking results in reduction in the masonry Young's modulus which would increase the damping level. (Elmenschawi et al., 2010c)

b) Damping model

The effect of viscous damping on the seismic response is influenced by the used mathematical model for its representation. The damping can be modeled using mass-proportional, stiffness-proportional or Rayleigh damping computed from either the initial elastic or the tangent inelastic system properties. The Rayleigh damping is widely used due to its mathematical simplicity. (Léger and Dussault, 1992)

The Rayleigh damping (c) is defined as a combination of the mass (m) and the stiffness (k):

$$c = a_0 \cdot m + a_1 \cdot k \quad \text{Equation 2.6}$$

where, a_0 and a_1 are the Rayleigh damping coefficients. These two coefficients can be determined from the damping ratios (ξ_i and ξ_j) and the angular frequencies (ω_i and ω_j) of the i^{th} and j^{th} modes as follows:

$$\frac{1}{2} \begin{bmatrix} 1/\omega_i & \omega_i \\ 1/\omega_j & \omega_j \end{bmatrix} \begin{Bmatrix} a_0 \\ a_1 \end{Bmatrix} = \begin{Bmatrix} \xi_i \\ \xi_j \end{Bmatrix} \quad \text{Equation 2.7}$$

The damping (ξ_n) of any mode n^{th} with angular frequency (ω_n) can be determined as:

$$\xi_n = \frac{a_0}{2} \cdot \frac{1}{\omega_n} + \frac{a_1}{2} \cdot \omega_n \quad \text{Equation 2.8}$$

When applying this procedure, the two modes (i^{th} and j^{th}) should be reasonably chosen such that the obtained values of a_0 and a_1 result in reasonable damping ratios for all the modes contributing in the dynamic behavior of the structure. (Chopra, 2000)

2.8.3.4 Recommendations for time step

When applying the Newmark method (Newmark, 1959), the choice of the time step size (Δt) should be chosen so that:

(1) it is sufficiently small compared with the accelerogram duration (t_d)

$$\Delta t \ll t_d \quad \text{Equation 2.9}$$

(2) to correctly reproduce the system response, preferably 20 time steps must be applied in the small period (T_i) of the highest mode

$$\Delta t \leq \frac{1}{20} T_i \quad \text{Equation 2.10}$$

thus ensuring the correct computation of the contribution of high-frequency modes (DIANA, 2009). According to Eurocode 8 (CEN, 2004) enough number of modes should be taken into account to ensure correct consideration of all modes contributing significantly to the dynamic response. This condition is satisfied by considering a number of modes corresponding to a cumulative mass participation of at least 90% in relevant directions of the analysis.

2.8.4 Limit analysis

2.8.4.1 Background

The limit analysis is a simple tool, yet effective, for estimating the ultimate capacity of masonry structures. The method as proposed by Heyman (1966) includes three basic assumptions: (1) masonry has infinite compressive strength, (2) masonry has no tensile strength and (3) sliding failure cannot occur. The first assumption is not conservative as it may appear because collapse of masonry structures is mostly due to cracking rather than crushing (Betti and Galano, 2012). The second assumption is near to reality since very small tension forces are transferred across mortar joints (Betti and Galano, 2012). These assumptions lead to the definition of the term mechanism in which the structure fails due to the formation of hinges corresponding to disconnections and localized cracking that divide the structure into macro-elements (Castellazzi et al., 2013). Macro-elements can also be proposed based on experience gained from surveys of damage patterns of structures already experienced earthquakes. The reader is referred to the following references for more about how to propose possible mechanisms of historical Catholic churches (Lagomarsino, 2012), Orthodox churches (Mosoarca and Gioncu, 2013), towers (Sepe et al., 2008), adobe structures (Tolles et al., 2003), masonry buttresses (Ochsendorf et al., 2004), masonry arches (Block et al., 2006a), masonry vaults (Huerta, 2001) and other types of historical construction (Jaiswal et al., 2011; D'Ayala and Speranza, 2003; Augusti et al., 2001; Garocci, 2001).

Today, limit analysis is used as a powerful tool able to realistically assess the safety and collapse of structures composed by blocks including arches, vaults, towers, façades and entire buildings. Notwithstanding, it can hardly be used to predict the damage for moderate or service load levels not leading to a limit condition. It should be considered as a complementary tool when performing alternative numerical analyses. Previous studies showed that, regardless the level of sophistication of the used numerical method, it will

produce, at ultimate condition, results predictable by means of limit analysis. (Roca et al., 2010)

2.8.4.2 Theorems of limit analysis

The assumptions of the limit analysis enable the application of the three limit theorems of plasticity: the lower-bound (or safe), the upper-bound (or unsafe) and uniqueness. In the first theorem, the structure is safe and the collapse is prevented if a statically admissible state of equilibrium can be found. This occurs when a thrust line can be determined in equilibrium with the external loads and falls within the boundaries of the structure. The load applied is a lower-bound of the actual ultimate load which causes failure. In the second theorem, if a kinematically admissible mechanism can be found for which the work developed by external forces is positive or zero, then the load is an upper-bound of the actual ultimate load. The application of the upper bound theorem leads to the so-called kinematic limit analysis for analyzing masonry buildings. For the last theorem, a limit condition can be reached and the structure will be about to fail if a both statically and kinematically admissible collapsing mechanism can be found. The failure configuration is reached when a thrust line can be found causing as many hinges (Hinges are caused by the thrust line becoming tangent to the boundaries) as needed to develop a mechanism. When this occurs, the load is the true ultimate load, the mechanism is the true ultimate mechanism, and the thrust line is the only possible one. (Heyman, 1995)

2.8.4.3 Calculations of the kinematic limit analysis

The collapse multiplier (α_0) is calculated from:

$$\alpha_0 \left(\sum_{i=1}^n P_i \delta_{x,i} + \sum_{j=n+1}^{n+m} P_j \delta_{x,j} \right) - \sum_{i=1}^n P_i \delta_{y,i} - \sum_{h=1}^k F_h \delta_h = L_{fi} \quad \text{Equation 2.11}$$

where: P_i is the self-weight of each macro-element part (n entries) composing the kinematic mechanism, P_j is the weight transmitted to the macro-element by adjacent structures (m entries), F_h is the generic external force applied to a macro-element part (k entries), $\delta_{x,i}$ and $\delta_{x,j}$ are the horizontal virtual displacements of each macro-element centroid, $\delta_{y,i}$ and δ_h are the vertical virtual displacements of each point of application of P_j and F_h respectively, L_{fi} is the work done by internal forces, and finally, φ is the given rotation to initiate the mechanism. The seismic acceleration of the activation of the mechanism (a_0^*) is calculated from (Circ. NTC08, 2009):

$$a_0^* = \frac{\alpha_0 \sum_{i=1}^{n+m} P_i}{M^* \cdot FC} = \frac{\alpha_0 g}{e^* \cdot FC} \quad \text{Equation 2.12}$$

$$e^* = \frac{g M^*}{\sum_{i=1}^{n+m} P_i} \quad \text{Equation 2.13}$$

$$M^* = \frac{(\sum_{i=1}^{n+m} P_i \delta_{x,i})^2}{g \cdot \sum_{i=1}^{n+m} P_i \delta_{x,i}^2} \quad \text{Equation 2.14}$$

where: g is the gravity acceleration, e^* is the fraction of the participation mass of the structure, M^* is the participating mass in the mechanism and FC is a confidence factor. FC takes a minimum value of 1 when extensive information is available about the structure's geometry, construction details and properties of materials, FA takes a maximum value of 1,35 when very limited information is available about the structure, and FC intermediate value is 1,2.

2.8.5 N2 method

2.8.5.1 General

The N2 method (Fajfar, 2002; Fajfar, 2000; Fajfar and Gaspersič, 1996; Fajfar and Fischinger, 1988) is a relatively simple method for the performance evaluation of structures. It combines the pushover analysis of a MDOF model with the response spectrum analysis of an equivalent SDOF system. It is derived in the acceleration-displacement format which allows the visual interpretation of the procedure and of the relations between the basic quantities controlling the seismic behavior. Two differences between this method and the capacity spectrum method (Freeman, 2004; Freeman, 1998) can be distinguished: (1) the inelastic spectra rather than elastic spectra (with equivalent damping and period) are utilized; (2) demand quantities can be obtained without the need to iterations. The results of this method are reasonably accurate when the structure oscillates predominantly according to the first mode. Some other limitations in the method exist and are corresponding to the limitations of the pushover analysis and the inelastic spectra. (Fajfar, 2000)

This method is already considered in some codes for earthquake design like Eurocode 8 (CEN, 2004) and the Italian code (O.P.C.M 3274, 2004) and its further modifications (O.P.C.M 3431, 2005). It was successfully applied for seismic performance evaluation of many types of masonry structures (Carpentieri, 2011; Pelá et al., 2009; Aprile et al., 2006; Resemini, 2003; Lagomarsino et al., 2002).

2.8.5.2 The procedure

The procedure of the method is detailed in (Fajfar, 2002). Here, a brief of the main steps is presented. The procedure is graphically shown in Figure 2.24. In the first step, the elastic response spectrum in the format of time (T)-elastic acceleration (S_{ae}) (Figure 2.24, a) is transformed to the displacement (S_{de})-acceleration format (Figure 2.24, b) for the same viscous damping ratio using the following relation (Fajfar, 2002):

$$S_{de} = \frac{T^2}{4\pi} S_{ae} \quad \text{Equation 2.15}$$

In the second step, the capacity curve obtained from the pushover analysis is transformed to the equivalent bi-linear curve using the approximate approach of equal area, i.e., the area under the capacity curve is equal to the area under the bi-linear curve (Figure 2.24, c). The ratio between the maximum displacement and the yield displacement is the ductility factor (μ).

In the third step, the obtained spectrum in the new format is transformed to the inelastic spectrum (Figure 2.24, d) using as reported by Fajfar (2002) the following relations proposed by Vidic et al. (1994):

$$S_a = \frac{S_{ae}}{R_\mu} \quad \text{Equation 2.16}$$

$$S_d = \mu \frac{T^2}{4\pi^2} S_a \quad \text{Equation 2.17}$$

where, R_μ is the reduction factor due to ductility and is evaluated from (Fajfar, 2002):

$$R_\mu = (\mu - 1) \frac{T}{T_C} + 1 \quad T < T_C \quad \text{Equation 2.18}$$

$$R_\mu = \mu \quad T \geq T_C \quad \text{Equation 2.19}$$

where, T_C is the characteristic period of the ground motion. The last step in the method is the intersection between the bi-linear capacity curve and the inelastic response spectrum to determine the performance point which defines the performance acceleration and the performance displacement of the structure (Figure 2.24, d).

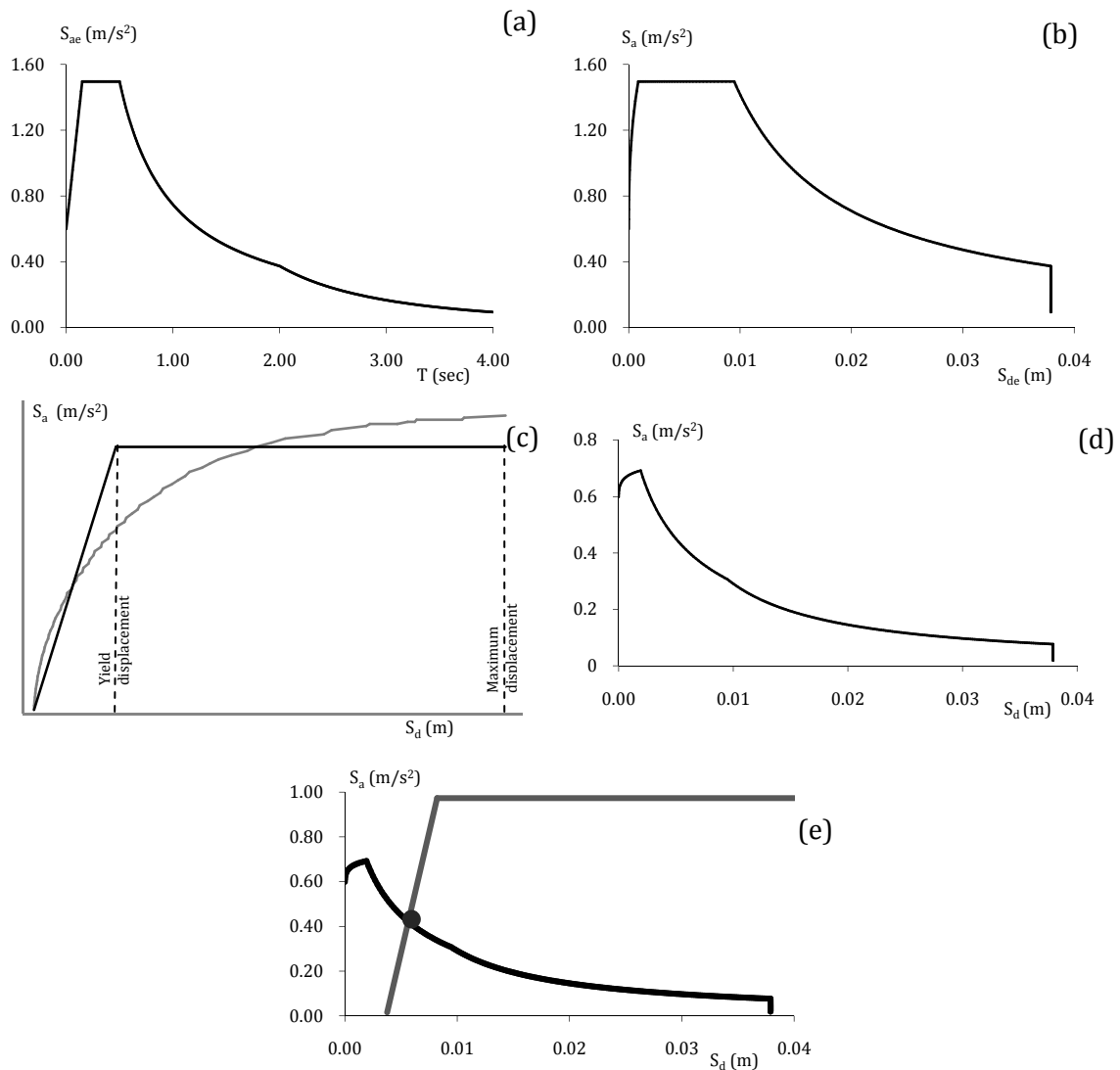


Figure 2.24. N2 method procedure: (a) elastic response spectrum; (b) elastic response spectrum in AD format; (c) the capacity curve (in grey) and the equivalent bi-linear curve (in black); (d) inelastic response spectrum; and (e) performance point.

2.8.6 Case studies

In the literature a large number of publications that addressed the issue of seismic assessment of historical structures can be found. The pushover analysis is widely used and some researchers confirm its results using the kinematic limit analysis; on the contrary, still the usage of the time history analysis is limited. Few case studies have been studied using both of the pushover and the time history analyses.

Peña et al. (2010) used the pushover analysis and the nonlinear dynamic analysis in the assessment of the seismic behavior of a historical minaret dates back to the 13th century called Qutb Minar. The FE model of the structure was calibrated based on the results of the AVT (Ramos et al., 2006a). The used models were (1) a 3D one that used

beam elements to simulate the minaret (Beam model) (2) a 3D one that used solid and shell elements (Solid model) and (3) a 2D in-plane model (Rigid model) based on the Rigid Element Method. Rather similar behaviors were found for the three models. It was observed that the load factor (the base shear/the self weight) was around 0,21 for the Beam and the Rigid models, while it was around 0,18 for the Solid model. For the collapse mechanism, the three models showed that the minaret materials did not fail by compressive stresses and the structure collapsed by overturning at the base. To study the effect of the used load pattern on the pushover results, two other load patterns were considered: the linear distribution of the displacement along the height and the forces proportional to the first mode shape. It was noticed that the resisted load factor depended very much on the distribution of the forces. The load factor proportional to the first mode was only 35% of the load factor proportional to the mass, while the load factor proportional to the linear distribution was 53%. Moreover, the collapse section changed and moved from the base in case of mass proportional load pattern to the first balcony for the two new load patterns. For the nonlinear dynamic analysis, five synthetic accelerograms compatible with the design spectrum of the Seismic Indian code were used. The Rayleigh damping model was used in which the experimentally identified damping of 2,5% was used and other two values of 5 and 8% were also tried. This analysis showed, on contrast to the pushover analysis, that the last two levels of the minaret were the most vulnerable, especially the last level which presented the highest drift, Figure 2.25 (a). The difference in results was attributed to the great influence of the higher modes of vibration on the seismic response of the minaret.

Minghini et al. (2014) in their study on a brick masonry chimney damaged by May 2012 Emilia earthquake (Italy) found that the nonlinear dynamic analysis estimated the same collapse mechanism (the upper part of the chimney, Figure 2.25b) that was observed in the damage survey carried out after the earthquake. The authors also found that the pushover analysis estimated the collapse of the lower part of the chimney which is not consistent with actual damage.

António et al. (2012) investigated the seismic response of two churches in Pico Island (Portugal) that were damaged by an earthquake in 1998. The authors carried out a detailed survey of earthquake damage, AVT and model updating. For the seismic safety analysis, they used a linear time history analysis and applied the already occurred earthquake. Good agreement was found between the numerical results and the actual surveyed damage.

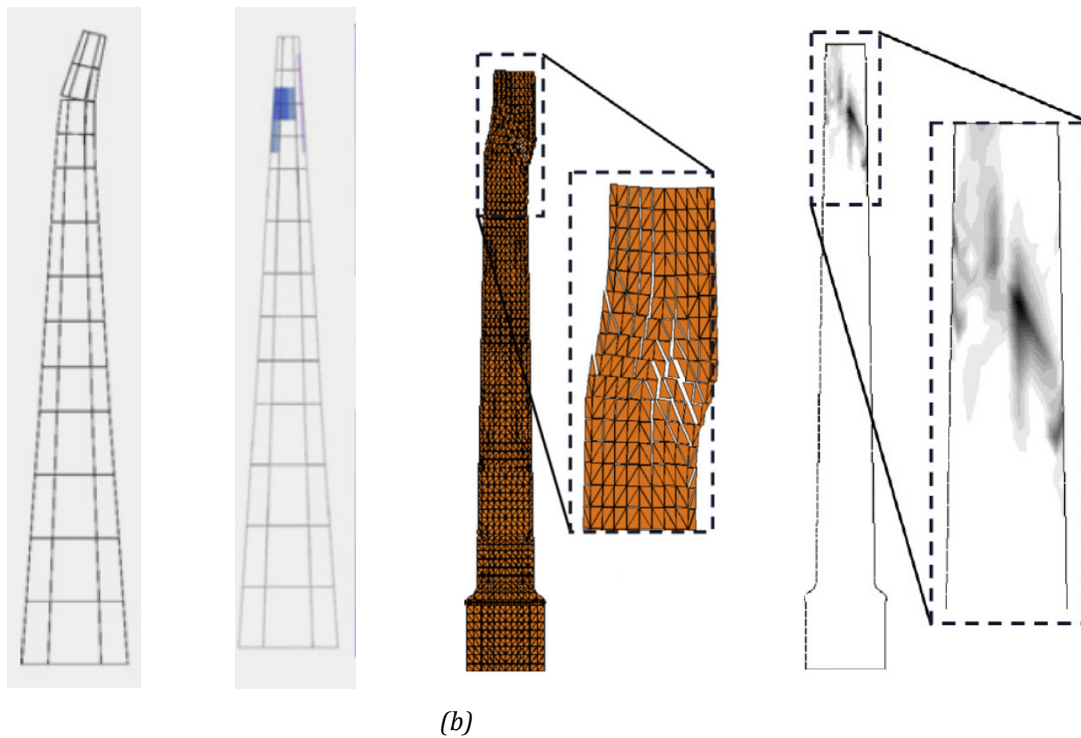


Figure 2.25. Nonlinear dynamic analysis of (a) minaret: deformed shape (left) and collapsed part in blue (right) (Peña et al., 2010); and (b) chimney: deformed shape (left) and collapsed part in dark gray (right) (Minghini et al., 2014).

Ramos and Lourenço (2004) assessed the seismic safety of a typical building typology in Lisbon using the pushover analysis. They studied the influence of the group of buildings in the seismic behavior of the individual buildings that constitute the block, what was called the *block effect*. It was concluded that this effect was beneficial and increased the safety against earthquakes. Thus, safety analysis of historical buildings belonging to larger compounds can be carried out with isolated buildings, which can reduce the effort and time to great extent. However, it must be stressed that the difference in the results were rather large and, if the isolated building analysis would indicate unsafe condition, it may be suitable and economically justifiable to refine the analysis using the full compound.

A common building typology of stone masonry residential buildings in Lisbon called *Gaioleiro* was studied extensively using the pushover analysis employing different load patterns, including the adaptive pushover, and the nonlinear dynamic analysis. Moreover a detailed sensitivity analysis was carried out and the influence of the compressive and tensile strengths, the compressive and tensile fracture energies, the damping ratio and the modulus of elasticity of walls and floors was discussed, see Mendes and Lourenço (2013) and Meneses (2013).

2.9 Conclusions

This chapter has presented the recent state-of-the-art of many interconnected activities usually carried out in an integrated methodology to end up with the structural assessment of a historical structure. In the following the main conclusions concerning each of these activities are presented.

On the dynamic identification tests:

- For modern structures, these tests are useful to 1) give insight about their dynamic behavior, 2) find out if their performance fall within particular criteria, 3) detect signs of damage and 4) propose guidance for improved future modeling and/or design.
- For historical structures, these tests are used to 1) obtain modal parameters of the structure, 2) update the numerical model of the structure, 3) assess the level of connection between different parts of the structure partially separated by cracks, 4) reveal the damage effect on dynamic behavior, 5) appraise the benefits of repair/strengthening interventions and 6) select the optimal sensors locations for the following dynamic monitoring activity.
- AVT is more used than FVT in the dynamic identification of historical structures because it is quicker and cheaper, less equipments and operators are needed, and tests can be realized while a structure is in service. However, it has some limitations, for instance, the difficulty in exciting some modes, the assumption of stationary white noise excitation and the low signal to noise ratio. Therefore, these limitations require the usage of robust output-only dynamic identification methods.
- The sensors are selected based on many aspects; above all are the frequency range, the dynamic range and the sensitivity.
- In AVT, the testing time should not be less than 1000 to 2000 times structure's fundamental period.
- It is important to carry out the modal parameters identification process using more than one dynamic identification method. In spite of this, normally damping will be a difficult parameter to determine. Moreover, some modes may not be identified due to low excitation levels.
- The identification of structures with one predominant direction like bridges and bell towers is easier than in more complex structures like churches and cathedrals.

On the dynamic monitoring of historical structures:

- Monitoring is carried out to 1) study the evolution of modal parameters in time, 2) reveal the effect of environmental actions on modal parameters, 3) capture the dynamic response in the vicinity of possible seismic events and 4) verify the effectiveness of any possible intervention, specifically the incremental intervention.
- The dynamic monitoring systems are classified according to the type of used instrument into wired systems and wireless systems. The first systems are still widely in use, and more research is still in need for facilitating and increasing the usage of the second systems. According to the activation regime of the recording devices, there are three types of systems: dynamic monitoring system with threshold, periodical dynamic monitoring system and continuous dynamic monitoring. Although the last system gives more information than the other two systems, it is not widely used because it needs large storage capacity and more post processing.
- Some of the few available case studies in the literature have been discussed. Based on these cases, it can be concluded that 1) the natural frequencies increase with the temperature due to the closing of cracks and vice versa, 2) under the effect of a seismic event with a considerable magnitude, the natural frequencies decrease and they may recover their initial value after the event if no residual damage has occurred, 3) the damping ratios increase significantly during a seismic events of a considerable magnitude, 4) mode shapes change lesser than natural frequencies and damping ratios under the effect of earthquakes.
- The automated dynamic identification of modal parameters from dynamic monitoring data is a new trend that it is highly needed to speed up the identification process by reducing the amount of human interfering.

On the modal parameters identification methods:

- Some basic concepts of signal processing like sampling, white noise, signal conditioning, spectral analysis and Fast Fourier Transform (FFT) were introduced. From these concepts, the following can be concluded 1) the sampling rate must be chosen to be five to ten times the signal's highest frequency component otherwise the aliasing error may occur, 2) Windows like Hanning are applied to signals to reduce leakage error, 3) filters are applied to reduce noise in signals by removing some unwanted frequencies, 4) decimation reduces the time of processing a signal without losing any information it contains.

- Five modal parameters identification methods were discussed. Those are the PP, the FDD, the SSI-COV, the SSI-DATA and the pLSCF. For each of them the background theory was briefly given and a focus was made on the advantages and the limitations of each method.
- The PP method is fast and user friendly but it is not efficient in case of closely spaced modes. Moreover, picking the peaks is always a subjective task. The FDD method allows for the accurate separation of closely spaced modes but its results are satisfactory in condition that the excitation is a white noise, the structure is lightly damped and the mode shapes of closely spaced modes are geometrically orthogonal. Also, it cannot estimate the damping ratios. The SSI methods are more accurate than the PP and the FDD; however, they don't afford an absolute scaling of the identified mode shapes. The pLSCF method yields a very clear stabilization diagram, compared to the SSI method. Nevertheless, the damping estimates associated with some stable poles decrease with increasing noise levels and this situation becomes worth for poorly excited modes.

On the IR thermography:

- This technique has two approaches, the passive and the active. The passive approach doesn't require pre-heating of the investigated structure, whereas, in the active approach pre-heating is required.
- The IR has main advantages of being a non-contact technique, large coverage area, easy to carry and easy data manipulation.
- The technique is useful to investigate the moisture problems due to rainwater seepage, to reveal the masonry texture covered by plaster layers, to observe the activeness of cracks, to show the homogeneity of the used construction materials and to estimate the efficiency of FRP strengthening to masonry structures.

On the model updating:

- Creating a reliable FE model of a heritage building is often a difficult task because of the challenges usually involved by this type of buildings such as their complex geometry, and possible existing damage and previous repairs. Consequently, it is always required to validate the historical structure FE model against possible modeling inaccuracies and uncertainties. A common approach is to carry out dynamic identification tests on the structure and extract the experimental natural frequencies and mode shape. Then, by correlating them to their numerical counterparts (using for

instance D_f and MAC), it may be possible to update the material properties, in specific the modulus of elasticity, and the boundary conditions could be updated.

- There are several methods of model updating. These include the direct methods, the indirect methods, the manual method, the automated method and the stochastic method. For historical structures, the manual method is the most widely used. The automated model updating has been used in few cases, and the indirect methods and stochastic methods have been used in very few cases.
- From the reviewed case studies, it can be stated that in case of bridges (and similar structures) and towers (and similar structures), very good correlation in terms of D_f and MAC can be found between experimental and numerical modal parameters. For other types of historical structures, like churches, it is difficult to find a good correlation between numerical and experimental mode shapes.

On the modeling of masonry nonlinear behavior:

- The linear analysis is not reliable for masonry structures that exhibit very early cracking process under applied load because of its almost null tensile resistance.
- Non-linear analysis is the recommended method for structural assessment of historical structures, because it allows for the tracing of the complete response of a historical structure from the elastic range, through cracking and crushing, up to complete failure. Moreover, different types of non-linear behavior may be combined like physical and geometrical ones.
- A literature review about historic masonry mechanical properties was carried out by reviewing several case studies. The methodologies followed in assuming the tensile strength, the modulus of elasticity and the fracture energies in tension and compression were discussed. For tensile strength, some researches assign zero or very low values to it. Others assume it as a ratio between 5 to 10% of the compressive strength. The modulus of elasticity can be empirically estimated from the compressive strength using a multiplier factor. Some codes assign an absolute value for this parameter based on the masonry type. For tensile fracture energy, values from 0,01 to 0,10 N.mm/mm² have been found in the literature. For compressive fracture energy, values from 6 to 20 N.mm/mm² have been used.

On the seismic assessment of historical structures:

- Assessing the seismic capacity of historic structures via numerical models is a difficult task and the usage of other simplified methods like the kinematic limit analysis is advisable to cross check the results.

- The pushover analysis is nowadays well recognized and adopted in many modern seismic codes. It has no rigorous theoretical base. It has some significant limitations, for instance, in case that the higher modes of vibration become important, the nonlinear dynamic response may differ from the predictions of the pushover analysis.
- The nonlinear dynamic analysis is generally preferred to the pushover analysis. However, it has several challenges. Among them are the dependency of the results on the used earthquakes records, the complexity of time-integration algorithms, the difficulties in damping representation, and the large needed of computational and storage resources.
- The N2 method is a relatively simple method for the performance evaluation of structures. It is now considered in some modern codes of seismic assessment of structures. It has two differences from the capacity spectrum method. First, the inelastic spectra rather than elastic spectra are used. Second, the demand quantities can be obtained without the need for iterations.